Technische Universität München

Fakultät für Medizin

Contribution of HOXD10, HOXD11 and HOXD13 to malignancy of Ewing sarcoma

Laura Roth

Vollständiger Abdruck der von der Fakultät für Medizin der Technischen Universität München zur Erlangung des akademischen Grades eines Doktors der Medizin genehmigten Dissertation.

Vorsitzender: Prof. Dr. Ernst J. Rummeny

Prüfer der Dissertation:

1. Prof. Dr. Stefan Burdach

2. Prof. Dr. Uta Behrends

Die Dissertation wurde am 23.05.2019 bei der Technischen Universität München eingereicht und durch die Fakultät für Medizin am 04.12.2019 angenommen.

Table of contents

List of abbreviations

aa	amino acid
ADGRG2, GPR64	adhesion G protein-coupled receptor G2
ADP	adenosine diphosphate
AML	acute myeloid leukemia
ANTP	antennapedia
BCP	1-bromo-3-chloropropane
BET	bromodomain and extraterminal (BET) proteins
BGLAP	bone gamma-carboxyglutamate protein
BHA	butylated hydroxyanisole
CCK	cholecystokinin
CCND1	cyclin D1
CD99	CD99 molecule (Xg blood group)
cDNA	complementary DNA
CNMD	chondromodulin
CO_2	carbon dioxide
COL10A1	collagen type X alpha 1 chain
CXCR4	C-X-C motif chemokine receptor 4
DEPC	diethyl pyrocarbonate
DKK2	dickkopf WNT signaling pathway inhibitor 2
DMEM	Dulbecco's modified eagle medium
DMSO	dimethyl sulfoxide
DNA	deoxyribonucleic acid
dNTP	deoxyribonucleotide triphosphate
e.g.	exempli gratia
EGR2	early growth response 2
ERBB4	erb-b2 receptor tyrosine kinase 4
ERG	ETS transcription factor ERG

ES	Ewing sarcoma
ESFT	Ewing sarcoma family of tumors
et al.	et alii
ETS	E26 transformation-specific
ETV1	ETS variant 1
ETV4	ETS variant 4
EWS, EWSR1	EWS RNA binding protein 1
EZH2	enhancer of zeste 2 polycomb repressive complex 2 subunit
FAM	6-carboxyfluorescein
FBS	fetal bovine serum
FC	fold change
FEV	FEV, ETS transcription factor
FGF	fibroblast growth factor
FITC	fluorescein isothiocyanate
FLI1	Fli-1 proto-oncogene
FLT1, VEGFR1	fms related tyrosine kinase 1
FT	fetal tissue
GAP43	growth associated protein 43
GAPDH	glyceraldehyde-3-phosphate dehydrogenase
GFAP	glial fibrillary acidic protein
GRP	gastrin releasing peptide
H_2O	water
H3K4	lysine 4 of histone 3
H3K4m3	trimethylation at lysine 4 of histone 3
H3K27	lysine 27 of histone 3
H3K27m3	trimethylation at lysine 27 of histone 3
HBSS	Hank´s buffered salt solution
HDAC	histone deacetylase

HIF1A	hypoxia inducible factor 1 subunit alpha
HOM-C	homeotic complex
HOX	homeobox
HOXA	homeobox A
HOXA11	homeobox A11
HOXA13	homeobox A13
HOXB	homeobox B
HOXB5	homeobox B5
HOXB8A	homeobox B8a
HOXC	homeobox C
HOXC6	homeobox C6
HOXD	homeobox D
HOXD3	homeobox D3
HOXD9	homeobox D9
HOXD10	homeobox D10
HOXD11	homeobox D11
HOXD12	homeobox D12
HOXD13	homeobox D13
HOXL	HOX-like
H&E	hematotoxylin and eosin
IFITM1	interferon induced transmembrane protein 1
IFN	interferon
IGF1	insulin like growth factor 1
IGF1R	insulin like growth factor 1 receptor
IgG	immunoglobulin G
IgM	immunoglobulin M
IL6	interleukin 6
ISG15	ISG15 ubiquitin-like modifier

ITM2A	integral membrane protein 2A
JAG1	jagged 1
kb	kilo bases
kDa	kilo dalton
LDL	low density lipoprotein
LRP6	LDL receptor related protein 6
LSD1	lysine demethylase 1A
MMP	matrix metallopeptidase
MMP1	matrix metallopeptidase 1
MMP7	matrix metallopeptidase 7
MMP9	matrix metallopeptidase 9
MMP14	matrix metallopeptidase 14
mRNA	messenger RNA
MSC	mesenchymal stem cells
MSX1	msh homeobox 1
mTOR	mechanistic Target of Rapamycin
Na_2HPO_4	sodium phosphate dibasic
NaH_2PO_4	sodium phosphate monobasic
NaN_3	sodium acide
NaOH	sodium hydroxide
NB	neuroblastoma
NC-MSC	neural crest-derived mesenchymal stem cells
NCSC	neural crest stem cells
NEFM	neurofilament medium
NGF	nerve growth factor
NGFR	nerve growth factor receptor
NK cell	natural killer cell
NKL	NK-like

NKX2-2	NK2 homeobox 2
NPY1R	neuropeptide Y receptor Y1
NR0B1	nuclear receptor subfamily 0 group B member 1
NT	normal tissue
NTC	non template control
NUP98	nucleoporin 98
PARP1	poly(ADP-ribose) polymerase 1
PBS	phosphate buffered saline
PBX	pre-B-cell leukemia homeobox
PCR	polymerase chain reaction
PDGFB	platelet derived growth factor subunit B
PET	polyethylen terephthalate
PFA	paraformaldehyde
PNET	primitive neuroectodermal tumor
PSA	Prostate-specific antigen
PTHLH	parathyroid hormone like hormone
$Rag2^{-/-}\gamma c^{-/-}$	recombination activating gene 2 knock out
RANK, TNFRSF11A	receptor activator of NF-κB, TNF receptor superfamily member 11a
RANKL, TNFSF11	receptor activator of NF-κB ligand, TNF superfamily member 11
RB	retinoblastoma
RNA	ribonucleic acid
RNAi	transient RNA interference
RPMI	Roswell Park Memorial Institute
RT	room temperature
RUNX1	runt related transcription factor 1
RUNX2	runt related transcription factor 2
RUNX3	runt related transcription factor 3
SD	standard deviation

SEM	standard error of the mean
SHOX2	short stature homeobox 2
shRNA	small hairpin RNA
siRNA	small interfering RNA
SLIT2	slit guidance ligand 2
SOX9	SRY-box 9
spdh	synpolydactyly homolog
STEAP	six transmembrane epithelial antigen of the prostate family
STEAP1	STEAP family member 1
TALE	three amino acid loop extension
TGFB1	transforming growth factor beta 1
TGFBR2	transforming growth factor beta receptor 2
TNFRSF11B, OPG	TNF receptor superfamily member 11b
TP53	tumor protein p53
TRAP	tartrate-resistent acid phosphate
qRT-PCR	quantitative real-time PCR
VEGF, VEGFA	vascular endothelial growth factor A
Wnt family	Wingless-type MMTV integration site family
WNT3a	Wnt family member 3A
WNT5a	Wnt family member 5A
WNT11	Wnt family member 11

1. Introduction

1.1 Ewing sarcoma

Bone cancer has its origin in bone tissue or bone marrow itself, or in a tumor that developed in other tissues of the body. It can therefore be divided into two groups: primary and secondary bone malignancies (van Driel & van Leeuwen 2014). Secondary bone malignancies (bone metastases) are common events that mainly occur in adults as a consequence of breast, prostate or lung cancer, for example (Coleman 2001). Primary bone malignancies are, in contrast, rare diseases and account for less than 0.2 % of all cancers. Osteosarcoma is the most common form of primary bone cancer (35 %), followed by chondrosarcoma (30 %) and Ewing sarcoma (16 %) (Biermann *et al.* 2017). In children and younger adolescents, Ewing sarcoma (ES) is even the second most malignant bone tumor after osteosarcoma with an incidence of 3.3 / 1 million (Ward *et al.* 2014). It mainly occurs in the second decade of life with a mean age of 15 years, but 20 - 30 % of the cases are diagnosed in the first decade and about 20 % in patients over 20 years (Bernstein *et al.* 2006). Males are affected slightly more often than females (60:40 male:female ratio). In Caucasians, ES arises significantly more frequently than in Asians or Africans (Jawad *et al.* 2009), probably due to genetic polymorphisms resulting in extended GGAA microsatellite repeats, e.g. in the *EGR2* gene (Grünewald *et al.* 2015).

Patients with ES typically exhibit symptoms like severe local pain, swelling, hyperemia or additional local symptoms depending on the affected part of the body, as well as blood changes like anemia, leukocytosis and elevated serum levels of lactate dehydrogenase, alkaline phosphatase and c-reactive protein (Ozaki 2015). The main tumor sites are the long bones (46 %), especially the diaphyseal regions of the lower extremity, the pelvis (26 %) and the bones of the chest wall (16 %) (Bernstein *et al.* 2006). But ES can also occur in any extra-osseous region, like in the chest wall or abdominal wall, paraspinal, in the extremities, the head, the neck or the retroperitoneum (Raney *et al.* 1997).

At the time of diagnosis about 25 % of the patients exhibit distant metastases in lung and / or bone or bone marrow (Esiashvili *et al.* 2008). The prognosis of patients with metastasized disease is still poor, whereby patients with isolated pulmonary metastases have a better prognosis than patients with primary bone / bone marrow or combined bone and lung metastases (3 year event-free survival up to 52 % with isolated lung metastases vs. 19 % / 8 % with bone / bone marrow or combined metastases) (Gaspar *et al.* 2015; Ladenstein *et al.* 2010; Thiel *et al.* 2016). The overall survival rate of initially metastatic disease is about

13 - 30 % with current therapies and did not improve markedly in the last decades (Burdach *et al.* 2010; Stahl *et al.* 2011). In contrast, localized disease can be cured in about 70 % of the cases today due to multimodal therapeutic measures (Biswas & Bakhshi 2016).

Therapeutic strategies comprise a multidisciplinary approach depending on many factors like age, tumor site and size, operability, metastases and treatment side effects. The standard treatment options for localized ES include multi-agent chemotherapy and local tumor control via surgery and / or radiation therapy. Primary disseminated ES are treated with chemotherapy, surgery and radiation therapy (Biswas & Bakhshi 2016). Usually, the chemotherapy is applied in a neoadjuvant setting to reduce the tumor size and to eliminate metastasizing tumor cells. After local tumor control, an adjuvant chemotherapy follows to prevent relapse (Biswas & Bakhshi 2016; Gaspar *et al.* 2015). Every chemotherapy includes several different cytostatic drugs, like vincristine, dactinomycin, cyclophosphamide, doxorubicin, ifosfamide and etoposide (etoposide only in localized disease) (Biswas & Bakhshi 2016; Burdach *et al.* 2010; Grier *et al.* 2003; Paulussen *et al.* 2008; Yock *et al.* 2006). An example for an induction chemotherapy is VIDE (vincristine, ifosfamide, doxorubicin, etoposide) according to the EURO-E.W.I.N.G. 99 protocol (Biswas & Bakhshi 2016; Ladenstein *et al.* 2010; Juergens *et al.* 2006; Le Deley *et al.* 2014). After induction chemotherapy, local tumor control follows. It can be implemented by surgery, radiation therapy or a combination of both as ES is a radiosensitive tumor (Daw *et al.* 2016; Haeusler *et al.* 2010; Ning *et al.* 2016). Surgery is the most commonly used form of local control and the risk of local failure seems to be lower for surgery than for definite radiation therapy (Biswas & Bakhshi 2016; DuBois *et al.* 2015; Schuck *et al.* 2003). Nevertheless, irradiation is an important alternative and supplement to surgery. In particular, it is suitable for patients with inoperable tumors, in a postoperative setting when the tumor has not been excised with adequate tumor margins and for the treatment of bone and lung (Biswas & Bakhshi 2016; Casey *et al.* 2015; DuBois *et al.* 2015; Haeusler *et al.* 2010; Liu *et al.* 2011; Ning *et al.* 2016; Paulino *et al.* 2013). In metastatic disease with high-risk for relapse high-dose chemotherapy (including busulfan / melphalan) with or without total-body-irradiation or involved compartment irradiation followed by autologous stem cell rescue is a reasonable approach (Burdach & Jürgens 2002; Burdach *et al.* 2003; Burdach 2004; Burdach *et al.* 2010; Ladenstein *et al.* 2010).

In about 30 % of all cases ES relapses, resulting in dismal survival rates (Leavey & Collier 2008). The main type of recurrence is systemic, as well in primary localized as in primary disseminated diseases. The relapse mostly occurs within the first two years, associated

with a worse prognosis than later recurrence (Burdach 2004). For relapse therapy there is no standardized treatment. Treatment options are, in addition to the therapeutic approaches mentioned above, intensified forms of treatment as high-dose, myeloablative chemotherapy and involved compartment irradiation followed by stem cell therapy, for example. But they are also associated with a higher risk of treatment related complications (Burdach *et al.* 2000; Burdach *et al.* 2003; Marina *et al.* 2017). Nevertheless, relapsed or primary disseminated ES still has low rates of survival under conventional therapy strategies (Stahl *et al.* 2011).

For this reason, the so-called targeted therapy including new therapeutic agents targeting specific pathways and epigenetic alterations plays an increasingly important role (Arnaldez & Helman 2014; Burdach *et al.* 2018; Jiang *et al.* 2015; Kovar *et al.* 2016; Richter *et al.* 2009; Riggi *et al.* 2014; Yu *et al.* 2017). Determining the tumor specific gene expression profile will serve as a basis for this purpose. Especially, the contribution of the typical oncogenic fusion protein EWS-FLI1 to ES malignancy has been examined in various studies with pending therapeutic consequences (Kovar *et al.* 2016; Theisen *et al.* 2016; Yu *et al.* 2017). Promising approaches that are currently being investigated concern, inter alia, the effectiveness of mechanistic target of rapamycin (mTOR) inhibitors (Dancey 2006; Naing *et al.* 2012; Wagner *et al.* 2015), antibodies against insulin like growth factor 1 receptor (IGF1R) (Fassel *et al.* 2016; Juergens *et al.* 2011; Tap *et al.* 2012), vascular endothelial growth factor A (VEGFA) (Ahmed *et al.* 2012; Vornicova & Bar-Sela 2016; Zhou *et al.* 2007), CD99 molecule (Xg blood group) (CD99) (Guerzoni *et al.* 2015; Manara *et al.* 2016; Scotlandi *et al.* 2000a) and poly (ADP-ribose) polymerase 1 (PARP1) inhibitors (Brenner *et al.* 2012; Engert *et al.* 2015; Stewart *et al.* 2014; Vormoor & Curtin 2014). Furthermore, it was demonstrated that immunotherapies using antigen-specific T cells and NK cells could be promising therapeutic opportunities too, even though ES is an only weakly immunogenic tumor (Blaeschke *et al.* 2016; Kirschner *et al.* 2017; Knott *et al.* 2016; Merchant *et al.* 2016; Schirmer *et al.* 2016; Thiel *et al.* 2011; Thiel *et al.* 2017). Recent studies about epigenetic deregulations in ES suggested epigenetic inhibitors like histone deacetylase (HDAC) inhibitors, lysine demethylase 1A (LSD1) inhibitors and JQ1, a BET bromodomain inhibitor, as auspicious novel treatment approaches in ES (Hensel *et al.* 2016; Jacques *et al.* 2016; Theisen *et al.* 2016; Zorzi *et al.* 2013). In summary, there are a lot of different options to directly target ES tumor cells, but there is still a lack of experience of their clinical applicability (Lawlor & Sorensen 2015). However, a study published by Weidenbush *et al.* in 2018 already demonstrated that the application of individual targeted

therapy in refractory pediatric sarcomas led to improved overall and progression free survival with no difference in the quality of life compared to non-targeted therapy. Precise knowledge of the carcinogenesis and the exact molecular pathways of ES provide the basis of all current and future therapeutic strategies.

The foundation for all subsequent investigations was laid out in 1921 when James Ewing first discovered ES. In his publication he described a round cell sarcoma in the radius of a fourteen-year-old girl as diffuse endothelioma of bone (Ewing 1972). Histologically, it belongs to the group of pediatric small round blue cell tumors that includes many tumor entities, like neuroblastoma, medulloblastoma, rhabdomyosarcoma, leukemia and others (Li & Siegal 2010; Roessner & Jürgens 1993). Because of their similar histological appearance there was a need for specific markers to clearly identify ES. By immunohistochemical analyses the expression of CD99 molecule at high levels was detected in ES cells (Ambros *et al.* 1991; Fellinger *et al.* 1991; Kovar *et al.* 1990). CD99, a transmembrane glycoprotein, is particularly highly expressed on the surface of T cells and ES cells. But, since positivity for CD99 can also be found in other tumors like synovial sarcomas or non-Hodgkin lymphomas, it proved to be too unspecific (Llombart-Bosch & Navarro 2001). Apart from CD99, also other markers over-expressed in ES were identified, but they were not specific enough for ES as well (Tirado *et al.* 2006). A groundbreaking improvement to specifically identify ES was the discovery of a specific chromosome translocation by Delattre *et al.* 1992. This typical translocation classifies ES, Askin tumors and primitive neuroectodermal tumors (PNET) as the Ewing sarcoma family of tumors (ESFT) and reveals their common histogenesis (Burchill 2008; Iwamoto 2007). The ESFT forms a heterogeneous group of aggressive malignancies that affect bone and soft tissue. Besides a similar histological appearance, all members of the ESFT have high gene expression levels of *CD99* and a rearrangement of the *EWS RNA binding protein 1* (*EWS, EWSR1*) gene on chromosome 22 band q12 with an E26 transformation-specific (ETS) transcription factor family member (Scotlandi *et al.* 2000a; Moore & Haydon 2014). In 85 % of all cases the *EWS* gene is fused to the *Fli-1 proto-oncogene* (*FLI1*) gene on chromosome 11 band q24 (translocation t(11;22)(q24;q12)) (Moore & Haydon 2014). In the most commonly ‘type 1’ translocation seven exons of *EWS* are fused with six exons of *FLI1* (Alava *et al.* 1998; Zoubek *et al.* 1996). Besides *FLI1*, also other ETS transcription factor family members including *ERG* (*ERG, ETS transcription factor*), *ETV1* (*ETS variant 1*), *ETV4* (*ETS variant 4*) and *FEV* (*FEV, ETS transcription factor*) can combine with *EWS*, but

less frequently. The second most translocation is *EWS-ERG* and can be found in about 5 - 10 % of cases (Peter *et al.* 1997; Sorensen *et al.* 1994; Warren *et al.* 2013).

The resulting oncogenic fusion protein EWS-FLI1 has dual functions. On the one hand, it acts as aberrant transcriptional activator. It binds to DNA with the conserved ets-domain and induces the expression of various genes that are involved in oncogenesis by promoting proliferation and regulating the cell cycle (Kauer *et al.* 2009; Kovar 2005). One of the most relevant direct target genes induced by EWS-FLI1 is *nuclear receptor subfamily 0 group B member 1* (*NR0B1*), an important cell-cycle progression regulator with a key role in ES cell proliferation and growth (Cidre-Aranaz & Alonso 2015; García-Aragoncillo *et al.* 2008; Kinsey *et al.* 2009). Accordingly, knock down of EWS-FLI1 in ES cell lines resulted in growth inhibition and reduced invasiveness (Dohjima *et al.* 2003). On the other hand, EWS-FLI1 represses the expression of genes that are important for cell differentiation, communication and tumor suppression (Kauer *et al.* 2009; Kovar 2005; Rorie *et al.* 2004). Even though mutations of the tumor suppressor gene *tumor protein p53* (*TP53*) are rare in ES, the p53 pathway seems to be abrogated in ES (Gröbner *et al.* 2018). It was demonstrated that EWS-FLI1 suppresses p53 in ES cell lines resulting in impaired p53-dependent growth inhibition, but induces growth arrest and apoptosis in primary human fibroblasts by stimulating p53 (Ban *et al.* 2008; Lessnick *et al.* 2002; Li *et al.* 2010b; Neilsen *et al.* 2011). Apart from p53, *transforming growth factor beta receptor 2* (*TGFBR2*), another tumor suppressor gene, is also repressed by EWS-FLI1 emphasizing the major contribution of EWS-FLI1 to oncogenesis of ES (Hahm *et al.* 1999; Im *et al.* 2000). Besides modulating gene expression directly via transcriptional activation or repression EWS-FLI1 also affects epigenetic mechanisms in ES. For instance, it induces EZH2 (*enhancer of zeste 2 polycomb repressive complex 2 subunit*) by binding to the EZH2 promotor. EZH2, which is over-expressed in ES, silences target genes that are important for neuroectodermal and endothelial differentiation by methylating H3K27 (lysine 27 of histone 3) and therefore preserves the undifferentiated phenotype of ES. Further, it was shown that EZH2 contributes to ES tumor growth and metastasis *in vivo* (Burdach *et al.* 2009; Richter *et al.* 2009). Thus, epigenetic alterations play a key role in ES oncogenesis indicating that the malignant stemness phenotype of ES is maintained by epigenetic mechanisms.

Despite of this great progress in research the question about the precise cell of origin of ES remains unresolved to date although the neuroectodermal histogenesis of ES was already demonstrated in 1985 (Schmidt *et al.* 1985). Mesenchymal stem cells (MSC) and / or neural crest stem cells (NCSC) are currently accepted as the most probable cells of origin.

Previous studies showed that human MSC expressing EWS-FLI1 mimicked the typical gene expression profile and phenotype of ES cells and expressed genes normally involved in neuronal and neuroectodermal differentiation (Miyagawa *et al.* 2008; Riggi *et al.* 2008; Riggi *et al.* 2010). They further retained their undifferentiated state and presented a high ability to self-renewal (Javaheri *et al.* 2016). It was further demonstrated that EWS-FLI1 silencing enabled differentiation along the adipogenic and osteogenic lineage in ES cell lines. Inhibition of EWS-FLI1 resulted in a gene expression profile similar to the expression pattern of MSC indicating that EWS-FLI1 silencing allows ES cells to regain their mesenchymal stem cell features (Tirode *et al.* 2007). Moreover, both MSC and NCSC displayed permissiveness for EWS-FLI1 with transition to an ES like cell type (Levetzow *et al.* 2011; Todorova 2014). Altogether, these findings elucidate the genetic relationship of ES cells to NCSC / MSC and suggest that ES might develop due to malignant transformation of MSC and / or NCSC from an undifferentiated state to a more differentiated state of the chondro-osseus lineage (Hauer *et al.* 2013).

In order to learn more about the origin of ES and to identify an ES specific expression pattern, Staege *et al.* performed high-density DNA microarray analyses of different ES cell lines compared to normal tissue (Staege *et al.* 2004). A list of genes over-expressed in ES was published. Thirty three of thirty seven up-regulated genes are expressed in neuronal tissues or during neuronal differentiation supporting the research results, NCSC as presumable cells of origin, as described above. Subsequently, other genes were identified and could enable new therapeutic approaches for targeted therapy (Burdach *et al.* 2009). Among them, three genes of the posterior *HOXD* locus, *HOXD10 (homeobox D10)*, *HOXD11 (homeobox D11)* and *HOXD13 (homeobox D13)*, were identified.

1.2 Genes of the posterior *HOXD* locus

1.2.1 General information on *HOX* genes

The beginning of research on *Homeobox* genes stretches back to the year 1894 when W. Bateson first introduced the term of “homeosis”. He observed special mutations in animals in which one part of the body was transformed into another one and designated this phenomenon as “homeosis” (Bateson 1894). In 1921, T.H. Morgan and C. Bridges studied homeotic transformations in Drosophila melanogaster (D. melanogaster). They found correct body structures located on the wrong body site and presumed special genes to be

responsible for correct spatial body patterning (Bridges 1921). 57 years later, E.B. Lewis discovered the homeotic complex (HOM-C) containing eight genes (*HOX* genes) and the chromosomal arrangement in two complexes, the antennapedia complex and the bithorax complex, determining the correct segmentation along the anterior-posterior body axis in D. melanogaster (Lewis 1978). In the 1980s, a characteristic DNA sequence included in all *HOX* genes, the homeobox, was identified (Garber *et al.* 1983; Gehring & Hiromi 1986). Thereupon, the existence of evolutionary highly conserved *HOX* genes has also been proven in the genome of plants, fungi, animals and humans, substantiating their ancient origin (Duboule 1992; Lappin *et al.* 2006; McGinnis & Krumlauf 1992; Rubock *et al.* 1990; Scott 1992).

In the human genome over 200 genes contain a homeobox and therefore belong to the homeobox gene superclass, but most of them are widely distributed across the entire genome and do not contribute to homeotic transformations. The homeobox gene superclass includes eleven classes under which the ANTP (antennapedia) class homeobox forms the largest subset containing two subclasses, the HOXL (HOX-like) and the NKL (NK-like) subclass. The actual *HOX* genes responsible for homeosis are part of the HOXL subclass. As a characteristic feature these 39 genes are organized in four clusters (A - D) on different chromosomes (HOXA on 7p15.2, HOXB on 17q21.32, HOXC on 12q13.13, HOXD on 2q31.1). Every cluster comprises 9 - 11 genes due to evolutionary loss of some *HOX* genes (Holland *et al.* 2007; Holland 2013; Lappin *et al.* 2006). The position of the genes on the chromosome is arranged in a collinear manner. Thus, the four clusters can be divided into 13 paralog groups illustrating the similar position and sequence of paralog genes although being located on different chromosomes (Kmita & Duboule 2003; Sharkey *et al.* 1997). As mentioned above, human *HOX* genes are orthologues to the genes of the HOM-C cluster of D. melanogaster. The paralog groups 1 - 8 display resemblance to the anntenapedia complex of D. melanogaster, whereas the groups 9 - 13 show close relation to abdominal B, part of the bithorax complex (Lappin *et al.* 2006).

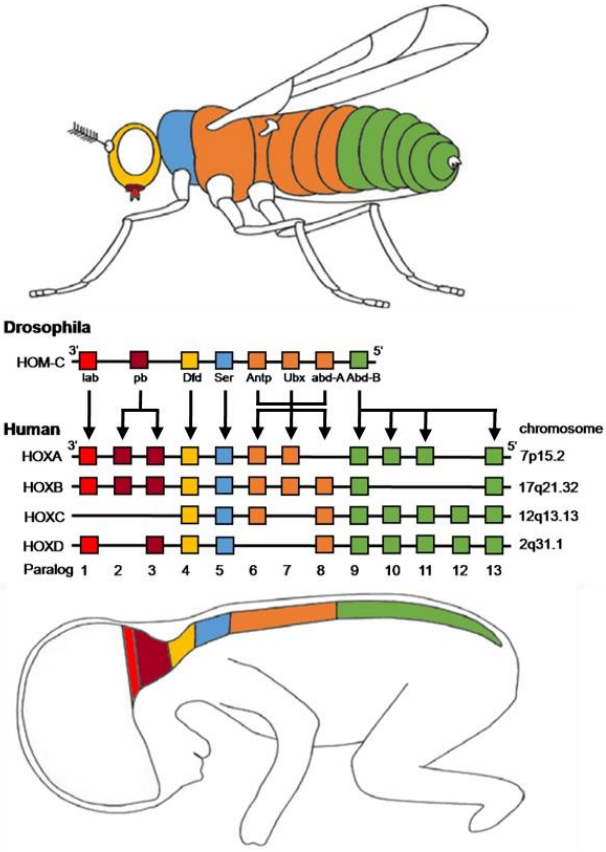

Figure 1: *HOX* gene arrangement on the HOM-C cluster of D. melanogaster in comparison to the arrangement in four clusters in the human genome

Eight *HOX* genes on the HOM-C cluster of D. melanogaster (above) developed to 39 *HOX* genes arranged in four clusters (HOXA - HOXD) in the human genome (below). Paralog groups 1 to 13 represent similarity of the genes across different chromosomes. lab: labial; pb: proboscipedia, Dfd: deformed; Ser: serrate; Ubx: ultrabithorax, abd-A: abdominal A, Abd-B: abdominal B. Modified illustration of an image by Lappin, T.R.J; Grier, D.G.; Thompson, A., Halliday, H.L.; HOX genes: seductive science, mysterious mechanisms; 2006 (Lappin *et al.* 2006).

HOX genes are relatively small genes from less than 200 bases to several kilobases. They only consist of two exons and one intron. The second exon always contains the characteristic homeobox, a 180 base pair DNA sequence which encodes the homeodomain (Gehring *et al.* 1994; Gehring & Hiromi 1986). The homeodomain is an evolutionary highly conserved helix-turn-helix motif of 60 amino acids (aa) that binds DNA sequence-specific. It forms three alpha helices and one unstructured N-terminal arm, whereby the third alpha helix contacts the major groove of DNA and the N-terminal arm strengthens the binding (Bürglin & Affolter 2016; Gehring *et al.* 1994). Several cofactors, such as members of the TALE (three amino acid loop extension) family, are known to play an important role to recognize the DNA-binding site and to stabilize the binding (Mann *et al.* 2009). The protein products of *HOX* genes, homeodomain proteins, work as DNA-binding transcription factors that can either repress or activate their target genes involved in cell adhesion, cell migration, proliferation and differentiation (Mann *et al.* 2009; Pearson *et al.* 2005).

HOX genes are key regulators of embryonic development. They determine the anterior-posterior body axis and are therefore essential genes for forming the axial skeleton. During development, *HOX* genes are activated in a highly-coordinated order. The spatial and temporal sequence of transcriptional activation corresponds to the position on the chromosome. Genes at the 3' end like paralog group 1 genes are transcribed earlier and in more anterior regions of the embryo than genes at the 5' end of the cluster like paralog group 13 members (Kmita & Duboule 2003; Krumlauf 1994; McGinnis & Krumlauf 1992; Wellik 2007). *In vivo* studies in mice demonstrated, for example, that disruption of HOXD3 resulted in defects of the first two cervical vertebrae while loss of function of HOXD11 induced sacral region deformities (Condie & Capecchi 1993; Davis & Capecchi 1994). This sequential activation of *HOX* genes from 3′ to 5′ is the so-called principle of collinearity (Kmita & Duboule 2003; Pineault & Wellik 2014; Seifert *et al.* 2015). To prevent premature transcriptional activation the expression of *HOX* genes is under epigenetic control. Epigenetic mechanisms can either activate or repress transcriptional activity of *HOX* genes corresponding to the temporal sequence (Beh *et al.* 2016; Rinn *et al.* 2007). For instance, *in vivo* studies showed that transcriptional activation of *HOX* genes in embryonic stem cells was clearly determined by the distribution of H3K27m3 (trimethylation at lysin 27 of histone 3) and H3K4m3 (trimethylation at lysin 4 of histone 3). H3K27m3 was necessary to maintain the inactive, silenced status of *HOX* genes to inhibit early activation, while high levels of H3K4m3 were associated with the beginning of transcriptional activity (Soshnikova & Duboule 2009). Furthermore, other mechanisms including changes of the chromatin structure and regulatory elements are involved in regulating *HOX* gene expression. To the present day, these complex interactions remain a current research topic (Montavon & Soshnikova 2014; Srivastava *et al.* 2015).

In addition to their popular function in determining the anterior-posterior body axis, posterior *HOX* genes (*HOX9 - HOX13*) pattern the limb skeleton along the proximo-distal axis in vertebrates. Similar to the axial skeleton, collinearity is given here, too. Mutations of paralog group 9 and 10 genes mainly affect the stylopod. The zeugopod can be malformed by defects of paralog group 11 genes, whereas the autopod can be affected by paralog group 13 mutations (Pineault & Wellik 2014).

Besides their function in body patterning, *HOX* genes fulfill manifold additional tasks during embryogenesis. They are involved in the development of various other body tissues and partially continue to be expressed in postnatal life. *HOX* genes are known to play a crucial role in the differentiation of stem cells towards their respective lineages (Seifert *et al.* 2015).

Inter alia, they contribute to lung morphogenesis (Kim & Nielsen 2000; Mollard & Dziadek 1997), neuronal development (Philippidou & Dasen 2013; Wang *et al.* 2013), adipogenesis (Cowherd *et al.* 1997; Procino & Cillo 2013), angiogenesis (Gorski & Walsh 2000; Kachgal *et al.* 2012) and hematopoiesis (Alharbi *et al.* 2013; Fröhling *et al.* 2007). But also postnatal, *HOX* genes, highly expressed in connective tissue, are known to have certain functions. For instance, some *HOX* genes were shown to be reactivated during bone regeneration after fracture and contribute to fracture healing by initiating differentiation of MSC to chondrocytes and osteoblasts (Bais *et al.* 2009; Gersch *et al.* 2005; Rux & Wellik 2016). Furthermore, several *HOX* genes participate in wound healing via induction of angiogenesis (Kachgal *et al.* 2012; Rux & Wellik 2016). In contrast to these useful properties *HOX* genes are also involved in the development of many congenital and acquired diseases, like congenital malformations, endocrinopathies, metabolic diseases, and in particular cancer (Abate-Shen 2002; Boncinelli 1997; Daftary & Taylor 2006; Mann *et al.* 2009; Procino & Cillo 2013; Quinonez & Innis 2014).

As already stated, *HOX* genes strongly affect cell proliferation, differentiation, apoptosis and angiogenesis providing a rationale for their involvement in cancer development. Indeed, deregulated *HOX* gene expression is evident in different types of cancer, but both carcinogenesis and tumor suppression can be associated with altered *HOX* gene expression (Abate-Shen 2002; Shah & Sukumar 2010). In most cases, *HOX* genes that are usually expressed during embryonic development, but not in adult age, are re-expressed in the respective malignant cells (Abate-Shen 2002; Grier *et al.* 2005). Altered HOX levels can be found in various solid tumors, such as in gynecological and gastrointestinal tumors, lung and prostate cancer, neuroblastoma or leukemia (Cheng *et al.* 2005; Horton *et al.* 2005; Pilato *et al.* 2013; Taketani *et al.* 2002; Truong *et al.* 2012; Vardhini *et al.* 2014; Yang *et al.* 2015; Zha *et al.* 2012; Zhang *et al.* 2015; Zhang *et al.* 2003). Additionally, aberrant *HOX* gene expression is present in ES cells and could contribute to ES genesis. As particularly *HOXD10*, *HOXD11* and *HOXD13* are over-expressed in ES (Burdach *et al.* 2009), this study focusses on their contribution to ES pathogenesis. In the following, a short summary of the current knowledge on these genes and their protein products including their structure, function and involvement in carcinogenesis will be given.

1.2.2 Current knowledge on HOXD10

All *HOXD* genes are located on chromosome 2q31.1. The 3.18 kb (2 exons) long *homeobox D10* gene (*HOXD10*, formerly known as *HOX4D, HOX4E, HOX4*) encodes a 340 aa protein with a molecular mass of 38.4 kDa (Redline *et al.* 1992). Like all posterior *HOX* genes, the gene *HOXD10* is involved in limb development. Mutations of HOXD10 are associated with midfoot malformations like congenital vertical talus and Charcot-Marie-Tooth disease (Dobbs *et al.* 2006; Shrimpton *et al.* 2004). In addition, HOXD10 plays an important role in the development of the lumbar spinal cord by regulating the motoneuron patterning (Choe *et al.* 2006; Hedlund *et al.* 2004; Lance-Jones *et al.* 2001; Lin & Carpenter 2003). In postnatal life, it is predominantly expressed in the female reproductive tract, particularly in the endometrium (Hu *et al.* 2004; Osborne *et al.* 1998; Xu *et al.* 2014). In keeping with that, mis-expression of HOXD10 can be found in gynecological tumors like breast cancer, ovarian cancer and endometrial adenocarcinoma (Nakayama *et al.* 2013; Osborne *et al.* 1998; Vardhini *et al.* 2014). Interestingly, HOXD10 seems to have tumor suppressive properties here. Studies demonstrated that HOXD10 appears to maintain the differentiated state of breast and endometrial cells (Carrio *et al.* 2005). Furthermore, down-regulated HOXD10 expression levels were associated with high-grade breast cancer, whereas normal HOXD10 expression impaired the tumor growth of breast cancer cells *in vivo* (Carrio *et al.* 2005; Vardhini *et al.* 2014). Similar tumor suppressive characteristics were also detected in gastric cancer and cholangiocellular carcinoma. In contrast, HOXD10 is up-regulated in colorectal cancer and could thereby participate in oncogenesis (Abdelmaksoud-Dammak *et al.* 2017; Joo *et al.* 2016; Wang *et al.* 2012; Yang *et al.* 2015).

1.2.3 Current knowledge on HOXD11

The *Homeobox D11* gene (*HOXD11*, previously known as *HOX4F, HOX4*), also located on chromosome 2q31.1, comprises 2.23 kb (2 exons). The 228 aa protein product has a molecular mass of 35.1 kDa (Boulet & Capecchi 2002). During embryogenesis, HOXD11 is important for the correct growth of radius and ulna. *In vivo* studies revealed that disruptions of HOXD11 lead to zeugopod alterations like distal growth plate anomalies, insufficient chondrocyte differentiation and shortened final length of radius and ulna (Boulet & Capecchi 2004; Davis & Capecchi 1994; Gross *et al.* 2012; Pineault *et al.* 2015). But also malformations of metacarpals and phalanges as well as transformations of the lumbar and sacral vertebrae are associated with HOXD11 mutations (Davis *et al.* 1995). Similar to

HOXD10, HOXD11 seems to participate in motoneuron patterning of the caudal spinal cord (Misra *et al.* 2009). Furthermore, proper HOXD11 expression in conjunction with adequate HOXA11 expression is required for correct metanephric kidney development (Mugford *et al.* 2008; Schwab *et al.* 2006). In oncology, an involvement of HOXD11 can be found in hematologic malignancies like acute myeloid leukemia where it forms a fusion gene with NUP98 (nucleoporin 98), and thus contributes to leukemogenesis (Taketani *et al.* 2002; Terui *et al.* 2003). Moreover, altered HOXD11 levels were detected in prostate cancer, laryngeal squamous cell carcinoma, ovarian cancer and head and neck squamous cell carcinoma. Depending on the cancer type, HOXD11 alterations have differential impact, but HOXD11 over-expression usually has a carcinogenic effect (de Barros E Lima Bueno, R. *et al.* 2016; Cai *et al.* 2007; Hayano *et al.* 2016; Sharpe *et al.* 2014).

1.2.4 Current knowledge on HOXD13

Homeobox D13 (*HOXD13*, formerly known as *HOX4I*, *SPD*) is a gene of 3.13 kb (2 exons). It encodes a protein of 343 aa with a molecular mass of 36.1 kDa (Akarsu *et al.* 1996). Correct HOXD13 expression is essential to avoid congenital limb malformations. There are several innate disorders associated with HOXD13 mutations that mainly affect the development of hand and foot bones and joints. A polyalanine expansion in exon 1 of the *HOXD13* gene causes synpolydactyly type II, a combination of soft-tissue syndactyly between the third and fourth digit or the fourth and fifth toe with digit duplication of the same dactyls (Bruneau *et al.* 2001; Goodman & Scambler 2001; Sarfarazi *et al.* 1995; Sayli *et al.* 1995). *In vivo* studies further proved that additional alanines in the poyalanine repeat of *HOXD13* lead to disturbed ossification, impaired development of perichondrial cells and a homeotic transformation from metacarpals into bones similar to carpal bones (Kuss *et al.* 2014; Villavicencio-Lorini *et al.* 2010). Other rarer congenital anomalies related to mutations of *HOXD13* are brachydactyly type D (shortened and broadened distal phalanx of the thumb), brachydactyly type E (shortened metacarpals / metatarsals) and synpolydactyly type V (metacarpal / metatarsal synostosis), caused by missense mutations (Johnson *et al.* 2003; Quinonez & Innis 2014; Zhao *et al.* 2007). Furthermore, HOXD13 is involved in the development of the urogenital tract, especially in the development of the male accessory sex glands with sustained expression in the adult prostate gland (Akarsu *et al.* 1996; Huang *et al.* 2007; Podlasek *et al.* 1997; Warot *et al.* 1997). Though, deregulated HOXD13 expression was demonstrated in various malignancies such as in gynecological, urological

and gastrointestinal tumors, hematologic neoplasms and others. In most tumor tissues increased HOXD13 expression was detected, suggesting an involvement in carcinogenesis (Cantile *et al.* 2009). In contrast, some gastrointestinal tumors like pancreatic and gastric cancer exhibit reduced HOXD13 levels. In pancreatic cancer HOXD13 could even act as tumor suppressor, since low expression was associated with poorer prognosis (Cantile *et al.* 2009).

Summarizing, posterior *HOXD* genes, the major regulators of limb development, have distinct functions in oncogenesis depending on the tumor type. Although they can act tumor-suppressive in some cases, they seem to have a crucial part in the malignant cell transformation in most forms of cancer. However, their contribution to the malignancy of ES is still unknown to a large extent. Therefore, this issue appeared to be an interesting and promising field of research.

1.3 Aim of this study and overview of the experimental approach

This doctoral thesis includes experiments with the aim to elucidate the involvement of the over-expressed posterior *HOXD* genes, *HOXD10*, *HOXD11* and *HOXD13*, in the malignancy and the phenotype of ES. Initially, it was examined if the typical ES fusion protein EWS-FLI1 and two other key regulators of ES, EZH2 and DKK2, regulate the expression of posterior *HOXD* genes. For this purpose, EWS-FLI1, EZH2 and DKK2 were knocked down in two ES cell lines (A673 and SK-N-MC) via RNA interference. The effect on posterior HOXD expression was analyzed by qRT-PCR. As a basis for all subsequent experiments, HOXD10, HOXD11 and HOXD13 were down-regulated in A673 and SK-N-MC cells via constitutive and transient RNA interference. A673 and SK-N-MC cells with posterior HOXD knock down were used for various *in vitro* and *in vivo* experiments. Each time, the results of posterior HOXD knock down cells were compared to those of respective control cells with normal HOXD expression. As NSCS are putative cells of origin of ES, it was initially investigated whether posterior *HOXD* genes may affect the neuronal differentiation capacity of ES cells and could thereby contribute to the undifferentiated phenotype of ES. Subsequent assays focused on the question whether and how posterior *HOXD* genes affect the osteotropism and osteolytic tumor growth of ES. Herein, the influence of HOXD knock down on bone-associated genes was examined using qRT-PCR in order to find possible downstream target genes. Thereupon, an orthotopic xeno-transplantation model was used to explore the impact of HOXD down-regulation on

colonization, invasion into bone / bone marrow and osteolysis. Ensuing experiments focused on the effect posterior *HOXD* genes have on tumor growth and invasiveness of ES. For this purpose, their influence on proliferation, colony formation and invasiveness was investigated *in vitro*. It was further examined if posterior *HOXD* genes could mediate their invasive effect via matrix metallopeptidases. Finally, a xeno-transplantation model with intravenous injection of HOXD knock down cells was performed to investigate whether posterior *HOXD* genes influence the metastatic spread of ES.

In summary, this study shall illuminate the consequences of the over-expression of HOXD10, HOXD11 and HOXD13 on the malignant phenotype of ES. It should increase the knowledge about the pathogenesis of ES and particularly help to understand the role of posterior *HOXD* genes in this malignancy. This work could further offer new basic knowledge which may help to develop future target-orientated therapeutic strategies.

2. Material

2.1 List of manufacturers

Manufacturers	Locations
Abbott	Wiesbaden, Germany
ACEA Biosciences	San Diego, USA
Ambion	Austin, TX, USA
Applied Biosystems	Darmstadt, Germany
ATCC	Rockyville, MD, USA
B. Braun Biotech Int.	Melsungen, Germany
BD Biosciences Europe	Heidelberg, Germany
Becton Dickinson (BD)	Heidelberg, Germany
Berthold detection systems	Pforzheim, Germany
Biochrom	Berlin, Germany
BioRad	Richmond, CA, USA
Biozym	Hess. Olendorf, Germany
Brand	Wertheim, Germany
Calbiochem	Darmstadt, Germany
DSMZ	Braunschweig, Germany
Eppendorf	Hamburg, Germany
Eurofins MWG GmbH	Ebersberg, Germany
Falcon	Oxnard, CA, USA
Feather	Osaka, Japan
Fermentas	St. Leon-Rot, Germany
Genzyme	Neu-Isenburg, Germany
GLW	Würzburg, Germany
Greiner Bio one	Nürtingen, Germany
Hamilton	Bonaduz, Switzerland
Heidolph Instruments	Schwabach, Germany
Heraeus	Hanau, Germany
Implen	München, Germany
Invitrogen	Karlsruhe, Germany

Jackson ImmunoResearch Laboratories	Baltimore, MD, USA
Kern	Balingen-Frommern, Germany
Köttermann	Uetze/Hänigsen
Leica	Wetzlar, Germany
LMS	Brigachtal, Germany
Lonza	Basel, Switzerland
Memmert	Schwabach, Germany
Merck	Darmstadt, Germany
Metabion	Martinsried, Germany
Millipore	Billerica, MA, USA
Molecular BioProducts, MbP	San Diego, CA, USA
Nalgene	Rochester, NY, USA
Nunc	Naperville, IL, USA
Qiagen	Chatsworth, CA, USA
R&D Systems	Minneapolis, MN, USA
Ratiopharm	Ulm, Germany
Roche	Mannheim, Germany
Roche/ACEA Biosciences	San Diego, CA, USA
Scientific Industries	Bohemia, NY, USA
Scotsman	Milan, Italy
Sempermed	Wien, Austria
Sigma	St. Louis, MO, USA
Siemens	München, Germany
Sony	Berlin, Germany
Systec	Wettenberg, Germany
Taylor-Wharton	Husum, Germany
Techlab	Braunschweig, Germany
TKA GmbH	Niederelbert, Germany
TPP	Trasadingen, Switzerland
Thermo Fisher Scientific	Ulm, Germany
Thermo Scientific	Braunschweig, Germany
Zeiss	Jena, Germany

2.2 General material

Materials	Manufacturers
Cryovials	Nunc
Culture dishes (Nunclon™ surface 100 mm)	Nunc
E-plates (96-well)	Roche
Flasks for cell culture (25 cm^2, 75 cm^2 and 175 cm^2)	TPP
Flasks for cell culture (75 cm^2 and 175 cm^2)	Falcon
Gloves (nitrile, latex)	Sempermed
Hypodermic needle (23 G, 30 G)	B. Braun
Petri dishes	Falcon
Pipettes (2, 5, 10 and 25 ml)	Falcon
Pipette tips (10, 200 and 1000 µl)	Thermo Scientific
Pipette tips (10, 200 and 1000 µl with a filter)	Biozym
Plates for cell culture (6-well, 24-well and 96-well)	TPP
Plates for invasion-assay (24-well)	Becton Dickinson
Plates for qRT-PCR (96-well)	Applied Biosystems
Scalpels (Nr. 12, 15, 20)	Feather
Syringes (27 G x 318'', 0.45 mm x 10 mm)	BD Biosciences
Syringes (Hamilton 100 µl, 250 µl)	Techlab
Syringes (Omnifix-F, 9161406V)	B. Braun
Tubes for cell culture (polypropylene, 15 ml and 50 ml)	Falcon
Tubes for molecular biology, Safelock (1.5 ml and 2 ml)	Eppendorf

2.3 Instruments and equipment

Type of device		Manufacturer
Airflow		Köttermann
Autoclave	2540EL	Systec
Autoclave	V95	Systec
Camera	DSC-W150	Sony
Centrifuge	Multifuge 3 S-R	Heraeus
Centrifuge	Biofuge pico	Heraeus
Controlled-freezing box		Nalgene
Drying cabinet		Memmert
Freezer (-80 °C)	Hera freeze	Heraeus
Freezer (-20 °C)	Cool vario	Siemens
Fridge (+4 °C)	Cool vario	Siemens
Ice machine	AF 100	Scotsman
Incubator	BBD 6220	Heraeus
Incubator	Hera cell 150	Heraeus
Liquid Nitrogen Tank	L-240 K series	Taylor-Wharton
Luminometer	Sirius Luminometer	Berthold detection systems
Multichannel pipette	(10-100 µl)	Eppendorf
Hemocytometer	Neubauer	Brand
Microliter syringe	710NR	Hamilton
Micropipettes	(0.5-10 µl, 10-100 µl, 20-200 µl, 100-1000 µl)	Eppendorf
Microscope (fluorescence)	AxioVert 100	Zeiss
Microscope	DMIL	Leica
Mini centrifuge	MCF-2360	LMS
PCR cycler	iCycler	BioRad
PCR cycler	Mastercycler ep gradient	Eppendorf
Pipetting assistant	Easypet	Eppendorf
qRT- PCR cycler	7300 Real-Time PCR	Applied Biosystems
qRT- PCR cycler	StepOnePlus Real-Time PCR	Applied Biosystems
Rotator		GLW

Scales	770	Kern
Scales	EW3000-2M	Kern
Shaker	Polymax 2040	Heidolph Instruments
Spectrophotometer		Implen
Sterile Bench	40498435	Heraeus
Sterile Bench	40492110	Heraeus
Vortexer	Vortex-Genie 2	Scientific Industries
Water bath		GFL
Water purification system	TKA GenPure	TKA GmbH
xCELLigence	RTCA XC - SP, W380	ACEA Biosciences

2.4 Chemical and biological reagents

Reagents	**Manufacturer**
BCP (1-bromo-3-chloropropane)	Sigma
BHA (butylated hydroxyanisole)	Sigma
Calcein AM	Merck
DEPC (diethyl pyrocarbonate)	Sigma
dNTPs	Roche
DMEM medium	Invitrogen
DMSO (dimethyl sulfoxide)	Merck
Ethanol	Merck
FBS (fetal bovine serum)	Biochrom
37 % Formaldehyde	Merck
Gentamycin	Biochrom
HBSS (Hank's buffered salt solution)	Invitrogen
HiPerFect Transfection Reagent	Qiagen
Human IgG	Genzyme
Isoflurane	Abbott
Isopropanol	Sigma
L- glutamine	Invitrogen
Matrigel matrix	BD Biosciences

Maxima™ Probe / ROX qPCR Master Mix (2 x)	Fermentas
Methylcellulose	R&D Systems
Na_2HPO_4 (sodium phosphate dibasic)	Merck
NaH_2PO_4 (sodium phosphate monobasic)	Merck
NaN_3 (sodium azide)	Merck
Novaminsulfon	Ratiopharm
PBS 10 x (phosphate buffered saline)	Invitrogen
PCR Buffer (10 x)	Invitrogen
Penicillin / streptomycin	Invitrogen
PFA (paraformaldehyde)	Merck
Puromycin	PAA
RPMI 1640 medium	Invitrogen
Triton X-100	Sigma
Trypan blue	Sigma
Trypsin / EDTA	Invitrogen

2.5 Commercial reagent kits

Name	Manufacturer
Cell Invasion Assay	BD Biosciences
High-Capacity cDNA Reverse Transcription Kit	Applied Biosystems
Human Methylcellulose Base Media	R&D Systems
MycoAlert Mycoplasma Detection Kit	Lonza
TRI Reagent RNA Isolation Kit	Ambion
TaqMan® Gene Expression Assays	Applied Biosystems

2.6 Media and solutions

Table 1: Cell culture media and universal solutions

Name	Ingredients
Standard tumor medium	500 ml RPMI 1640, 10 % FBS, 2 mM L-glutamine, 100 µg/ml gentamycin
Freezing medium	45 ml FBS, 10 % DMSO
1×PBS	900 ml sterile water, 100 ml 10 × PBS
1×Trypsin/ EDTA	45 ml 1 × PBS, 5 ml 10 × Trypsin/ EDTA
4 % formaldehyde	4 % Formalin, 55 mM Na_2HPO_4, 12 mM NaH_2PO_4, 2 H_2O
4 % paraformaldehyde	4 % PFA in 1 x PBS, adjusted to pH 7.4 with NaOH
Immunofluorescence staining buffer	49 ml 1 × PBS, 2 % FBS, 0,05 % NaN_3

Table 2: Media for neuronal differentiation assay

Name	Ingredients
Neuronal differentiation medium	50 ml DMEM, 2 % DMSO, 0.2 mM BHA, 100 µg/ml gentamycin
Control medium	50 ml DMEM, 0.2 mM ethanol, 100 µg/ml gentamycin

2.7 Antibodies for immunofluorescence

Table 3: Antibodies for immunofluorescence

Antibody	Source	Dilution	Product No.	Manufacturer
anti-GFAP	mouse	1:100	556330	BD Biosciences
anti-mouse IgG+IgM F(ab`)$_2$-FITC	goat	1:100	115-096-068	Jackson ImmunoResearch

2.8 Small interfering RNAs

Small interfering RNAs (siRNAs) were obtained from Qiagen, except EWS-FLI1_1 and EWS-FLI1_2 siRNAs (Dohjima *et al.* 2003), which were synthesized by Eurofins MWG GmbH.

Table 4: Small interfering RNA used for transient transfection

siRNA Name	Target Sequence (5'-3')
Control (non-silencing) siRNA	5´-AAT TCT CCG AAC GTG TCA CGT- 3`
EWS-FLI1_1 siRNA	5´-GCT ACG GGC AGC AGA ACC CTT- 3`
EWS-FLI1_2 siRNA	5´-GCA GAA CCC TTC TTA TGA CTT- 3`
EZH2_2 siRNA	5´-AAG CAA ATT CTC GGT GTC AAA- 3`
EZH2_val siRNA	5´-AAC CAT GTT TAC AAC TAT CAA- 3`
HOXD10_1 siRNA	5´-CAG GGT AAC TAT TAT TGC GCA- 3`
HOXD10_4 siRNA	5´-CTC CTT CAC CAC CAA CAT TAA- 3`
HOXD10_5 siRNA	5´-CCG AAC AGA TCT TGT CGA ATA- 3`
HOXD11_3 siRNA	5´-CCC GTC TGA STT CGC TAG CAA- 3`
HOXD11_5 siRNA	5´-CTC AAC CTC ACT GAC CGG CAA- 3`
HOXD11_6 siRNA	5´-TTG GCC GAG CGG ATC CTA ATA- 3`
HOXD13_1 siRNA	5´-AAG AGA GTG CCT TAC ACC AAA- 3`
HOXD13_2 siRNA	5´-ACG AAC CTA TCT GAG AGA CAA- 3`
HOXD13_3 siRNA	5´-GCC AGT ATA AAG GGA CTT GAA- 3`

2.9 Oligonucleotides for retroviral gene transfer

All oligonucleotides were obtained from Metabion International AG.

Table 5: Oligonucleotides used for retroviral gene transfer

Name	Sequence (5'3')
HOXD10 sense	5´-GAT CCG GGG TAA CTA TTA TTG CGC ATT CAA GAG ATG CGC AAT AAT AGT TAC CCC TTT TTT CTA GAG- 3`
HOXD10 antisense	5´-AAT TCT CTA GAA AAA AGG GGT AAC TAT TAT TGC GCA TCT CTT GAA TGC GCA ATA ATA GTT ACC CCG- 3`
HOXD11 sense	5´-GAT CCG CGT CTG ACT TCG CTA GCA ATT CAA GAG ATTGCT AGC GAA GTC AGA CGC TTT TTT CTA GAG- 3`

HOXD11 antisense	5´-GAT CCG CGT CTG ACT TCG CTA GCA ATT CAA GAG ATTGCT AGC GAA GTC AGA CGC TTT TTT CTA GAG- 3`
HOXD13 sense	5´-GAT CCG GAA CCT ATC TGA GAG ACA ATT CAA GAG ATTGTC TCT CAG ATA GGT TCC TTT TTT CTA GAG- 3`
HOXD13 antisense	5´-AAT TCT CTA GAA AAA AGG AAC CTA TCT GAG AGA CAA TCT CTT GAA TTG TCT CTC AGA TAG GTT CCG- 3`
DKK2 sense	5´-GAT CCG GGG ATT TGC TAT CAT AAT ATT CAA GAG ATA TTA TGA TAG CAA ATC CCC TTT TTT CTA GAG- 3`
DKK2 antisense	5´-AAT TCT CTA GAA AAA AGG GGA TTT GCT ATC ATA ATA TCT CTT GAA TAT TAT GAT AGC AAA TCC CCG- 3`
Negativ control sense	5´-GAT CCG TTC TCC GAA CGT GTC ACG TTT CAA GAG AACGTG ACA CGT TCG GAG AAC TTT TTT CTA GAG- 3`
Negativ control antisense	5´-AAT TCT CTA GAA AAA AGT TCT CCG AAC GTG TCA CGT TCT CTT GAA ACG TGA CAC GTT CGG AGA ACG- 3`

2.10 Primers for PCR and qRT-PCR

The concentration of primers was 900 and 250 nM, respectively.

Table 6: Primers for PCR and qRT-PCR

Name	Sequence (5'-3')
EWS-FLI1 for	5'-TAG TTA CCC ACC CAA ACT GGA T-3'
EWS-FLI1 rev	5'-GGG CCG TTG CTC TGT ATT CTT AC-3'
pSIREN for	5`-GGG CAG GAA GAG GGC CTA T-3`
pSIREN rev	5`-GAG ACG TGC TAC TTC CAT TTG TC-3`

2.11 Gene expression assays for qRT-PCR

All TaqMan Gene Expression Assays were obtained from Applied Biosystems.

Table 7: TaqMan Gene Expression Assays

Gene	Assay ID
CXCR4	Hs00237052_m1
DKK2	Hs00205294_m1
EZH2	Hs00544830_m1
FLT1	Hs00176573_m1
GAPDH	Hs02758991_g1

GAP43	Hs00176645_m1
GFAP	Hs00157674_m1
HOXD10	Hs00157974_m1
HOXD11	Hs00360798_m1
HOXD13	Hs00968515_m1
HIF1A	Hs00153153_m1
IFITM1	Hs01652522_g1
IL6	Hs00985639_m1
ISG15	Hs00192713_m1
ITM2A	Hs04176575_m1
JAG1	Hs01070032_m1
MMP1	Hs00899658_m1
MMP7	Hs01042796_m1
MMP9	Hs00234579_m1
MMP14	Hs00237119_m1
NGFR	Hs00609977_m1
PTHLH	Hs00174969_m1
RUNX2	Hs00231692_m1
SLIT2	Hs00191193_m1
TGFB1	Hs00998133_m1

2.12 Human cell lines and mouse strain

2.12.1 Human cell lines

Table 8: Description of utilized human cell lines

Cell line	Description
A673	ES cell line with type 1 translocation (t (11;22)(q24;q12)), typical EWS-FLI1 fusion gene, p53 mutation, established from the primary tumor of a 15-year old girl with Ewing Sarcoma (Giard *et al.* 1973), purchased from ATCC
SK-N-MC	ES cell line with type 1 translocation, established from metastasis from the supra orbital area of a 14- year old girl with Askin`s tumor (related to ES) (Dunn *et al.* 1994), purchased from the German Collection of Microorganisms and Cell Cultures (DSMZ)

2.12.2 Mouse strain

Table 9: Description of utilized mouse strain

Mouse strain	Characteristics	Origin
BALB/c $Rag2^{-/-}\gamma c^{-/-}$	Absence of all T-lymphocyte, B-lymphocyte and NK cell function	Central Institute for Experimental Animals (Kawasaki, Japan)

The *Recombination activating gene 2* (Rag2)-*gamma(c)* knock out ($Rag2^{-/-}\gamma c^{-/-}$) mouse is a gene mutated mouse strain with severe immunodeficiency by absence of all T- and B-lymphocyte and natural killer (NK) cell function. Thus, it is a suitable model for *in vivo* studies which is utilized in vaccine development, research on organ transplantation or in cancer research. It was developed by back-crossing of two immuno-compromised mouse models, the *gamma(c)* knock out and the *Rag2* knock out mice. Homozygous *gamma(c)* knock out mice have a deficiency of the *gamma(c)* receptor gene which is essential for the development of lymphocytes and NK cells. NK cells are substantially depleted, whereas a small number of B- and T- lymphocytes persists. For this reason, the *gamma(c)* knock out mouse was back-crossed onto the *Rag2* knock out mouse. Homozygous *Rag2* knock out mice lack several exons of the *Rag2* gene. This gene defect results in an inability to initiate V(D)J rearrangement, an essential step to generate mature, functional B- and T-lymphocytes. Thus, $Rag2^{-/-}\gamma c^{-/-}$ exhibit a lack of all T- and B-lymphocyte and NK cell functions (Goldman *et al.* 1998).

3. Methods

3.1 Cell culture

ES cell lines A673 and SK-N-MC were cultured in standard tumor medium (see Table 1) at 37 °C in 5 % CO_2 in a humidified atmosphere. Cell lines were grown in middle-sized culture flasks (75 cm^2 adherence surface) filled with 20 ml medium or in large-sized flasks (175 cm^2 adherence surface) filled with 30 ml medium depending on the number of cells needed for the experiments. When cells grew to confluence (every 3 - 4 days) the medium was removed and cells were split 1:2 to 1:10. To detach the cells they were washed once with 1 x PBS and incubated 5 min with 2 - 3 ml 1 x trypsin at 37 °C (5 % CO_2). Detached cells were re-suspended in 5 ml fresh standard tumor medium, converted in a 15 ml tube, centrifuged at 1200 rpm for 7 min and filled in new culture flasks with pre-warmed standard tumor medium.

For storage the cells were re-suspended at a concentration of 1 - 2 x 10^6 per ml freezing medium (see Table 1) and 1 ml aliquots of the cell suspension were transferred into cryovials. The cryovials were put in controlled freezing boxes for 12 - 18 h in order to gradually reach a temperature of -80 °C. Then, they were stored in the -80 °C freezer. To re-culture cryopreserved cells, the cryovials thawed at room temperature (RT) until the content began to defrost. The content was then transferred into a 50 ml Falcon tube with 10 ml of fresh standard medium and centrifuged at 1200 rpm for 7 min. Afterwards, the cell pellet was re-suspended in 20 ml pre-warmed fresh standard tumor medium. The cell suspension was transferred into a middle-sized culture flask and stored in an incubator at 37 °C (5 % CO_2) in a humidified atmosphere.

The number of cells was counted with a Neubauer hemocytometer. The cell viability was evaluated by the trypan blue (Sigma) exclusion method.

Mycoplasma contamination was checked every 6 - 8 weeks for cells cultivated in flasks and always after thawing of cryopreserved cells using MycoAlertTM Mycoplasma Detection Kit according to the manufacturer's instructions (Lonza).

3.2 RNA isolation

For gene expression analyses, RNA of cultivated cells had to be isolated. Therefore, TRI Reagent RNA Isolation Kit (Ambion Manual Version 0610) was used according to the

manufacturer's instructions. A cell pellet of approximately 1 × 10^6 - 10^7 cells was lysed in 1 ml TRI Reagent and homogenized with a micropipette (1000 µl). The homogenate incubated for 5 min at RT. Then, 100 µl BCP (1-bromo-3-chloropropane) per 1 ml TRI Reagent was added, the sample was vortexed for 20 s and incubated for 5 - 15 min at RT. Subsequently, the sample was centrifuged at 4000 rpm for 20 min at 4 °C. The content divided into three phases. The aqueous RNA phase on top was transferred into a new tube. Afterwards, RNA was precipitated by adding 500 µl isopropanol, vortexing for 10 s and incubating for 8 min on ice. Then, the sample was centrifuged at 4000 rpm for 12 min at 4 °C. To purify the RNA pellet from isopropanol the supernatant was discarded and the pellet was washed with 1 ml 75 % ethanol centrifuging at 4000 rpm for 8 min at 4 °C. The ethanol was removed, the pellet was air-dried for 5 min on ice and the isolated RNA was dissolved in 20 - 60 µl RNase-free water. The RNA concentration was determined photometrically at 260 nm. For later analyses RNA was stored in the - 80 °C freezer.

3.3 cDNA synthesis

To analyze gene expression via qRT-PCR, isolated RNA had to be reverse transcribed into complementary DNA (cDNA). Therefore, High-Capacity cDNA Reverse Transcription Kit was used according to the manufacturer's instructions (Applied Biosystems Insert P/N 4375222 REV B). The mastermix was prepared as follows:

Table 10: cDNA master mix

Component	Volume (µl)
10 × Reverse Transcriptase (RT) Buffer	2.0
10 × RT Random Primers	2.0
25 × dNTPs (100mM)	0.8
MultiScribe™ Reverse Transcriptase (RT)	1.0
RNAse free water	10
Total	15.8

Depending on the RNA concentration measured photometrically the appropriate volume of RNA solution (containing 1 µg purified RNA, usually 0,5 - 4 µl RNA solution) was added. To complete the volume of 20 µl for each tube, the residual volume was filled up with RNAse free water. cDNA was synthesized under the following thermal cycling conditions:

Table 11: Thermal cycling conditions

	Step 1	Step 2	Step 3	Step 4
Temperature	25 °C	37 °C	85 °C	4 °C
Time	10 min	120 min	5 min	∞

cDNA which was not used for gene expression analyses directly was stored at -20 °C.

3.4 Quantitative Real-Time PCR (qRT- PCR)

3.4.1 Standard qRT-PCR

To investigate differential gene expression on mRNA level, synthesized cDNA was quantified via qRT- PCR as the amount of cDNA corresponds to the amount of cellular mRNA (messenger RNA). qRT- PCR was performed using Maxima™ Probe/ROX qPCR Master Mix (2x) (containing Hot Start Taq DNA Polymerase, PCR buffer and dNTPs) and specific TaqMan® Gene Expression Assays (Applied Biosystems, see Table 7) which consist of two unlabeled PCR primers and a FAM™ dye-labeled TaqMan® MGB probe. The reaction mix was prepared according to the manufacturer's instructions (Fermentas PureExtreme™ Insert):

Table 12: qRT-PCR reaction mix

Component	Volume (µl)
Maxima™ Probe/ ROX qPCR Master Mix (2x)	10.0
TaqMan® Gene Expression Assay	1.0
RNase-free water	8.5
cDNA	0.5
Total	20.0

The final concentration of primers and probe were 0.9 and 0.25 µM respectively. The assays were performed in duplicate in a 96-well plate. Before starting the qRT- PCR, the plate was centrifuged briefly. To review a possible contamination, a no template control (NTC) was made for every analyzed Gene Expression Assay. The gene expression profiles were normalized to the mRNA levels of the housekeeping gene *glyceraldehyde 3-phosphate dehydrogenase* (*GAPDH*). For the routinely performed posterior *HOXD* gene expression

analyses the AB 7300 Real-Time PCR system was used. For gene expression analyses of other genes the StepOnePlus Real-Time PCR system was used (both Applied Biosystems). The reason for using two systems was the high number of qRT- PCRs made in the laboratory, and thus limited availability, not functional differences. For both systems, the following cycler conditions were applied:

Table 13: Thermal cycler conditions for qRT-PCR systems

	Step 1	**Step 2**	**Step 3**	
Repetitions	1	1	40	
Temperature	50 °C	95 °C	95 °C	60 °C
Time	1 s	10 min	15 s	1 min

The calculation afterwards was made in Microsoft Excel using the 2^{-ddCt} method. The mean value and standard deviations of duplicates were displayed graphically, as well as standard error of the mean of at least two independent experiments. The t-test was used to check statistical significance.

3.4.2 Detection of EWS-FLI1

For the detection of EWS-FLI1, primers detecting EWS (sense) and FLI1 (antisense) were previously designed in the laboratory:

Table 14: Gene expression assay to detect *EWS-FLI1* mRNA by qRT-PCR

sense primer	5'-TAG TTA CCC ACC CAA ACT GGA T-3'
antisense primer	5'-GGG CCG TTG CTC TGT ATT CTT AC-3'
FAM probe	5'-FAM-CAG CTA CGG GCA GCA GAA CCC TTC TT-TAMRA -3'

The reaction mix for qRT-PCR was prepared as described in Table 15. Fluorescence was measured with the AB 7300 Real-Time PCR system. Gene expression profiles were normalized to *GAPDH* mRNA levels and calculated using the 2^{-ddCt} method.

Table 15: qRT-PCR reaction mix for detecting EWS-FLI1

Component	Volume (µl)
Maxima™ Probe/ ROX qPCR Master Mix (2x)	10.0
Primer detecting EWS (0.3 µM)	0.6
Primer detecting FLI1 (0.3 µM)	0.6
FAM probe (0.2 µM)	0.4
RNase-free water	7.6
cDNA	0.5

3.5 Transient RNA interference (RNAi)

Transient transfection was performed by use of small interfering RNA (siRNA, see Table 4) and HiPerFect Transfection Reagent in accordance with the standard procedures (Qiagen Handbook 05/2008) in order to induce transient protein knock down. As there were differences in the response to the treatment of A673 cells and SK-N-MC cells, different quantities of siRNA and transfection reagent were applied. In A673 cells, 2 x 10^6 cells were plated into 100 mm culture dishes with 10 ml standard tumor medium and incubated for 5 - 10 min at 37 °C (5 % CO_2). 3.6 µl siRNA (5 nM, see Table 4) and 36 µl transfection reagent were mixed together in 2 ml pure RPMI medium, vortexed briefly and incubated for 8 min at RT to build effective transfection complexes. Then, the mixture was cautiously dripped on the cells in the culture dishes. After incubation for 48 h at 37 °C (5 % CO_2) in a humidified atmosphere, RNA was isolated (see 3.2.) and reverse transcribed into cDNA (see 3.3.). mRNA levels of transient knock down cells were analyzed by qRT-PCR and compared to mRNA levels of cells transfected with control siRNA (si.control) (see 3.4.). For the transient transfection of SK-N-MC cells, 5 µl siRNA (5 nM) and 36 µl transfection reagent were used. Apart from that, the procedure was the same. Triple HOXD knock down was performed analogically, but the triple amount of siRNA (3.6 µl of each kind of siRNA for A673/ 5 µl of each kind of siRNA for SK-N-MC) and 50 µl transfection reagent were applied. To exclude unspecific suppression of the examined gene, at least two different types of siRNA were analyzed for each gene (see Table 4). To make sure that there is no induction of an interferon (IFN) response, mRNA levels of the two IFN responsive genes *ubiquitin-like modifier ISG15* (*ISG15)* and *interferon induced transmembrane protein 1* (*IFITM1)* were measured (see Table 7). If the specific siRNA induced the mRNA expression of *ISG15* or

IFITM1 more than twofold, the respective siRNA was no longer used for transient RNA interference.

3.6 Retrovirus-mediated stable RNA interference

Stably transfected ES cell lines with constitutive protein knock down were required for many experiments. These cell lines had previously been produced at the laboratory by retroviral gene transfer (see doctoral thesis of M. Ertl). To select successfully transfected cells and preserve stable gene suppression, cells were treated with 2 - 10 µg/ml puromycin from 12 h to 5 days depending on the cell proliferation.

3.7 *In vitro* assays

3.7.1 xCELLigence proliferation assay

The cell proliferation was measured with an impedance-based instrument system according to the manufacturer's instructions (see product information, ACEA Biosciences: The xCELLigence Real-Time Cell Analysis (RTCA) assay principle 2017). In this method, cells are seeded on special 96-well E-plates containing gold sensor electrodes. Due to cell proliferation, the local ionic environment in the wells changes and the impedance of the electrodes increases. Thus, higher cell proliferation is associated with increase in electrode impedance. Cell index values like doubling time and slope are monitored by the system.

For the cell line A673, 1×10^4 cells suspended in 200 µl standard tumor medium were seeded into each well of the E-plate. Due to slower growth and proliferation of SK-N-MC cells, 2.5×10^7 SK-N-MC cells per well were seeded. To get a reliable result, a row of eight wells was filled with the same cell type. One row was filled with standard tumor medium as a no template control. The cells were allowed to grow in a humified atmosphere at 37 °C and 5 % CO_2. The assay ran for 168 h with a measurement interval of 4 h. The mean values and standard deviations were calculated by the RTCA Software.

3.7.2 Colony forming assay

The contact independent growth was analyzed by a methylcellulose-based colony forming assay (R&D Systems, Manual HSC002). It was performed according to the manufacturer's

instructions. This assay is based on the ability of cells to form colonies in a semi-solid medium in response to cytokine stimulation (see product information, Human Methylcellulose Base Media: R&D Systems). The number of colonies can be counted and compared.

1 x 10^4 cells were dissolved in 10 µl standard tumor medium and re-suspended in 300 µl cell re-suspension solution. This solution was transferred in 2 ml methylcellulose media and was vortexed vigorously. After a incubation time of 30 min at RT the air bubbles vanished and the mixture was pipetted into a 35 mm plate in duplicate. The assay was cultured for 10 - 14 days at 37 °C and 5 % CO_2 in a humidified atmosphere. For the evaluation newly formed colonies were photographed and counted using the image processing package Fiji.

3.7.3 Invasion assay

To examine the invasive potential, the BioCoat™ Angiogenesis System (BD Biosciences Manual SPC-354141-G rev 3.0) was used according to the manufacturer's instructions. This system contains a 24-well insert plate with a 3.0 micron pore size polyethylene terephthalate (PET) membrane that has been coated with BD Matrigel matrix. The Matrigel matrix forms a barrier for non-invasive cells, since it occludes the pores of the PET membrane. Cells with high invasive potential are able to detach themselves from and can migrate through the Matrigel matrix. The invading cells can be detected on the underside of the PET membrane by fluorescent staining (see product information). Thus, the different invasiveness of tumor cells can be compared.

The 24-well plate was removed from -20 °C storage and allowed to adjust to RT. Afterwards, the plate was re-hydrated by adding 500 µl pre-warmed pure RPMI medium per well and incubation for 1 h at 37 °C (5 % CO_2). Then, the medium was removed carefully and the insert wells were filled with 5 x 10^4 cells in 250 µl RPMI medium (without additives) in duplicate. 750 µl medium containing 10 % FBS were added to each of the bottom wells to promote invasiveness. The assay incubated for 48 h at 37 °C (5 % CO_2) in a humidified atmosphere. The cell invasion was measured by staining the invasive cells on the bottom of the membranes with Calcein AM solution and counting them. For this purpose, the insert plate was transferred into a second BD Falcon 24-well plate containing 4 µg/ml Calcein AM in 500 µl pre-warmed HBSS with 0.15 % DMSO per well and incubated for 90 min at 37 °C (5 % CO_2). To examine the result microscopically, the insert plate was again transferred

into another 24-well plate containing 500 µl pre-warmed 1 × PBS per well. The invasive cells were visualized by fluorescence microscopy using a Zeiss AxioVert 100 with attached AxioCam MRm and the visualizing program AxioVision Rel. 4.7 (Carl Zeiss). Then, they were photographed and counted by the use of the image processing package Fiji.

3.7.4 Neuronal differentiation assay

The ability of cells to differentiate into a neuronal phenotype was examined by treating them with neuronal differentiation medium (see Table 2) containing BHA (butylated hydroxyanisole), according to a protocol of Woodbury *et al*. and Safford *et al.* (Safford *et al.* 2002; Woodbury *et al.* 2000).

5 x 10^4 cells were seeded at a final volume of 3 ml DMEM medium with 10 % FBS and 100 µg/ml gentamycin into 6-well plates and incubated for 24 h at 37 °C (8 % CO_2) in a humidified atmosphere to grow to adherence. Then, cells were treated with neuronal differentiation medium for 6 days to induce neuronal differentiation. As negative control, the same number of cells was incubated in control medium without BHA (see Table 2) under equal conditions. After 6 days, cells that incubated in differentiation medium exhibited a neuronal phenotype. To verify this observation the differentiated cells were identified with immunofluorescence against glial fibrillary acid protein (GFAP). The immunofluorescence staining and measurement was performed as follows (Burdach *et al.* 2009; Richter *et al.* 2009): cells were fixed by adding 500 µl 4 % paraformaldehyde per well and shaking for 20 min at RT. Then, they were washed two times with 1 x PBS. To perforate cell membranes, cells incubated for 30 min with 500 µl 0.1 % Triton X-100 per well at RT. Two washing cycles with 1 × PBS followed. Afterwards, unspecific binding sites were blocked with 50 µg human IgG (500 µl of a 100 µg/ml stock solution) by incubating for 30 min. Then, cells were stained with a mixture of staining buffer (see Table 1), human IgG and the antibody anti-GFAP (see Table 3) in a ratio of 20:10:1 for 12 - 18 h at 4 °C. After three washing steps with 1 x PBS, samples were incubated with a mixture of staining buffer, human IgG and the adequate secondary antibody anti-mouse IgG+IgM F(ab`)$_2$-FITC (see Table 3) in a ratio of 100:50:1 for 2 - 3 h at RT in the dark. Then, cells were washed three times with 1 x PBS, dried and imaged by fluorescence microscopy using a Zeiss AxioVert 100 with attached AxioCam MRm and the visualizing program AxioVision Rel. 4.7 (Carl Zeiss). To illustrate diverse cell growth depending on the medium (control medium vs. differentiation medium), also bright field illumination pictures were taken.

For analyses of neuronal marker gene expression, RNA was isolated (see 3.2.) and cDNA was synthesized (see 3.3.). The genes of interest were *nerve growth factor receptor (NGFR)*, *slit guidance ligand 2 (SLIT2)* and *growth associated protein 43 (GAP43)* (see 4.4.), all involved in neurogenesis. Gene expression analyses were made using qRT-PCR (see 3.4.).

3.8 *In vivo* experiments

3.8.1 Investigation of local tumor growth

To examine colonization, invasion into bone tissue and osteolysis *in vivo,* A673 cells were detached with 2 - 3 ml 1 x trypsin, washed twice with 1 x PBS and counted with a Neubauer hemocytometer. 6 × 10^6 cells were re-suspended in a final volume of 0.4 ml 1× PBS (equivalent to 3 × 10^5 cells in 20 µl 1× PBS per injection). The immunodeficient Rag2$^{-/-}$γc$^{-/-}$ mice (see Table 9) were anesthetized with 500 mg/ml Novaminsulfon (Ratiopharm) and isoflurane (Abbott). A 30-gauge needle was introduced through the proximal tibia plateau and 3 x 10^5 A673 cells in a volume of 20 µl 1× PBS were injected into the medullary cavity with the Hamilton syringe (Corey *et al.* 2002). When a tumor grew over 10 mm in diameter (determined with a caliper), the mouse was sacrificed through breathing an appropriate volume of isoflurane. The tumor was recovered and processed for histological analysis. Intra-tibial tumor formation was monitored by X- ray radiography.

3.8.2 Investigation of invasive tumor growth

To analyze *in vivo* invasive growth and metastatic spread*,* A673 cells were detached with 2 - 3 ml 1 x trypsin, washed twice with 1 x PBS and counted with a Neubauer hemocytometer. 2 × 10^7 cells were re-suspended in a final volume of 2 ml 1× PBS (equivalent to 2 × 10^6 cells in 200 µl 1× PBS per injection). The cells in a volume of 200 µl 1× PBS were injected into the tail vein of immunodeficient Rag2$^{-/-}$γc$^{-/-}$ mice with a 27-gauge needle. Mice were euthanized with isoflurane after four weeks. Then, metastatic spread was examined in the individual organs. Affected organs were excised, photographed and fixated with 4 % formaldehyde for immunohistochemistry (see below) (Grünewald *et al.* 2012a; Richter *et al.* 2009). All apparent metastases within an organ were counted.

3.9 Immunohistochemistry of murine samples

Histological analyses were performed with the collaboration of Dr. Julia Calzada-Wack and Dr. Frauke Neff (Institute of Pathology, Helmholtz Centre Munich, Neuherberg, Germany). Tumor samples and organs containing metastases were fixated in 4 % formaldehyde and embedded in paraffin. Following steps were performed by the pathologists: 3 - 5 µm thick sections from these tissues were cut and stained with hematoxylin and eosin (H&E). Osteoclasts were detected by tartrate-resistant acid phosphatase (TRAP) staining. The number of TRAP positive osteoclasts was counted in up to 20 segments to get the average number per mm^2. All samples were reviewed and interpreted by two pathologists (Dr. J. Calzada-Wack and Dr. F. Neff).

3.10 Statistical analysis

Error bars represent the mean ± standard deviation (SD) of duplicates. When two or more independent experiments were performed, error bars show the mean ± standard error of the mean (SEM). Differences were analyzed by unpaired two-tailed student's t-test using Excel (Microsoft); p values < 0.05 were considered statistically significant ($p < 0.05$ (*), $p < 0.005$ (**), $p < 0.0005$ (***)).

4. Results

4.1 Over-expression of posterior *HOXD* genes in ES

To examine which genes are involved in the pathogenesis of ES, microarray data of ES were analyzed to find an ES-specific gene expression pattern. Genes which are over-expressed in primary ES in comparison to normal tissue were detected by using high-density DNA microarrays. ES RNA was hybridized onto HG U133A arrays (GSE1825, GSE15757 by Affymetrix (Burdach *et al.* 2009)) and compared to public array data of normal tissue (GSE2361 by Affymetrix). Among the 50 most up-regulated genes with over-expression in ES, three genes of the posterior *HOXD* locus, *HOXD10*, *HOXD11* and *HOXD13*, were identified. Table 16 gives a short summary of the relevant microarray results and shows that *HOXD10*, *HOXD11* and *HOXD13* are significantly up-regulated in ES, recognizable by the high amount of fold changes (FC).

Table 16: Summary of *HOXD* genes up-regulated in ES

Probe set ID	Gene symbol	Gene description	FC	p value
207373_at	*HOXD10*	*homeobox D10*	41.91	0.002592756
214604_at	*HOXD11*	*homeobox D11*	11.22	0.000217162
207397_s_at	*HOXD13*	*homeobox D13*	28.42	0.004564739

Extract of the list of the 50 most up-regulated genes with the strongest over-expression in ES compared to normal tissue (GSE1825, GSE15757, and GSE2361) published 2009 (Burdach *et al.* 2009). Data of *HOXD10*, *HOXD11* and *HOXD13* are shown. FC = fold change.

Furthermore, microarray data analyses revealed a strong over-expression of some posterior *HOXD* genes in ES in comparison to neuroblastoma (NB), normal (NT) and fetal tissue (FT). While other posterior *HOXD* genes, like *HOXD9* and *HOXD12,* were also highly expressed in NB, NT or FT, *HOXD10*, *HOXD11* and *HOXD1*3 were only over-expressed in ES, as can be seen in Figure 2. Due to these findings, *HOXD10, HOXD11* and *HOXD13* were chosen for further studies.

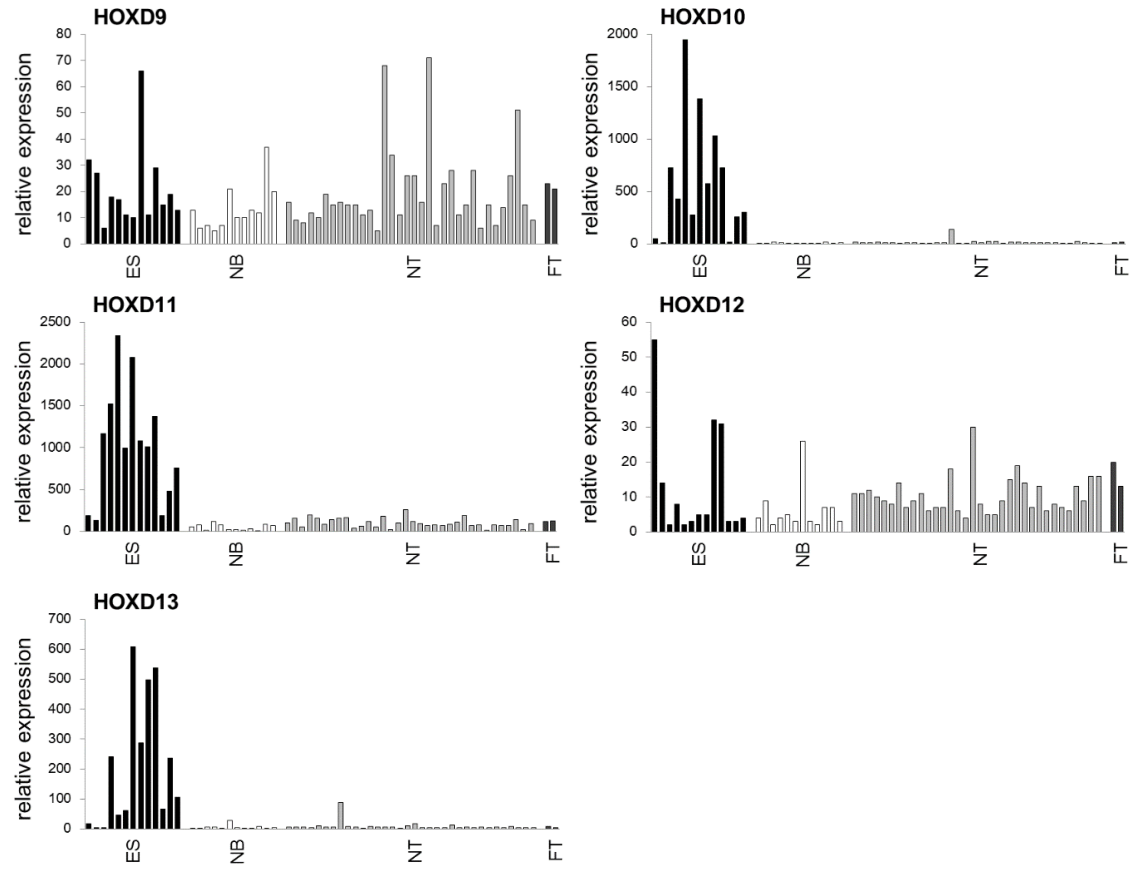

Figure 2: Posterior *HOXD* gene expression in ES in comparison to neuroblastoma, normal and fetal tissue

Microarray data that show the expression profile of posterior *HOXD* genes (*HOXD9- HOXD13*) on mRNA level in primary ES samples (black bars) in comparison to neuroblastoma (NB; white bars), normal (NT; light grey bars) and fetal tissue (FT; dark grey bars). ES and NB RNA were hybridized onto HG U133A arrays (Affymetrix; GSE1825, GSE15757) and compared to a published microarray study of normal tissue (GSE2361).

4.2 Potential regulatory mechanisms of posterior *HOXD* genes in ES

4.2.1 No Regulation via EWS-FLI1

The typical *EWS-FLI1* gene fusion leads to the oncogenic fusion protein EWS-FLI1 which is a key player for ES malignancy (Paronetto 2013). Preceding experiments in the laboratory revealed that posterior *HOXD* genes are not influenced by EWS-FLI1 (see doctoral thesis of M. Ertl). For review, EWS-FLI1 was down-regulated by transient RNA interference (see 3.5.) in two ES cell lines (A673, SK-N-MC) with two different types of specific siRNA (EWS-FLI1_1, EWS-FLI1_2) and respective control (si.control, see Table 4). 48h after transfection, RNA was isolated and qRT- PCR analyses were made to quantify the mRNA expression of *EWS-FLI1* and posterior *HOXD* genes using specific gene expression assays (see Table 7 & 14). The results are shown in Figure 3. In A673 cells, treatment with EWS-FLI1 siRNA reduced the mRNA expression of *EWS-FLI1* down to 10 - 19 % of normal values compared to control cells. A significant up-regulation of *HOXD10* and *HOXD11* up to 233 - 300 % compared to control cells was observed. *HOXD13* expression was not affected by EWS-FLI1. After transient transfection of SK-N-MC cells, *EWS-FLI1* was suppressed down to 22 - 43 % compared to control cells. In contrast to A673 cells, *HOXD10* and *HOXD11* expression did not increase after EWS-FLI1 knock down. *HOXD13* expression was suppressed down to 49 % after treatment with si.EWS-FLI1_1, but si.EWS-FLI1_2 had no significant influence on *HOXD13*. As the results were not consistent in both cell lines, *HOXD* genes seem not to be affected by EWS-FLI1 regulation.

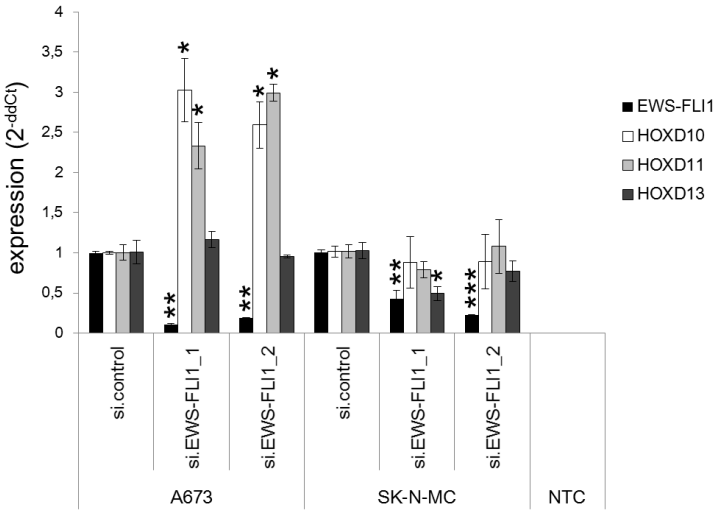

Figure 3: *EWS-FLI1* and posterior *HOXD* mRNA levels after transient EWS-FLI1 knock down in A673 and SK-N-MC cells

Results of qRT-PCR 48h after transfection are shown. si.EWS-FLI1_1 and si.EWS-FLI1_2 represent two specific siRNAs, si.control: non silencing siRNA. Error bars represent the mean ± SEM of two independent experiments; t-test ($p < 0.05$ (*), $p < 0.005$ (**), $p < 0.0005$ (***)); NTC: non template control.

4.2.2 No Regulation via EZH2

The histone methyltransferase enhancer of zeste 2 polycomb repressive complex 2 subunit (EZH2) is known to play a central role in ES pathology (Richter *et al.* 2009). Furthermore, EZH2 is involved in the regulation of *HOX* gene expression during development and in adult tissue (Rinn *et al.* 2007; Soshnikova & Duboule 2009). Thus, it was interesting to investigate the influence of EZH2 on *HOXD* gene expression in ES cell lines. Therefore, EZH2 was down-regulated in A673 and SK-N-MC cells by transient RNA interference (see 3.5.). The impact on *HOXD* genes was measured by qRT-PCR afterwards. A673 and SK-N-MC cells were transiently transfected with two kinds of specific siRNA for 48h (EZH2_2, EZH2_val, see Table 4). RNA was isolated and transient gene knock down of *EZH2* was measured by qRT-PCR on mRNA level in comparison to cells transfected with control siRNA (si.control). When reduced gene expression levels of *EZH2* were achieved, posterior *HOXD* mRNA levels were analyzed by qRT-PCR with respective gene expression assays (see Table 7). In A673 cells, *EZH2* gene expression was down-regulated to 40 - 63 % in comparison to control cells (see Figure 4). Expression levels of *HOXD10* and *HOXD13* were not affected. *HOXD11* was suppressed by si.EZH2_2, but not by si.EZH2_val. In SK-N-MC cells, *EZH2* mRNA expression was reduced down to 26 - 37 % compared to control cells. Expression levels of *HOXD10* and *HOXD13* slightly increased, whereas *HOXD11* was not affected. It can therefore be presumed that EZH2 has no influence on the three posterior *HOXD* genes.

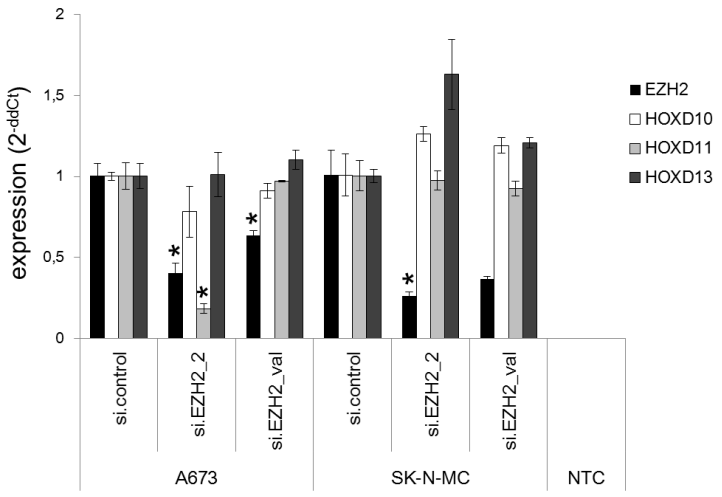

Figure 4: *EZH2* and posterior *HOXD* mRNA levels after transient EZH2 knock down in A673 and SK-N-MC cells

Results of qRT-PCR 48h after transfection are shown. si.EZH2_2 and si.EZH2_val represent two specific siRNAs, si.control: non silencing siRNA. Error bars represent the mean ± SD of duplicates; t-test ($p < 0.05$ (*)); NTC: non template control.

4.2.3 Regulation via DKK2

The bone-associated gene *DKK2* (*dickkopf WNT signaling pathway inhibitor 2)*, one of 38 genes highly over-expressed in ES (Staege *et al.* 2004), acts as agonist of the Wnt/ß-catenin signaling pathway in ES and is known to be important for the malignant and osteolytic phenotype of ES (Hauer *et al.* 2013). Furthermore, Wnt/ß-catenin signaling and the expression of single *HOX* genes seem to interrelate in diverse context (Breau *et al.* 2013; Yamamoto-Shiraishi & Kuroiwa 2013). To analyze if the canonical Wnt/ß-catenin agonist DKK2 may interact with posterior *HOXD* genes, DKK2 was constitutively suppressed by specific shRNA in different cell lines previously established in the laboratory by K. von Heyking (Hauer *et al.* 2013) (target sequence of constitutive gene knock down see Table 5). RNA was isolated and quantitative mRNA expression of *DKK2*, *HOXD10*, *HOXD11* and *HOXD13* was measured by qRT-PCR with specific gene expression assays (see Table 7). Figure 5 shows the results for A673 and SK-N-MC cells. *DKK2* was significantly reduced down to 7 - 19 % compared to control cells. Expression levels of *HOXD10*, *HOXD11* and *HOXD13* were suppressed down to 49 - 76 % (*HOXD10*), 23 - 44 % (*HOXD11*) and 50 - 59 % (*HOXD13*) in both cell lines indicating that posterior *HOXD* genes are stimulated via DKK2.

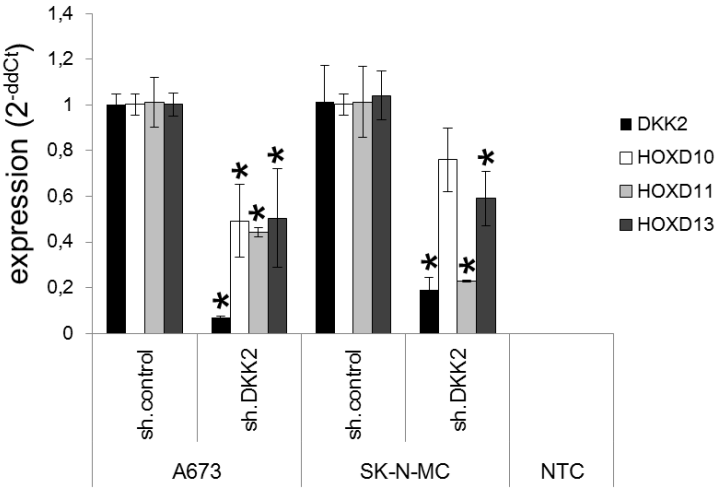

Figure 5: *DKK2* and posterior *HOXD* mRNA levels after constitutive DKK2 knock down in two ES cell lines

Results of qRT-PCR of A673 and SK-N-MC cells with stable DKK2 knock down are shown. sh.DKK2: expression after infection with specific DKK2 shRNA construct (pSIREN^{DKK2}) (Hauer *et al.* 2013); sh.control: negative control (transfected with pSIREN$^{neg.siRNA}$). Error bars represent the mean ± SEM of two independent experiments; t-test ($p < 0.05$ (*)); NTC: non template control.

4.3 Down-regulation of posterior *HOXD* genes via RNA interference

To examine the effect of posterior *HOXD* gene over-expression on ES pathogenesis and malignancy, HOXD10, HOXD11 and HOXD13 were down-regulated in A673 and SK-N-MC cells by RNA interference. When suppression was achieved, the transfected cells were utilized for diverse *in vitro* and *in vivo* assays and gene expression analyses.

4.3.1 Transient RNA interference of single *HOXD* genes

Especially for gene expression analyses A673 and SK-N-MC cells were transiently transfected with different types of siRNA (see 3.5., siRNAs see Table 4). 48 h after transfection, RNA was isolated and *HOXD10*, *HOXD11* and *HOXD13* mRNA levels were measured by qRT-PCR. Figure 6 shows the average suppression after *HOXD* gene knock down. In A673 cells, *HOXD10*, *HOXD11* and *HOXD13* were down-regulated from 26 - 44 % with the two most effective siRNAs. Transient transfection of SK-N-MC cells reduced *HOXD* mRNA levels down to 6 - 38 %. To exclude induction of an interferon (IFN) response, mRNA levels of the IFN responsive genes *ISG15 ubiquitin-like modifier* (*ISG15)* and *interferon induced transmembrane protein 1* (*IFITM1*) were monitored (data not shown). As *ISG15* and *IFITM1* mRNA expression levels were induced more than twofold after treatment with HOXD13_1 siRNA in A673 cells (in this case 6 - 24 - fold), si.HOXD13_1 was not used for subsequent experiments in A673 cells. Those two siRNAs that obtained reliably the most effective reduction of each *HOXD* gene expression, and without off-target effects, were used for subsequent experiments (si.HOXD10_1, si.HOXD10_5, si.HOXD11_5 and si.HOXD13_2 for both cell lines, si.HOXD11_3 and si.HOXD13_3 for A673 cells and si.HOXD11_6 and si.HOXD13_1 for SK-N-MC cells).

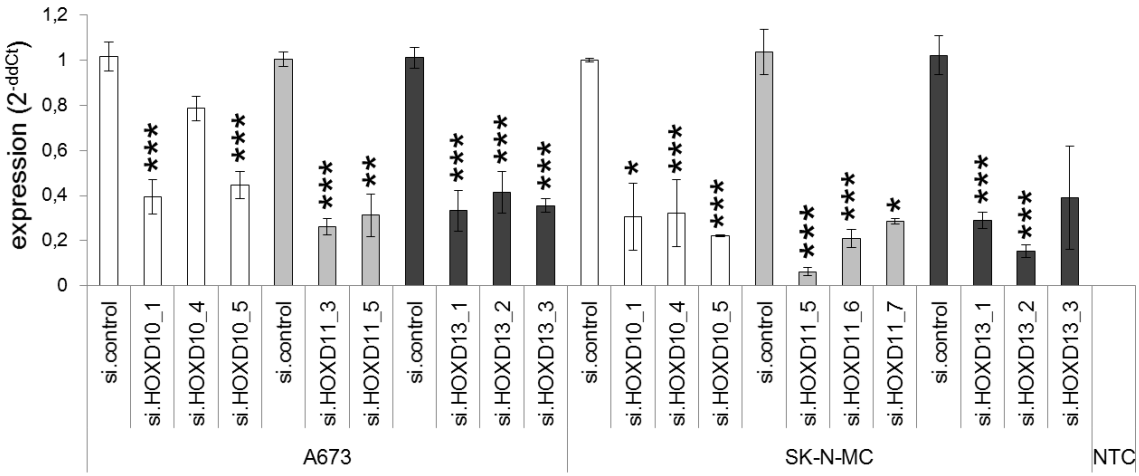

Figure 6: mRNA levels after transient *HOXD* knock down in A673 and SK-N-MC cells

Expression of *HOXD* genes 48h after transfection with specific siRNAs (si.HOXD) measured by qRT-PCR. **White bars:** HOXD10 knock down. **Light grey bars:** HOXD11 knock down. **Dark grey bars:** HOXD13 knock down. si.control: non silencing siRNA (negative control). Error bars represent the mean ± SEM of at least two independent experiments; t-test ($p < 0.05$ (*), $p < 0.005$ (**), $p < 0.0005$ (***)); NTC: non template control.

4.3.2 Triple *HOXD* gene knock down via transient RNA interference

To examine, if *HOXD* genes also interact with each other and whether their effects on other bone-associated genes increase after simultaneous knock down (see 4.5.1. and 4.6.4.), A673 and SK-N-MC cells were transiently transfected with a combination of three siRNAs at the same time (see 3.5., siRNAs see Table 4). RNA was isolated and *HOXD* mRNA levels were analyzed by qRT-PCR using special gene expression assays (see Table 7). Results are shown in Figure 7. In A673 cells, *HOXD10*, *HOXD11* and *HOXD13* were suppressed down to 22 - 46 % compared to control cells. In SK-N-MC cells, posterior *HOXD* mRNA expression was reduced down to 20 - 60 % in comparison to control cells.

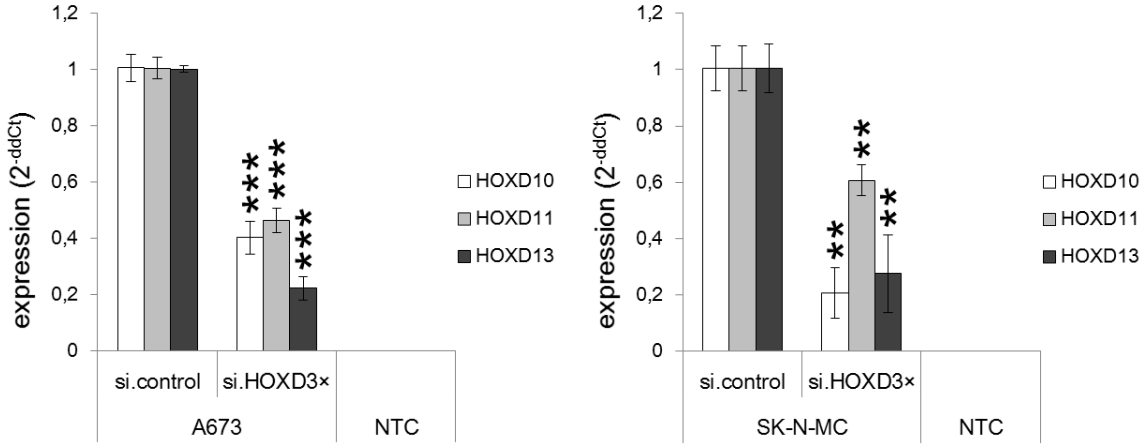

Figure 7: mRNA levels after transient triple *HOXD* knock down in two ES cell lines

Results of qRT-PCR 48h after transfection are shown. In A673, siRNA HOXD10_1, siRNA HOXD11_3 and siRNA HOXD13_2 achieved the most efficient *HOXD* down-regulation simultaneously. In SK-N-MC, siRNA HOXD10_1, siRNA HOXD11_7 and siRNA HOXD13_1 reduced *HOXD* mRNA expression most effective. si.control: non silencing siRNA. Error bars represent the mean ± SEM of two to three independent experiments; t-test ($p < 0.005$ (**), $p < 0.0005$ (***)); NTC: non template control.

4.3.3 Constitutive *HOXD* gene knock down via RNA interference

For the implementation of various *in vitro* and *in vivo* experiments, stable *HOXD* gene knock down cells were required. A673 and SK-N-MC cells with constitutive *HOXD10*, *HOXD11* and *HOXD13* gene knock down were previously generated in the laboratory (see doctoral thesis of M. Ertl and (Heyking *et al.* 2016)). Isolating RNA of transfected cells and measuring the *HOXD* mRNA expression with qRT-PCR was used to check the level of gene knock down. Figure 8 shows the average posterior *HOXD* gene suppression of transfected A673 and SK-N-MC cells when they were used for subsequent experiments. Constitutive gene knock down resulted in a significant knock down of all of the three *HOXD* genes down to 25 - 42 %.

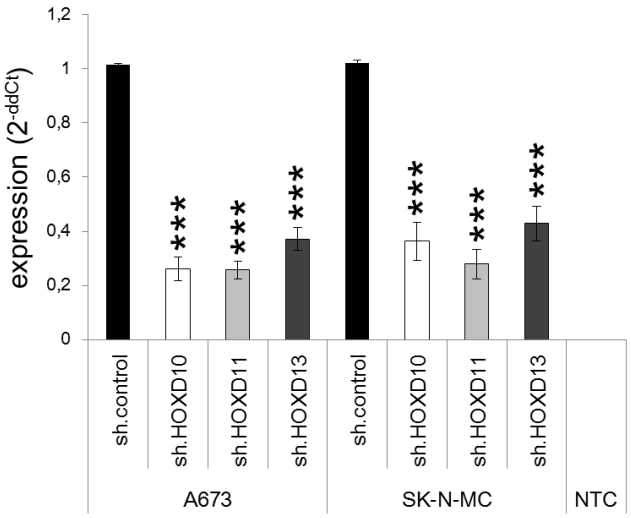

Figure 8: mRNA levels after constitutive posterior *HOXD* knock down in two ES cell lines

Results of qRT-PCR of A673 and SK-N-MC cells with stable *HOXD10*, *HOXD11* and *HOXD13* gene knock down are shown. sh.HOXD10, sh.HOXD11, sh.HOXD13: expression after infection with specific *HOXD* shRNA construct (pSIREN^{HOXD}, see Table 5); sh.control: negative control (transfected with pSIREN$^{neg.siRNA}$). Error bars represent the mean ± SEM of at least eighteen independent experiments; t-test ($p < 0.0005$ (***)); NTC: non template control.

4.4 Contribution of posterior *HOXD* genes to neuronal differentiation ability of ES cell lines

ES is a tumor with an immature stemness phenotype. Among others, NCSC are presumed cells of ES origin (Levetzow *et al.* 2011). Further, *HOX* genes are known to be critical key players for neuronal differentiation (Philippidou & Dasen 2013; Wang *et al.* 2013). Thus, it was investigated whether posterior *HOXD* genes may influence the neuronal differentiation capacity in ES. A673 and SK-N-MC cells with stable HOXD knock down and respective controls were treated with 0.1 mM BHA in 2 % DMSO for 6 days (see 3.7.4.). Subsequently, morphologic changes towards neuronal cell morphology were monitored. Differentiated cells were identified via immunofluorescence against glial fibrillary acid protein (GFAP, see Table 3), a gene encoding one of the major intermediate filament proteins of mature astrocytes (Choi & Kim 1984; Reeves *et al.* 1989). As shown in Figure 9, all infected A673 cells incubated in differentiation medium expressed GFAP significantly more than A673 sh.controls grown in control medium (without BHA, see Table 2). As expected, control cells without BHA neither demonstrated morphologic changes nor GFAP expression. In comparison to the expression of GFAP in sh.control infectants incubated in differentiation medium, there was no significant difference of the signal intensity in sh.HOXD10 infectants (see Figure 9, lower panel). HOXD11 suppression reduced the expression of GFAP down to 57 % compared to sh.control cells, whereas HOXD13 knock down significantly enhanced the expression of GFAP up to 309 %. In contrast to A673 cells, treatment with neuronal differentiation medium induced apoptosis in most of the SK-N-MC cells. The immunofluorescence staining against GFAP was therefore not feasible. Hence, the neuronal differentiation capacity of SK-N-MC cells was only measured by gene expression analyses of neuronal marker genes (see below).

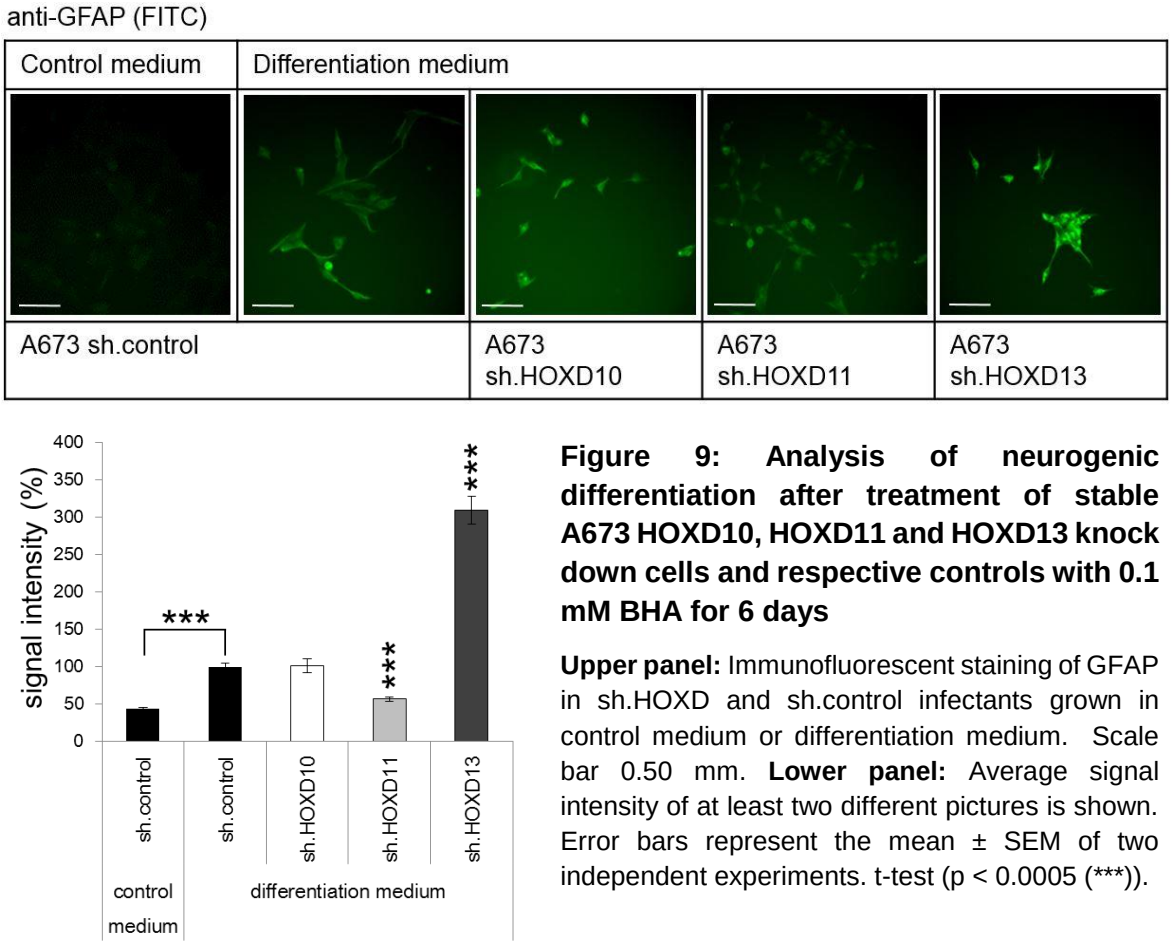

Figure 9: Analysis of neurogenic differentiation after treatment of stable A673 HOXD10, HOXD11 and HOXD13 knock down cells and respective controls with 0.1 mM BHA for 6 days

Upper panel: Immunofluorescent staining of GFAP in sh.HOXD and sh.control infectants grown in control medium or differentiation medium. Scale bar 0.50 mm. **Lower panel:** Average signal intensity of at least two different pictures is shown. Error bars represent the mean ± SEM of two independent experiments. t-test ($p < 0.0005$ (***)).

For gene expression analyses of the neuronal marker genes *nerve growth factor receptor* (*NGFR)* (Chao *et al.* 1986; Johnson *et al.* 1986; Matsushima & Bogenmann 1990), *slit drosophila homolog of 2 (SLIT2)* (Brose *et al.* 1999; Wang *et al.* 1999) and *growth-associated protein 43* (*GAP43)* (Aigner *et al.* 1995; Benowitz & Routtenberg 1997; Zhao *et al.* 2012), RNA was isolated and mRNA expression levels were measured by qRT-PCR with special gene expression assays (see Table 7). In A673 cells (Figure 10, left panel), HOXD10 knock down induced one of the early marker genes of neuronal differentiation, *NGFR*, but not *GAP43* and *SLIT2*. In contrast, HOXD11 knock down led to decreased *NGFR* levels, but enhanced *GAP43* expression. Suppression of HOXD13 increased the expression level of *GAP34* and *NGFR*, whereas *SLIT2* expression was slightly reduced. Thus, HOXD13 affects the expression of three neuronal maker genes unidirectionally (*GFAP*, *GAP43* and *NGFR*) indicating that HOXD13 inhibits the neurogenic differentiation potential in the ES cell line A673. In SK-N-MC cells (Figure 10, right panel), posterior HOXD knock down resulted in decreased mRNA levels of all of the three neuronal maker genes.

Especially *SLIT*2 was significantly reduced after HOXD10, HOXD11 and HOXD13 down-regulation. As described above, beginning apoptosis could probably have led to a loss of the original cell function and may therefore be a possible reason for the differing results in comparison to A673 infectants. In summary, posterior *HOXD* genes seem to have diverse effects on neuronal differentiation in ES cell lines with the exception of HOXD10 revealing minor impact. Suppression of HOXD11 decreased GFAP, *NGFR* and *SLIT2* in both cell lines, but induced *GAP43* in A673 cells. HOXD13 knock down, in contrast, enhanced the expression of GFAP, *GAP43* and *NGFR* in the cell line A673, but reduced *SLIT2* in both cell lines.

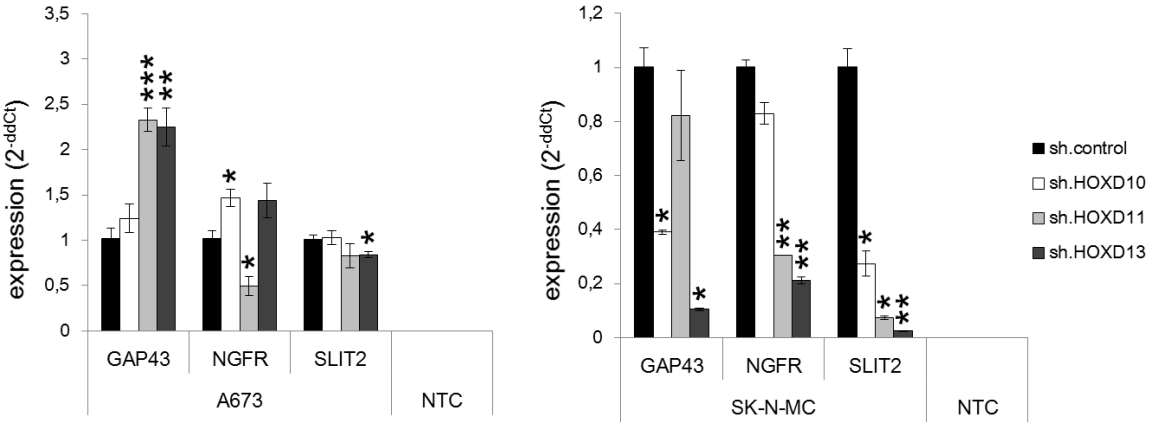

Figure 10: mRNA levels of neuronal marker genes after induction of neuronal differentiation in stable HOXD knock down cells in two ES cell lines

qRT-PCR of *GAP43*, *NGFR* and *SLIT2* after treatment of stable HOXD10, HOXD11 and HOXD13 knock down infectants and respective controls with 0.1 mM BHA for 6 days. **Left panel**: Results for A673 cells. Error bars represent the mean ± SEM of three independent experiments. **Right panel:** Results for SK-N-MC cells. Error bars represent the mean ± SD of one experiment. t-test ($p < 0.05$ (*), $p < 0.005$ (**), $p < 0.0005$ (***)); NTC: non template control.

4.5 Influence of posterior *HOXD* genes on bone-associated genes and osteotropic tumor growth of ES

ES is a high-grade malignancy occurring predominantly in the bones of children and adolescents (Ozaki 2015). It frequently arises in the diaphysis of long bones, in the pelvis and in the ribs and metastasizes to lung and bone (Ewing 1972; Schmidt *et al.* 1985; Tanaka *et al.* 2014). Due to this osteotropism, it was investigated if HOXD10, HOXD11 and HOXD13 may also have an impact on the osteolytic tumor growth of ES.

4.5.1 Suppressed expression of *RUNX2* after triple HOXD knock down

Runt-related transcription factor 2 (*RUNX2*) is a known key factor for bone development and especially for osteoblast differentiation (Bruderer *et al.* 2014; Liu & Lee 2013), but it is also involved in the carcinogenesis of several tumors (Sun *et al.* 2015). Individual posterior *HOXD* genes directly interact with RUNX2 in the chondrocyte differentiation program and during ossification (Gross *et al.* 2012; Villavicencio-Lorini *et al.* 2010). Hence, it was investigated whether HOXD10, HOXD11 and HOXD13 may also affect RUNX2 in ES. *RUNX2* gene expression of transiently and constitutively transfected HOXD knock down cells of two ES cell lines was analyzed by qRT-PCR using specific gene expression assays (see Table 7). The corresponding *HOXD* mRNA expression levels are shown in Figure 11, left panel. Single inhibition of individual *HOXD* genes did not affect the expression of *RUNX2* consistently, as shown in Figure 10, right panel. The mRNA levels of *RUNX2* differed depending on the cell line (A673 vs. SK-N-MC) and the type of RNA interference (transient vs. constitutive).

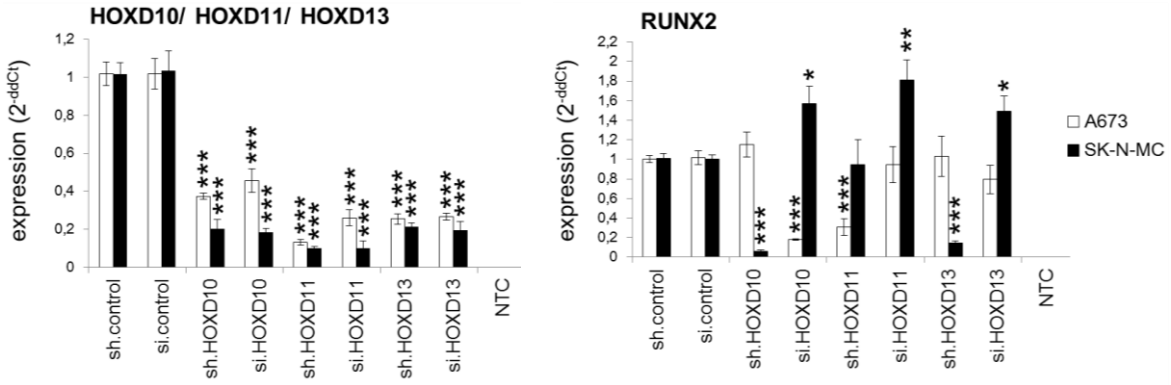

Figure 11: *HOXD* and *RUNX2* mRNA expression after transient and constitutive HOXD10, HOXD11 and HOXD13 knock down in A673 and SK-N-MC cells

qRT-PCR of *HOXD10*, *HOXD11*, *HOXD13* and *RUNX2* in two ES cell lines. **Left panel:** Reduced HOXD10, HOXD11 and HOXD13 expression after transient and constitutive HOXD gene knock down. **Right panel:** *RUNX2* mRNA expression after HOXD knock down. sh.HOXD10, sh.HOXD11, sh.HOXD13, sh.control: stably transfected ES cell lines and respective control. si.HOXD10, si.HOXD11, si.HOXD13, si.control: transiently transfected ES cell lines and respective control. Error bars represent the mean ± SEM of two independent experiments; t-test ($p < 0.05$ (*), $p < 0.005$ (**), $p < 0.0005$ (***)); NTC: non template control.

Subsequently, ES cells with triple HOXD knock down (see 4.3.2.) were examined accordingly. In contrast to the single inhibition, triple HOXD suppression clearly reduced the gene expression level of *RUNX2* down to 45 % (SK-N-MC) - 52 % (A673), as shown in Figure 12.

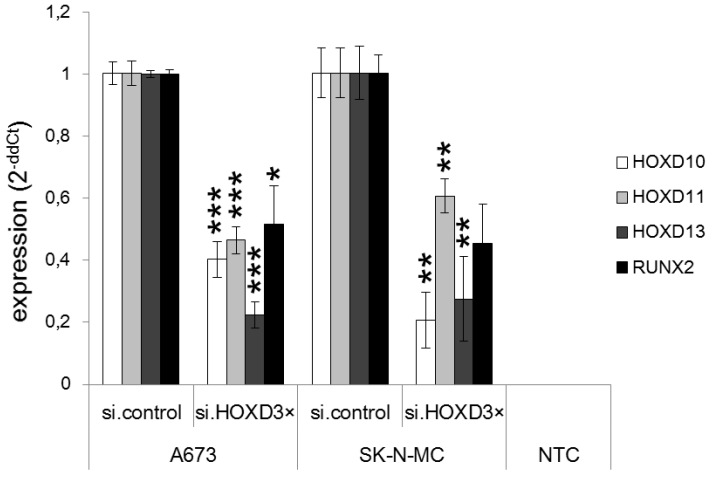

Figure 12: *HOXD10*, *HOXD11*, *HOXD13* and *RUNX2* mRNA levels after transient triple HOXD knock down in A673 and SK-N-MC cells

qRT-PCR of ES cell lines transiently transfected with si.HOXD3× (simultaneous suppression of HOXD10, HOXD11 & HOXD13); si.control: non silencing siRNA. Error bars represent the mean ± SEM of two independent experiments; t-test ($p < 0.05$ (*), $p < 0.005$ (**), $p < 0.0005$ (***)); NTC: non template control.

4.5.2 Influence of posterior *HOXD* genes on other bone-associated genes

Due to these findings, the impact of posterior HOXD knock down on other bone-associated genes was investigated by gene expression analyses. The RNA of transiently and constitutively HOXD transfected A673 and SK-N-MC cells was isolated and quantitative mRNA expression of *HOXD10*, *HOXD11*, *HOXD13* and the respective bone-associated gene was measured by qRT-PCR. On the left panel of Figure 11, corresponding mRNA levels of suppressed *HOXD* genes are plotted. As described above, DKK2, a critical mediator of osteolytic tumor growth, seems to promote posterior *HOXD* gene expression (see 4.2.3.). The question arose whether there is a reciprocal interference between DKK2 and posterior *HOXD* genes. As shown in Figure 13, left panel, HOXD10 and HOXD11 infectants did not exhibit consistently altered *DKK2* expression. Knock down of HOXD13 reduced the expression level of *DKK2* in A673 infectants (70 - 83 % compared to control cells) as well as in SK-N-MC infectants (2 - 58 % compared to control cells). Thus, there could be a mutual influence between DKK2 and HOXD13. In addition to DKK2, the BRICHOS domain containing gene *integral membrane protein 2A (ITM2A)* is over-expressed in ES (Staege *et al.* 2004). It was previously investigated concerning its contribution to ES malignancy (Heyking *et al.* 2014). Therefore, it was examined if posterior *HOXD* genes influence ITM2A. However, HOXD suppression did not affect the expression of ITM2A reproducible, as shown in Figure 13, right panel.

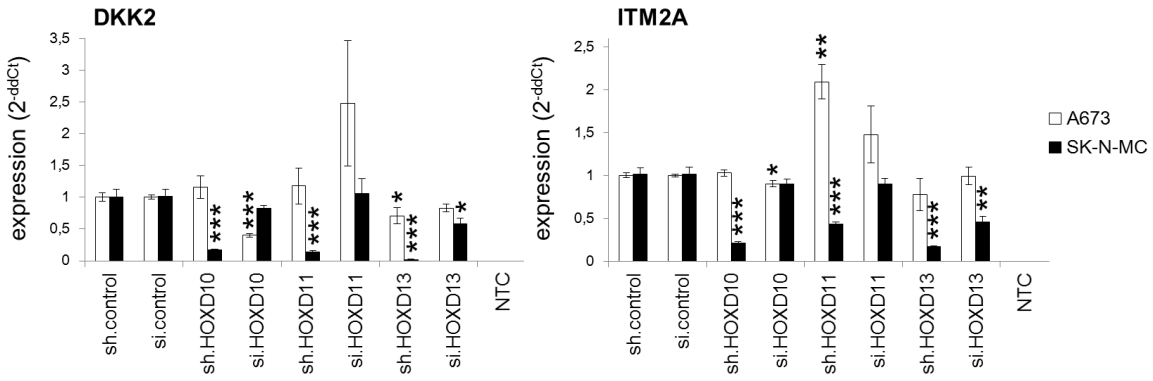

Figure 13: DKK2 and ITM2A expression after posterior HOXD knock down

Gene expression analyses of *DKK2* and *ITM2A* after posterior HOXD knock down in A673 and SK-N-MC cells measured by qRt-PCR. sh.HOXD10, sh.HOXD11, sh.HOXD13, sh.control: stably transfected ES cell lines and respective control. si.HOXD10, si.HOXD11, si.HOXD13, si.control: transiently transfected ES cell lines and respective control. Error bars represent the mean ± SEM of two independent experiments; t-test ($p < 0.05$ (*), $p < 0.005$ (**), $p < 0.0005$ (***)); NTC: non template control.

Subsequently, gene expression analyses of additional genes involved in osteolysis were made. *Hypoxia inducible factor 1 alpha subunit (HIF1A*), *fms related tyrosine kinase 1 (FLT1, VEGFR1*), *jagged 1* (*JAG1*), and *interleukin 6 (IL6*) were chosen, because all of them contribute to osteolysis and bone destruction in cancer (Guan *et al.* 2015; Knowles *et al.* 2010; Li *et al.* 2014a; Ohba *et al.* 2014; Rattigan *et al.* 2010; Sethi *et al.* 2011). HOXD10 knock down decreased the expression of *HIF1A* in transiently transfected A673 cells and in both, stably and transiently transfected SK-N-MC cells, but not in sh.HOXD10 A673 infectants (see Figure 14, top left). HOXD11 down-regulation did not affect *HIF1A*. Constitutive HOXD13 suppression enhanced expression of *HIF1A* in both cell lines, but in contrast, transient HOXD13 knock down significantly reduced the expression. To ensure reproducibility additional investigations are necessary. FLT1, a potent stimulator of angiogenesis, was examined next (Shibuya 2015). Reduced *FLT1* expression was observed after HOXD10 knock down (three of four values), whereas HOXD11 and HOXD13 did not affect the expression reproducible, as shown in Figure 14, top right. The canonical Notch ligand JAG1 is an important mediator of bone metastasis by activating the Notch pathway in bone cells (Sethi *et al.* 2011). *JAG1* gene expression analyses of SK-N-MC cells revealed significantly altered expression levels after HOXD knock down, either increase (after HOXD10 suppression) or decrease (after HOXD11 and HOXD13 suppression). But these observations were not reproducible in A673 cells. Finally, IL6, which contributes to ES tumor progression, was analyzed (Lissat *et al.* 2015). As shown in Figure 14, bottom right, HOXD10 suppression clearly reduced *IL6* expression compared to control cells. Constitutive HOXD11 knock down led to a significant decrease, but transient HOXD11 knock down did not affect *IL6*. Si.HOXD13 infectants revealed significantly suppressed *IL6* expression levels, whereas the results of stable sh.HOXD13 infectants differed in the two cell lines.

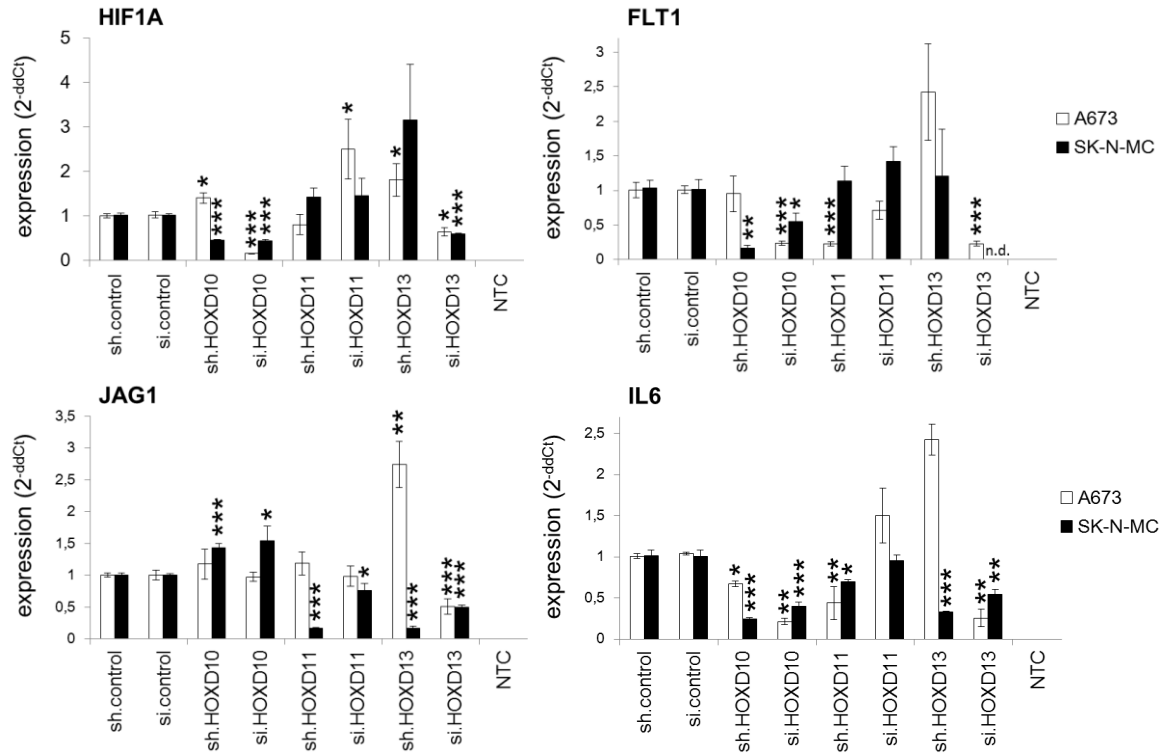

Figure 14: Expression of osteolytic genes after posterior HOXD knock down in A673 and SK-N-MC cells

Gene expression analyses of *HIF1A*, *FLT1*, *JAG1* and *IL6* after posterior HOXD knock down measured by qRT-PCR. sh.HOXD10, sh.HOXD11, sh.HOXD13, sh.control: stably transfected ES cell lines and respective control. si.HOXD10, si.HOXD11, si.HOXD13, si.control: transiently transfected ES cell lines and respective control. Error bars represent the mean ± SEM of two independent experiments; t-test ($p < 0.05$ (*), $p < 0.005$ (**), $p < 0.0005$ (***)); NTC: non template control; n.d.: not determined.

To further elucidate posterior *HOXD* genes contribute to the osteotropism and osteolytic growth of ES, their impact on genes associated with bone colonization was investigated. The examined genes, namely *C-X-C motif chemokine receptor 4 (CXCR4), parathyroid hormone like hormone (PTHLH),* and *transforming growth factor beta 1 (TGFB1)*, are all known to be involved in preparing the pre-metastatic niche, homing and invading bone (Weilbaecher *et al.* 2011). As shown in Figure 15, top left, HOXD10 and HOXD11 down-regulation did not unidirectionally affect the gene *CXCR4*, encoding a chemokine receptor known to play a key role in cancer cell proliferation, invasion and metastatic spread (Cojoc *et al.* 2013). But si.HOXD13 infectants of both cell lines and sh.HOXD13 SK-N-MC infectants revealed clearly reduced *CXCR4* mRNA expression. PTHLH, an important factor for osteolysis (Mak, Isabella W Y *et al.* 2013), was examined next. In Figure 15, top right, it

can be seen that there may be a regulation via HOXD10 and HOXD11, since sh.HOXD10 and sh.HOXD11 infectants of both cell lines and transiently transfected A673 si.HOXD10 and si.HOXD11 infectants revealed reduced *PTHLH* expression. HOXD13 did not clearly influence *PTHLH*. At least, gene expression analyses of *TGFB1*, a multifunctional cytokine involved in cell proliferation, growth, differentiation and cell movement (Kajdaniuk *et al.* 2013), were made. However, it seems not to be regulated by posterior *HOXD* genes as demonstrated by contrary or unaffected expression after posterior HOXD knock down (see Figure 15, bottom).

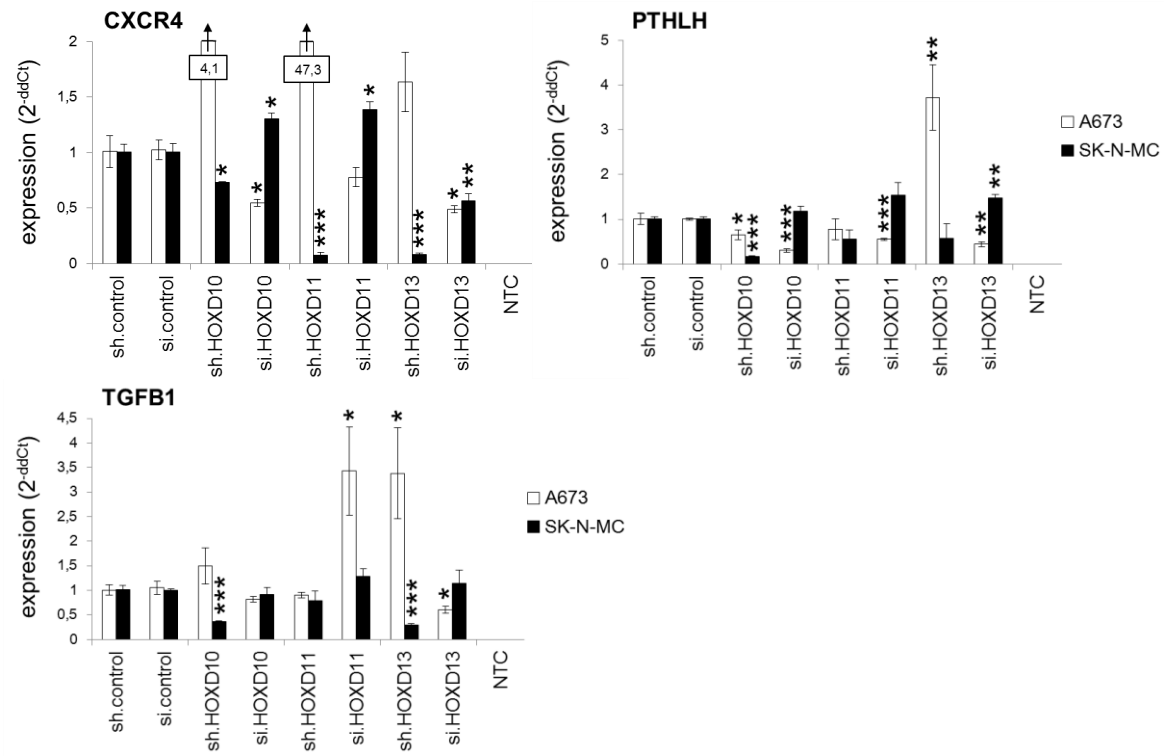

Figure 15: Expression of genes associated with bone colonization after HOXD10, HOXD11 and HOXD13 knock down in A673 and SK-N-MC cells

Gene expression analyses of *CXCR4*, *PTHLH* and *TGFB1* after posterior HOXD knock down measured by qRT-PCR. sh.HOXD10, sh.HOXD11, sh.HOXD13, sh.control: stably transfected ES cell lines and respective control. si.HOXD10, si.HOXD11, si.HOXD13, si.control: transiently transfected ES cell lines and respective control. Error bars represent the mean ± SEM of two independent experiments; t-test ($p < 0.05$ (*), $p < 0.005$ (**), $p < 0.0005$ (***)); NTC: non template control.

4.5.3 Contribution of posterior *HOXD* genes to osteolytic tumor growth *in vivo*

Based on these findings, the impact of posterior *HOXD* genes on colonization, invasion into bone and osteolysis was investigated *in vivo*. A673 sh.HOXD10, sh.HOXD11, sh.HOXD13 and sh.control infectants were injected in the tibiae of immunodeficient Rag2$^{-/-}$γc$^{-/-}$ mice. When the tumor grew to a certain size, it was recovered and fixed for histological analysis (see 3.8.1. and 3.9.). The intra-tibial tumor formation was monitored by X- ray radiography. As shown in Figure 16, posterior HOXD knock down did not significantly reduce bone invasiveness. But after suppression of HOXD10 and HOXD11, the invasiveness into the bone marrow was decreased as demonstrated by X-ray radiographies and H&E staining. Furthermore, a reduction of relative invasion into the bone marrow was observed after HOXD10, HOXD11 and even HOXD13 down-regulation (Figure 16, right panel).

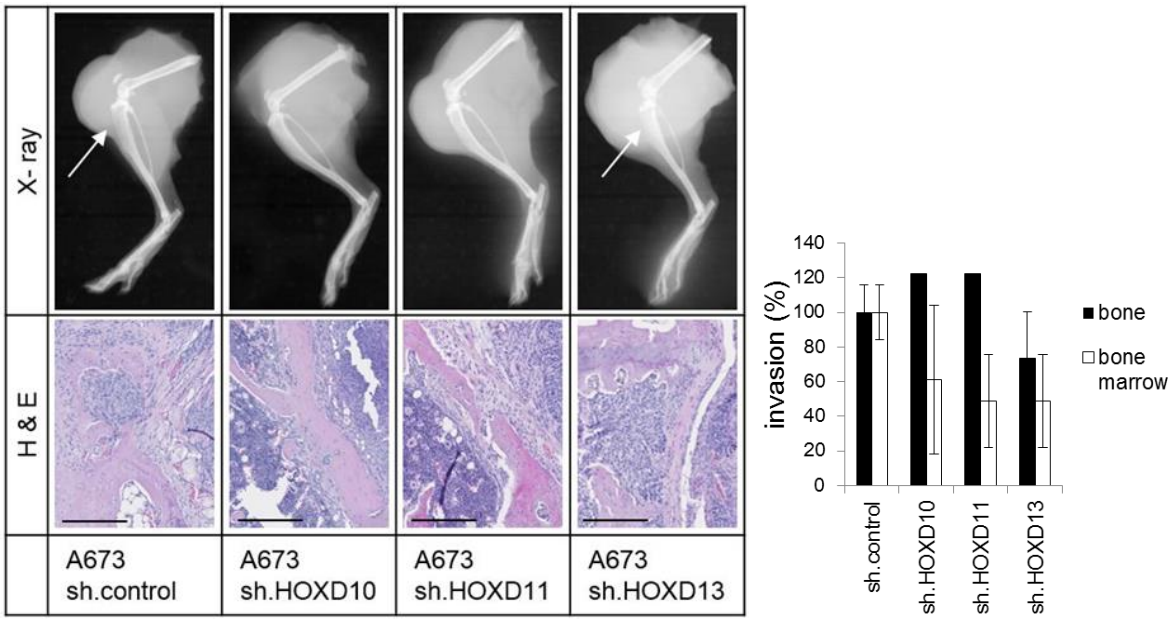

Figure 16: Analysis of bone and bone marrow invasiveness in an orthotopic bone xeno-transplantation model

A673 sh.control, sh.HOXD10, sh.HOXD11 and sh.HOXD13 infectants were injected into the tibiae of immunodeficient mice (5 - 11 mice/group). **Left panel:** Affected bones were assessed by X-ray radiography and histology (H&E staining). Representative pictures are shown. Scale bar 0.25 mm. **Right panel:** Percentage of mice exhibiting infiltration of cortical bone or bone marrow infiltration. Error bars represent the mean ± SEM.

To quantify osteolytic bone destruction, osteoclasts were stained with the tartrate-resistant acid phosphatase staining (TRAP) and counted thereafter in three different tumor samples per group. The number of TRAP positive osteoclasts in the bone did not differ between posterior HOXD knock down and control tumor samples, as can be seen in Figure 17. But in tumor tissue, a significant reduction of TRAP positive osteoclasts was observable after HOXD10, HOXD11 and HOXD13 suppression (see also Figure 17). Thus, posterior *HOXD* genes seem to enhance the number of TRAP positive osteoclasts ($1mm^2$) in the tumor.

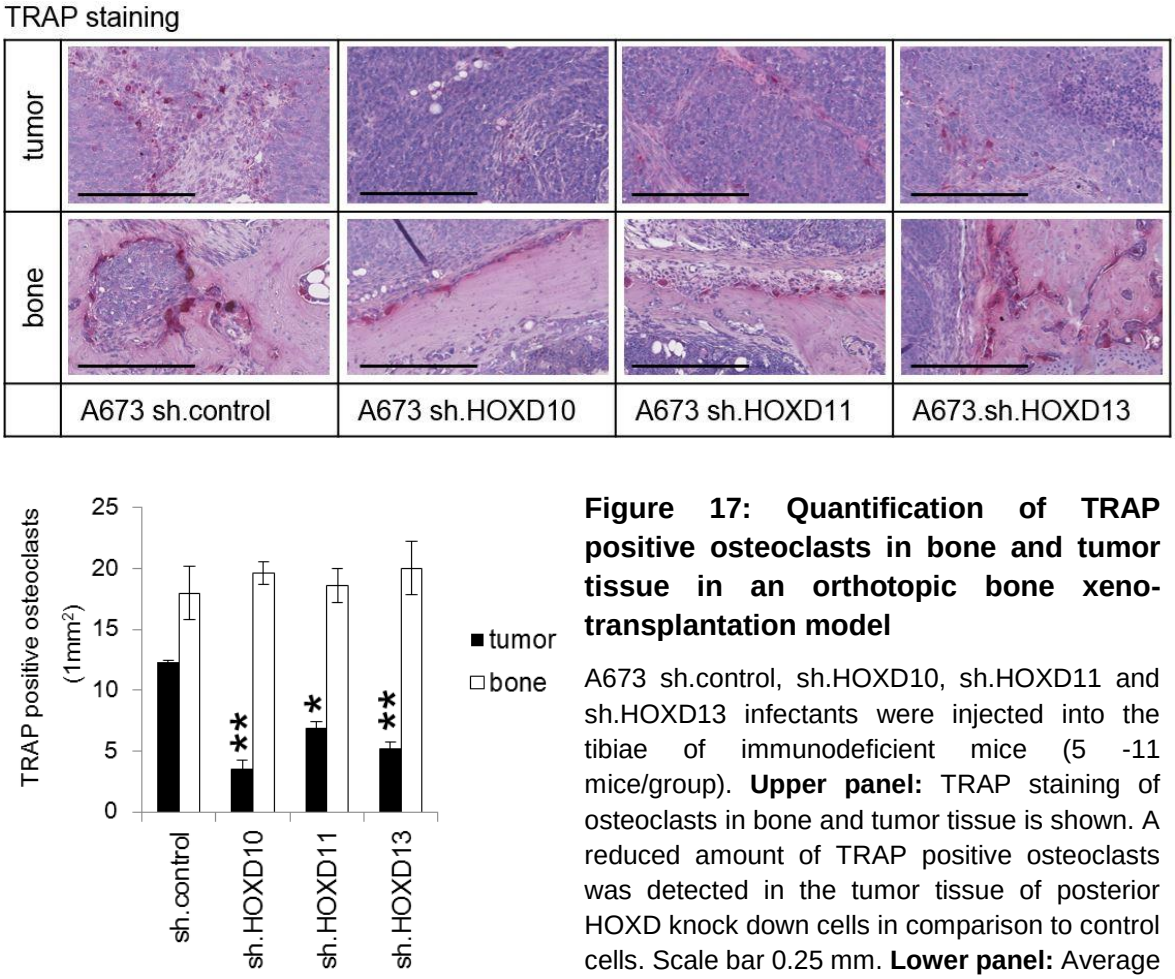

Figure 17: Quantification of TRAP positive osteoclasts in bone and tumor tissue in an orthotopic bone xeno-transplantation model

A673 sh.control, sh.HOXD10, sh.HOXD11 and sh.HOXD13 infectants were injected into the tibiae of immunodeficient mice (5 -11 mice/group). **Upper panel:** TRAP staining of osteoclasts in bone and tumor tissue is shown. A reduced amount of TRAP positive osteoclasts was detected in the tumor tissue of posterior HOXD knock down cells in comparison to control cells. Scale bar 0.25 mm. **Lower panel:** Average number of TRAP positive osteoclasts in bone and tumor tissue. Data are mean ± SEM of at least three tumor samples/group (20 segments counted).

4.6 Influence of HOXD10, HOXD11 and HOXD13 on ES growth and invasiveness

To determine the impact the over-expression of posterior *HOXD* genes in ES has on tumor growth and invasiveness, various *in vitro* and *in vivo* assays were performed. For these experiments, A673 and SK-N-MC cells with stable HOXD10, HOXD11 or HOXD13 knock down and respective controls were utilized.

4.6.1 Inhibition of proliferation after HOXD10 and HOXD13 knock down *in vitro*

The influence of HOXD10, HOXD11 and HOXD13 knock down on the proliferative capacity and contact dependent growth in A673 cells was measured with the xCELLigence system (see 3.7.1.). Stably transfected sh.HOXD10, sh.HOXD11, sh.HOXD13 and sh.control A673 infectants grew in a humidified atmosphere. Cellular impendence was measured at an interval of 4 h by the xCELLigence system. Then, cell index, doubling time and slope were analyzed. As shown in Figure 18, HOXD10 and HOXD13 suppression led to a significant inhibition of proliferation compared to control cells. The cell index of sh.HOXD13 infectants was clearly reduced over the whole measurement period. Moreover, the doubling time of sh.HOXD13 infectants was significantly extended (135 % compared to sh.control infectants). According to that, the slope of the growth curve was significantly smaller after HOXD13 knock down. Also HOXD10 down-regulation inhibited proliferation and thereby led to extended doubling time and smaller slope, but to a lesser extent than in sh.HOXD13 infectants. Similar, but not significant alterations were observed after HOXD11 suppression.

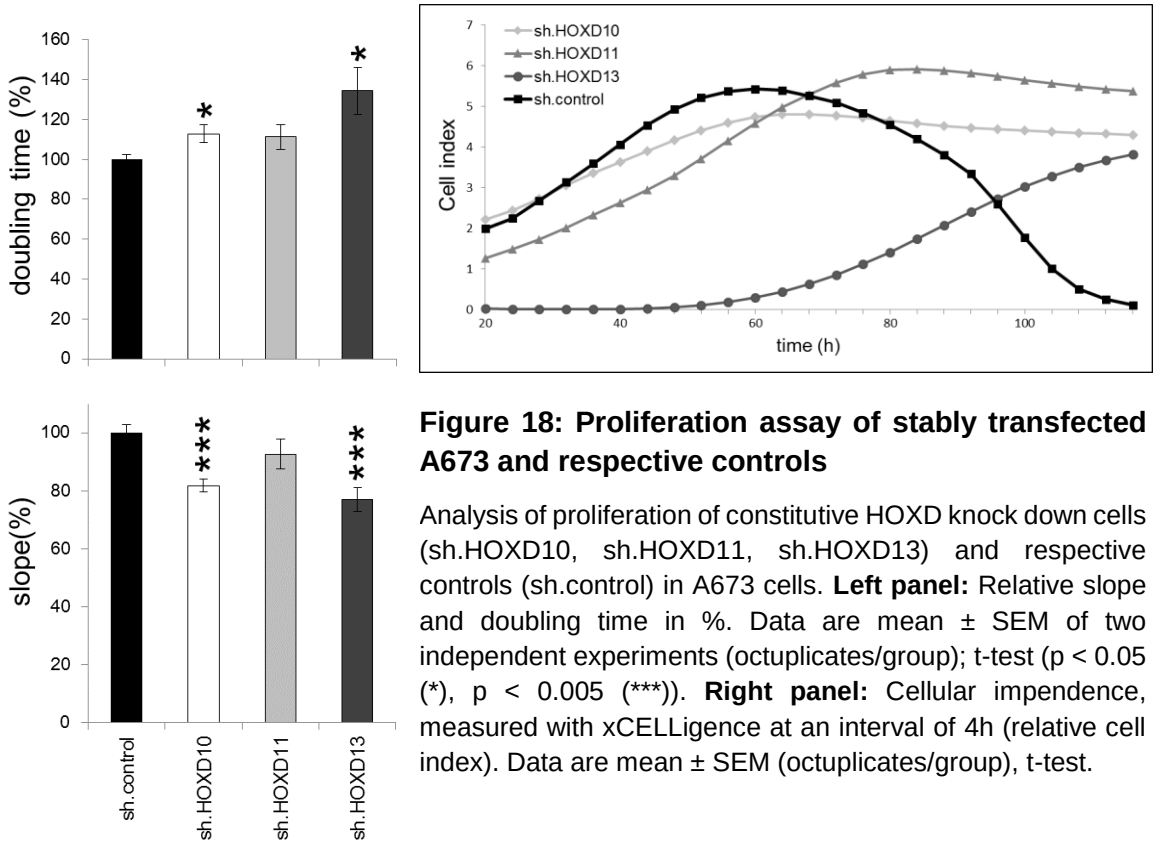

Figure 18: Proliferation assay of stably transfected A673 and respective controls

Analysis of proliferation of constitutive HOXD knock down cells (sh.HOXD10, sh.HOXD11, sh.HOXD13) and respective controls (sh.control) in A673 cells. **Left panel:** Relative slope and doubling time in %. Data are mean ± SEM of two independent experiments (octuplicates/group); t-test ($p < 0.05$ (*), $p < 0.005$ (***)). **Right panel:** Cellular impendence, measured with xCELLigence at an interval of 4h (relative cell index). Data are mean ± SEM (octuplicates/group), t-test.

4.6.2 Reduction of colony formation after HOXD11 and HOXD13 knock down *in vitro*

In addition to contact dependent growth, contact independent growth was examined as it can provide information about the malignant growth behavior of transfected ES cells. The capacity for anchorage independent growth had already been analyzed in the laboratory (see doctoral thesis of M. Ertl): sh.HOXD11 and sh.HOXD13 transfected A673 and SK-N-MC cells revealed reduced ability to form colonies in methylcellulose-based medium. This result was re-examined by repeating the colony forming assay with A673 cells (see 3.7.2.). Two different sh.HOXD clones for each gene were utilized to increase reliability. A673 cells with stable HOXD knock down and respective controls were inserted in culture dishes containing methylcellulose-based medium. Newly formed colonies were photographed and counted. The number of colonies formed by sh.HOXD10 infectants varied a lot for the two clones (see high standard deviation in Figure 19, right panel), but did not depend on the extent of HOXD10 suppression as both clones revealed significant, strong HOXD10 knock downs (data not shown). Thus, HOXD10 did not seem to affect the anchorage independent

growth. In contrast, down-regulation of HOXD11 and HOXD13 inhibited contact independent growth capacity of A673 cells significantly, as shown in Figure 19. The number of colonies was reduced down to 35 - 59 % compared to control cells.

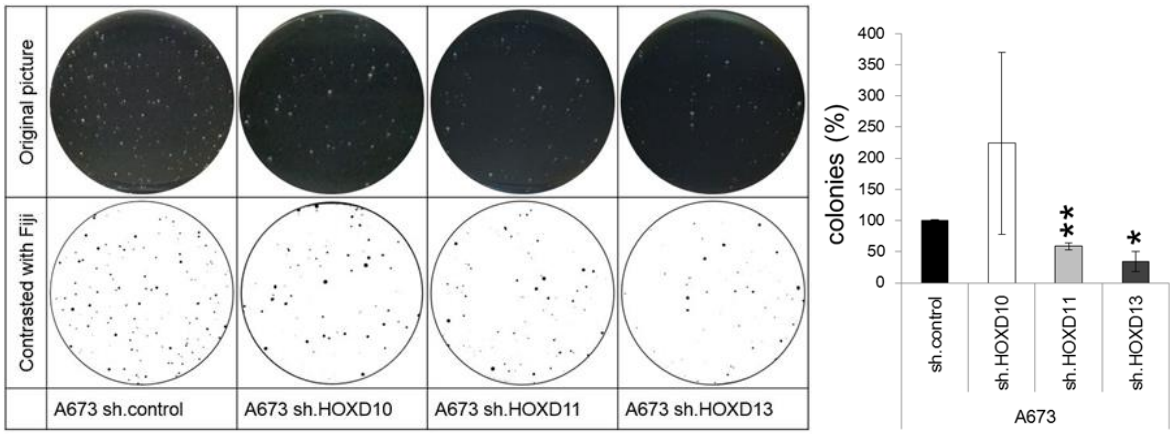

Figure 19: Colony forming assay of stably transfected A673 cells

Analysis of contact independent growth of A673 cells with constitutive HOXD10, HOXD11 or HOXD13 knock down (two clones/group, duplicates/clone) and respective control. **Left figure**: Pictures of one representative culture dish per group. Above: Original photographs of culture dishes. Below: Respective pictures, inverted and contrasted with Fijii. **Right figure:** Relative amount of colonies, counted with Fiji. Data are mean ± SD, t-test ($p < 0.05$ (*), $p < 0.005$ (**)).

4.6.3 Decrease of invasiveness after HOXD10 and HOXD13 knock down *in vitro*

To gain further knowledge about the invasive potential of ES cells with altered posterior *HOXD* gene expression under *in vitro* conditions, invasiveness was examined using the BioCoat™ Angiogenesis System. Invasive sh.HOXD10, sh.HOXD11, sh.HOXD13 and sh.control A673 and SK-N-MC infectants that migrated through the Matrigel were stained, photographed and counted (see 3.7.3.). In A673 cells, all of the three sh.HOXD infectants exhibited a significant reduction of invasions down to 4 - 9 % compared to sh.control infectants, as shown in Figure 20.

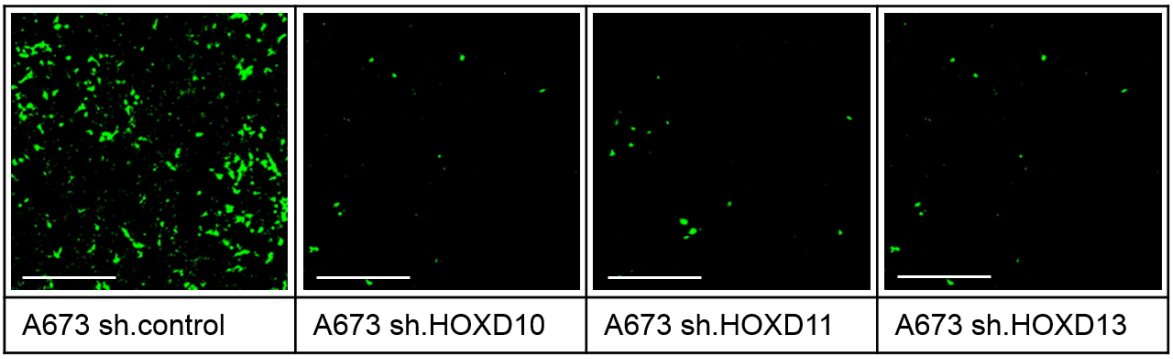

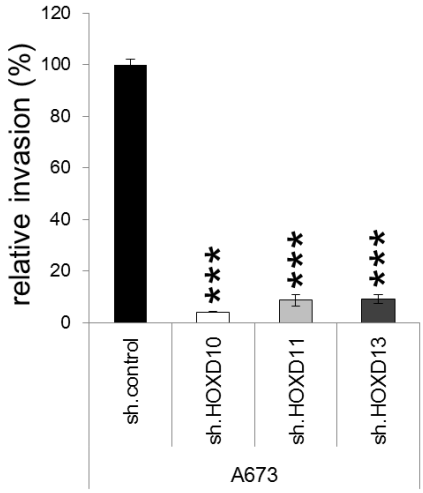

Figure 20: Invasion assay of stably transfected A673 cells and respective controls

Analysis of invasiveness of stable HOXD knock down cells (sh. HOXD10, sh.HOXD11, sh.HOXD13) and respective controls (sh.control) through Matrigel. **Upper panel:** Invasive cells 48 h after incubation. Image of one representative experiment is shown. Scale bar 0.50 mm. **Lower panel:** Relative amount of invasion, counted with Fiji. Data are mean ± SEM of at least two independent experiments; t-test ($p < 0.0005$ (***)).

SK-N-MC cells revealed less invasive potential than A673 cells in general, as can be seen in Figure 21, upper panel. HOXD10 and HOXD13 suppression significantly reduced the number of invasions down to 39 - 43 % (see Figure 21, lower panel). Compared to sh.control infectants, the invasiveness of sh.HOXD infectants were smaller and seemed not to form big cell clusters. Sh.HOXD11 infectants presented a lower number of counted invasions too, but the reduction was not significant compared to sh.control infectants. Thus, at least HOXD10 and HOXD13 clearly influenced *in vitro* invasiveness of ES cells, but there were also indications for the involvement of HOXD11.

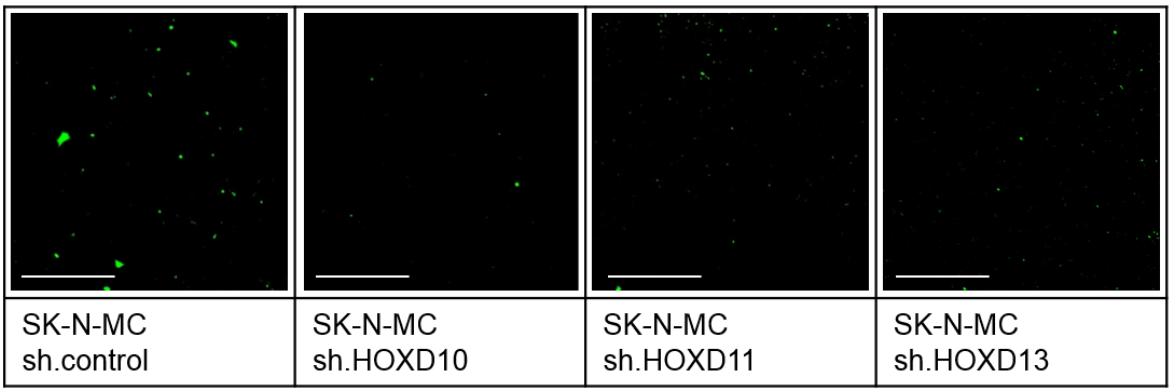

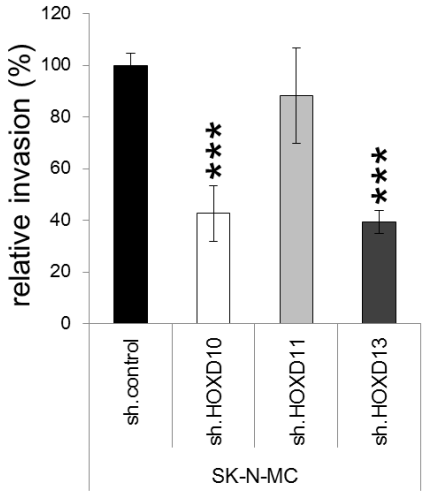

Figure 21: Invasion assay of stably transfected SK-N-MC cells and respective controls

Analysis of invasiveness of stable HOXD knock down cells (sh.HOXD10, sh.HOXD11, sh.HOXD13) and respective controls (sh.control) through Matrigel. **Upper panel:** Invasive cells 48 h after incubation. Image of one representative experiment is shown. Scale bar 0.50 mm. **Lower panel:** Relative amount of invasion, counted with Fiji. Data are mean ± SEM of two independent experiments; t-test ($p < 0.0005$ (***)).

4.6.4 Suppressed expression of *MMP1* after HOXD11, HOXD13 and triple HOXD knock down

Subsequently, possible causes for the reduced invasiveness after posterior HOXD knock down were investigated. It was examined whether posterior *HOXD* genes may have an influence on matrix metallopeptidases (MMP), major proteolytic enzymes which are known to play a key role in carcinogenesis concerning cell migration, invasion and metastasis (Wieczorek *et al.* 2015). Previous investigations in the laboratory revealed a major contribution of matrix metallopeptidase 1 (MMP1) to metastasis of ES (Grünewald *et al.* 2012a; Hauer *et al.* 2013; Richter *et al.* 2013). Consequently, the effect of *HOXD* gene suppression on the mRNA expression level of *MMP1* in A673 and SK-N-MC cells was analyzed by qRT-PCR (gene expression assay see Table 7). Stable as well as transient down-regulation of HOXD11 and HOXD13 suppressed *MMP1* in both ES cell lines, as shown in Figure 22. HOXD10 knock down only reduced *MMP1* expression in transiently

and stably transfected SK-N-MC cells. In A673 cells, constitutive HOXD10 knock down did not affect *MMP1*, whereas transient HOXD10 suppression resulted in a higher gene expression level. Hence, no reliable statement about the influence of HOXD10 on MMP1 can be made.

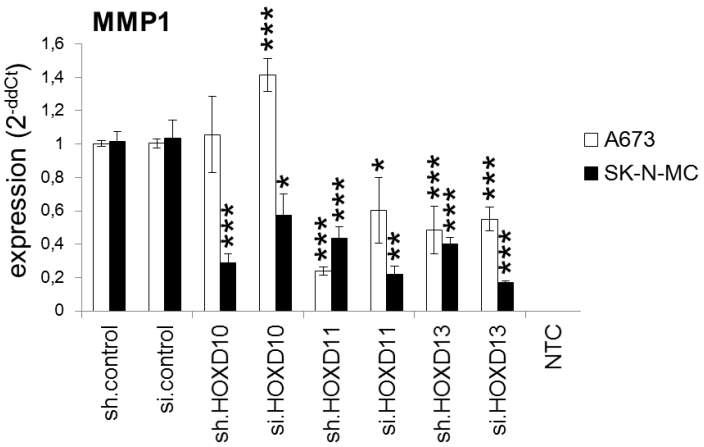

Figure 22: *MMP1* gene expression after constitutive and transient HOXD knock down in A673 and SK-N-MC cells

Results of qRT-PCR are shown. sh.HOXD10, sh.HOXD11, sh.HOXD13, sh.control: stably transfected ES cell lines and respective control. si.HOXD10, si.HOXD11, si.HOXD13, si.control: transiently transfected ES cell lines and respective control. Error bars represent the mean ± SEM of two independent experiments; t-test ($p < 0.05$ (*), $p < 0.005$ (**), $p < 0.0005$ (***)); NTC: non template control.

In addition to analyses of single HOXD knock down cells, A673 cells with triple HOXD-knock down (see 4.3.2.) were tested for *MMP1* gene expression. Figure 23 shows, that simultaneous down-regulation of HOXD10, HOXD11 and HOXD13 significantly reduced *MMP1*. In SK-N-MC cells, *MMP1* could not be determined by the qRT-PCR system in si.control and si.HOXD3× infectants probably due to very low gene expression levels of *MMP1* in these cells (data not shown).

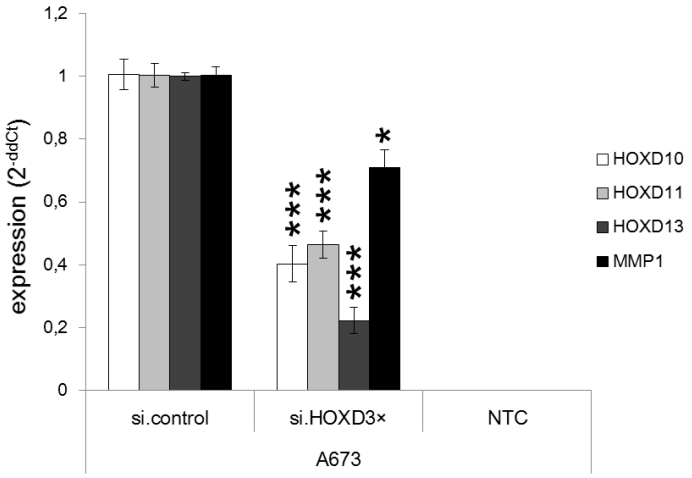

Figure 23: *HOXD10*, *HOXD11*, *HOXD13* and *MMP1* gene expression after transient triple HOXD knock down in A673 cells

qRT-PCR of A673 cells transiently transfected with si.HOXD3× (simultaneous HOXD suppression with siRNAHOXD10_1, siRNA HOXD11_5 and siRNA HOXD13_2); si.control: non silencing siRNA.. Error bars represent the mean ± SEM of three independent experiments; t-test ($p < 0.0005$ (***)); NTC: non template control.

4.6.5 Minor influence of posterior *HOXD* genes on other MMPs

Taking into account the known influence of posterior *HOXD* genes on other matrix metallopeptidases (MMPs), the gene expression of *MMP7*, *MMP9*, and *MMP14* was investigated by qRT-PCR (see Table 7). The apparently low gene expression levels of *MMP7* could not be determined by the qRT-PCR system in transiently transfected A673 and SK-N-MC cells. The values for constitutive knock down cells could partly be determined (see Figure 24), but an evaluation was hardly possible due to high dCT- values, and according low reliability. *MMP9* regulation by HOXD10 and HOXD11 differed in the two cell lines and seems not generally affected by these two genes (see Figure 24). A tendency to reduced *MMP9* levels after down-regulation of HOXD13 was observed, but one of four values (*MMP9* expression after constitutive HOXD13 knock down in A673 cells) did not differ from control cells. *MMP14* was not influenced by HOXD11 and HOXD13 as varying mRNA levels demonstrate. But down-regulation of HOXD10 reduced the expression of *MMP14* significantly in transiently and stably transfected A673 and SK-N-MC cells. Hence, MMP14 may contribute to the decreased invasiveness detected after HOXD10 suppression (see 4.6.3.).

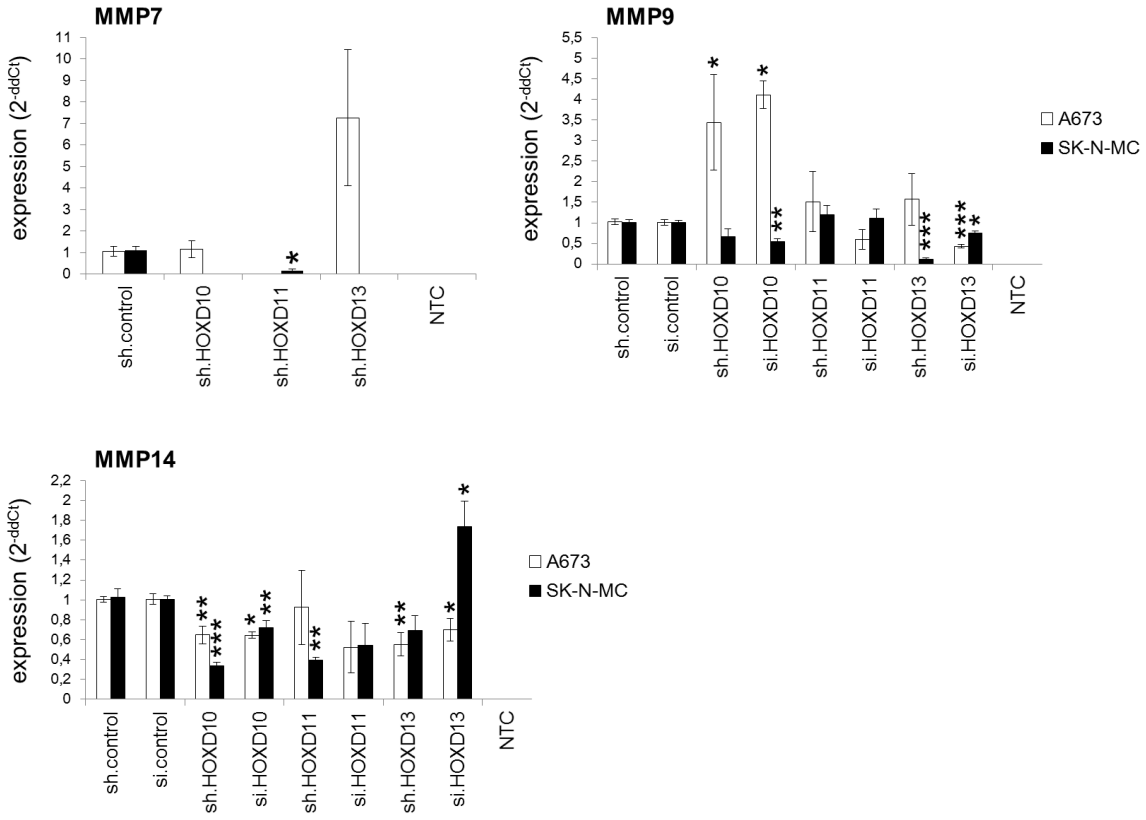

Figure 24: Gene expression analyses of *MMPs* after constitutive and transient HOXD knock down in A673 and SK-N-MC cells

Analyses of *MMP7*, *MMP9* and *MMP14* mRNA expression levels in A673 and SK-N-MC cells after posterior HOXD knock down, measured by qRT-PCR. sh.HOXD10, sh.HOXD11, sh.HOXD13, sh.control: stably transfected ES cell lines and control. si.HOXD10, si.HOXD11, si.HOXD13, si.control: transiently transfected ES cell lines and control. Error bars represent the mean ± SEM of two independent experiments; t-test (($p < 0.05$ (*), $p < 0.005$ (**), $p < 0.0005$ (***)); NTC: non template control.

4.6.6 Reduction of metastatic spread after HOXD11 and HOXD13 knock down *in vivo*

Based on all preceding observations the question arose, if *HOXD* genes may also have an influence on *in vivo* invasiveness of ES cells. To assess the impact of HOXD10, HOXD11 and HOXD13 knock down on the metastatic behavior, A673 cells with stable HOXD knock down and respective controls were injected into the tail vein of immunodeficient $Rag2^{-/-}\gamma c^{-/-}$ mice. After four weeks, metastatic spread was examined in possibly affected organs. All apparent metastases within an organ were counted (see 3.8.2., 3.9.). As shown in Figure 25, sh.control infectants caused the highest number of lung metastases, but barely liver metastases. The histological analysis demonstrated that sh.control infectants formed a large number of big tumor nodules with a high rate of necrosis in the lungs. HOXD10 knock down reduced the number of lung metastases slightly, but the histological examination revealed no difference in the appearance of the tumor nodules concerning size and amount of necrosis between sh.control and sh.HOXD10 infectants. Moreover, sh.HOXD10 infectants also colonized into the liver and formed ten metastases in average. However, HOXD11 and HOXD13 knock down significantly decreased the number of lung metastases. Furthermore, the lung metastases of sh.HOXD11 and sh.HOXD13 infectants were smaller and less necrotic. Some liver metastases occurred (2 - 3 in average), but less than after HOXD10 knock down. Even though ES is an osteolytic bone tumor, no bone metastases developed after injection of neither sh.control infected nor sh.HOXD infected A673 cells.

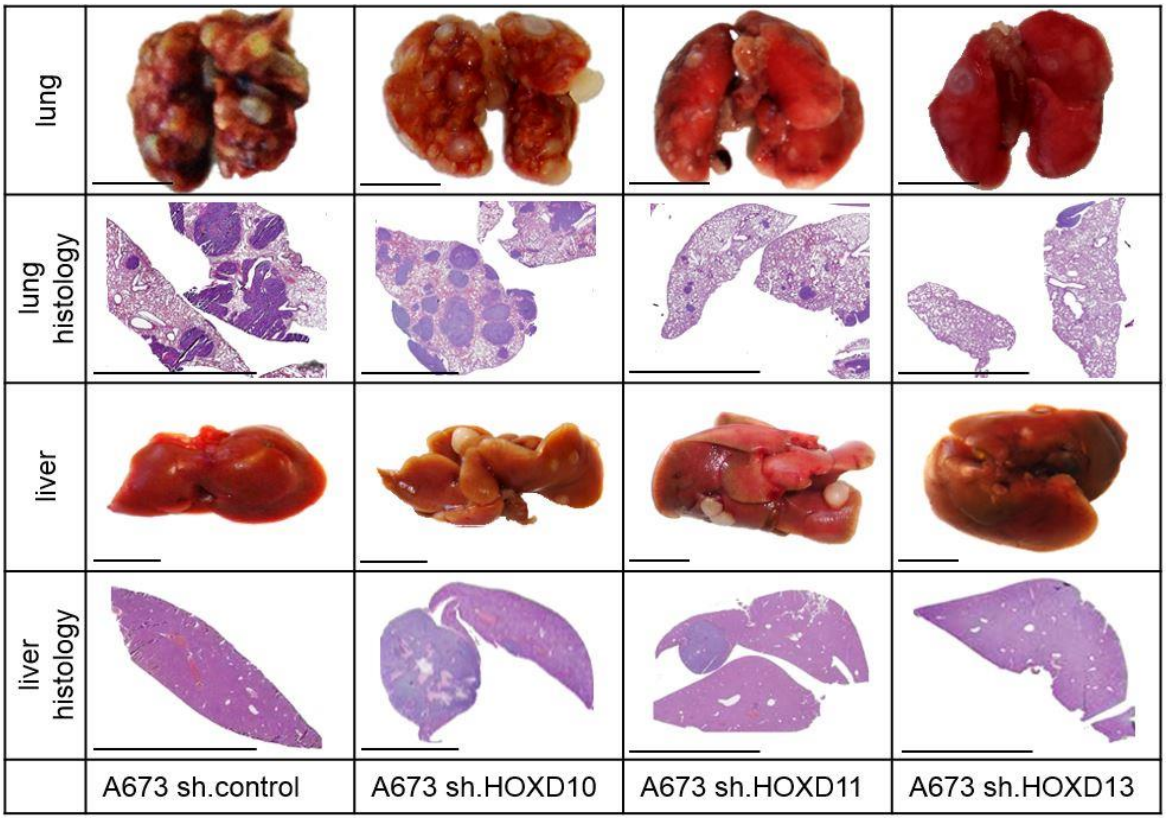

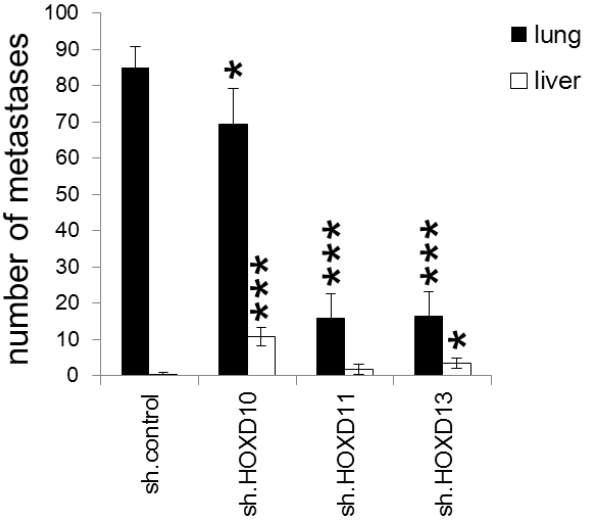

Figure 25: Affected organs after intravenous injection of posterior HOXD knock down cells into the tail vein of Rag2$^{-/-}$γc$^{-/-}$ mice

Analysis of the metastatic potential of A673 cells stably transfected with sh.control, sh.HOXD10, sh.HOXD11 and sh.HOXD13 in Rag2$^{-/-}$γc$^{-/-}$ mice (5 mice/group). **Upper panel:** Affected organs, photographed and analyzed by histology. Representative photographs of lungs and livers can be seen. HE stained sections of respective organs are shown below (scale bar 5mm). **Lower panel:** All macroscopically visible metastases were counted. Average numbers of apparent lung and liver metastases are shown; t-test ($p < 0.05$ (*), $p < 0.05$ (**), $p < 0.005$ (***)).

5. Discussion

5.1 Over-expression of posterior *HOXD* genes in ES

ES is a highly-malignant primary bone tumor, mainly occurring in children and adolescents, that tends to form metastases in lung and bone / bone marrow at an early stage. Even nowadays, patients in the metastatic stage have a poor prognosis despite continuous improvement of therapeutic options (Burdach *et al.* 2010; Gaspar *et al.* 2015; Ladenstein *et al.* 2010). Due to that it is necessary to gain more knowledge about basic pathological processes concerning tumor development, growth, invasion and metastatic behavior. High-density DNA microarray analyses were performed to identify an ES specific gene expression pattern in comparison to normal tissue (Burdach *et al.* 2009). The published list of the 50 most up-regulated genes in primary ES includes three genes of the posterior *HOXD* locus, *HOXD10*, *HOXD11* and *HOXD13*. Because of the putative neuroectodermal histogenesis of ES (Schmidt *et al.* 1985), posterior HOXD expression in ES was compared to neuroblastoma and fetal tissue. Not only in comparison to normal tissue, but also compared to neuroblastoma and fetal tissue, these three genes were over-expressed in ES, whereas other posterior *HOXD* genes were up-regulated in normal, neuroblastoma or fetal tissue, too (see Figure 2). Previous analyses of our laboratory examined whether HOXD10, HOXD11 and HOXD13 are over-expressed in other pediatric tumors with similar histology to ES like osteosarcoma by measuring posterior *HOXD* gene expression via qRT-PCR in diverse cell lines (see doctoral thesis of M. Ertl, (Heyking *et al.* 2016)). Interestingly, HOXD10, HOXD11 and HOXD13 were significantly higher expressed in ES cell lines than in osteosarcoma cell lines, though it is known that HOXD10, HOXD11 and HOXD13 play a major role in bone development (Kmita *et al.* 2002; Pineault & Wellik 2014; Zakany & Duboule 2007). These results show that the *HOX* gene expression profile in ES clearly differs from normal tissue and other pediatric malignancies. HOXD10, HOXD11 and HOXD13 could therefore be markers to distinguish ES from other pediatric tumors with similar histology. Furthermore, analysis of the impact of posterior *HOXD* gene over-expression in ES on tumor development, growth and metastasis was an interesting research approach.

5.2 Regulatory mechanisms of posterior *HOXD* genes

5.2.1 Absent regulation via EWS-FLI1 and EZH2

The typical gene translocation of the *EWSR1* gene and an ETS transcription factor family member, most frequently resulting in the fusion protein EWS-FLI1, defines classic ES and has far-reaching consequences on ES oncogenesis. A number of different EWS-FLI1 downstream target genes, either down- or up-regulated, were identified in the last decades, including *NR0B1* (García-Aragoncillo *et al.* 2008; Kinsey *et al.* 2009), *EZH2* (Burdach *et al.* 2009; Richter *et al.* 2009), *STEAP1* (*STEAP family member 1*) (Grünewald *et al.* 2012b; Grünewald *et al.* 2012a), *CCND1* (*cyclin D1*) (Kennedy *et al.* 2015; Matsumoto *et al.* 2001), *CCK* (*cholecystokinin*) (Carrillo *et al.* 2009; Cidre-Aranaz & Alonso 2015) and *CNMD* (*chondromodulin*) (Heyking *et al.* 2017; Heyking *et al.* 2014). NR0B1, STEAP1, EZH2 and CNMD are directly up-regulated by EWS-FLI1 and clearly contribute to oncogenesis of ES (Grünewald *et al.* 2012a; Grünewald *et al.* 2012b; Heyking *et al.* 2017; Heyking *et al.* 2014; Kinsey *et al.* 2009; Richter *et al.* 2009). In contrast, CCK and CCND1 are indirectly affected downstream targets with impact on ES cell proliferation and tumor growth (Carrillo *et al.* 2009; Carrillo *et al.* 2007; Cidre-Aranaz & Alonso 2015; Kennedy *et al.* 2015; Matsumoto *et al.* 2001). The question arose whether posterior HOXD expression also depends on EWS-FLI1. Svoboda *et al.* published that EWS-FLI1 transduction in NCSC significantly enhanced the expression of HOXA-D during stem cell differentiation. Especially posterior *HOXD* genes, but also posterior *HOXC* genes, were up-regulated in EWS-FLI1^{+} cells. After 4 to 7 weeks in differentiation conditions HOXD10, HOXD11 and HOXD13 showed the most remarkable up-regulation (Svoboda *et al.* 2014). However, the low posterior HOXD expression in neural crest-derived mesenchymal stem cells (NC-MSC) did not increase by transduction of EWS-FLI1 after 5 days in self-renewal media. But after 6 weeks in differentiation media EWS-FLI1^{+} NC-MSC displayed a significant up-regulation of HOXD13 (Heyking *et al.* 2016). In this doctoral thesis, mRNA levels of posterior *HOXD* genes were measured via qRT- PCR in two ES cell lines with transient EWS-FLI1 suppression, but no dependency of HOXD10, HOXD11 and HOXD13 on EWS-FLI1 was detected. Thus, posterior *HOXD* genes seem not to be regulated by EWS-FLI1 at early stages of NC-MSC or in differentiated ES cells, whereas their expression increases after EWS-FLI1 transduction in NCSC.

As studies have shown, *HOX* gene regulation depends on epigenetic mechanisms during embryogenesis. For instance, trimethylation of H3K27 is required for *HOX* gene silencing in embryonic stem cells (Montavon & Soshnikova 2014). Moreover, *in vivo* studies

demonstrated that sequential transcriptional activation of posterior *HOXD* genes is influenced by the methylation status of H3K27 and H3K4 during vertebrate development. Polycomb-dependent trimethylated H3K27 represses the expression of *HOXD* genes, whereas trithorax-dependent trimethylated H3K4 induces transcriptional activation (Soshnikova & Duboule 2009). Thus, epigenetic modifications seem to play an important role for the correct collinear expression of *HOX* genes during development. Apart from that, epigenetic alterations of *HOX* genes can be found in various human malignancies. In most cases, hypermethylation of *HOX* genes resulting in *HOX* gene silencing is associated with tumor suppressor gene silencing, and thus contributes to tumor development (Rodrigues *et al.* 2016). Hence, it was of great interest whether posterior *HOXD* genes are regulated by EZH2, an important epigenetic regulator in ES. EZH2 methylates H3K27 and thereby counteracts the differentiation of ES cells via gene silencing (Burdach *et al.* 2009; Richter *et al.* 2009). Furthermore, enhanced expression of EZH2 in ES promoted tumor growth and metastasis *in vivo* (Richter *et al.* 2009). However, it was shown that the over-expression of posterior *HOXD* genes in ES is related with absence of trimethylated H3K27 and enrichment of trimethylated H3K4 across the *HOXD* locus (Svoboda *et al.* 2014). This is in line with the finding that suppressed EZH2 expression has no impact on the expression of HOXD10, HOXD11 and HOXD13 in ES cells, as demonstrated in this study. Though, other epigenetic modifications on *HOXD* genes could play a role in ES. Advanced investigations are needed to further elucidate this issue.

5.2.2 Regulation via DKK2

The ES specific gene expression pattern with enhanced expression of a number of genes also comprises *DKK2*, part of the Wnt/ß-catenin pathway (Staege *et al.* 2004). The Wnt/ß-catenin pathway is a complex cascade including a wide variety of signal transduction elements like receptors, inhibitors or activators. It affects downstream targets by canonical (ß-catenin dependent) or non-canonical (ß-catenin independent) signaling mechanisms, and thereby regulates essential cell functions like cellular communication, cell fate, differentiation, proliferation and cell death. Hence, Wnt/ß-catenin signaling plays a key role in embryonic development. It influences limb patterning, chondrogenesis, osteogenesis and organogenesis, but also tumor development (Bonewald & Johnson 2008; Duan & Bonewald 2016; Moon *et al.* 2002; Polakis 2012; Tai *et al.* 2015). Aberrant activation of Wnt signaling was demonstrated in different malignancies such as in breast and lung cancer,

gastrointestinal tumors or leukemia, and contributes to proliferation, cancer cell survival and metastasis (Krishnamurthy & Kurzrock 2018; Polakis 2012; Tai *et al.* 2015).

As might be expected, Wnt/ß-catenin signaling has influence on *HOX* gene expression in embryonic development (Breau *et al.* 2013; Neijts *et al.* 2016; Yamamoto-Shiraishi & Kuroiwa 2013). A study in zebrafish showed that the expression of HOXB8A, which is critical for correct cell migration along the posterior lateral line, directly depends on Wnt activity (Breau *et al.* 2013). In mammals, Wnt signaling cooperates with *HOX* genes as with controlling the expression of transcription factors essential for limb tendon development (Yamamoto-Shiraishi & Kuroiwa 2013). Moreover, there seems to exist an inverse interference between the Wnt/ß-catenin pathway and different *HOX* genes, since HOX expression affects the Wnt/ß-catenin pathway during embryogenesis or carcinogenesis, as well (Hong *et al.* 2015; Kumar *et al.* 2017; Zhang *et al.* 2017). *In vitro* studies showed that knock down of HOXB5 led to reduced ß-catenin expression, and subsequently reduced non-small cell lung cancer cell proliferation and gastric cancer cell migration and invasion (Hong *et al.* 2015; Zhang *et al.* 2017). In ES, active Wnt/ß-catenin signaling is associated with enhanced tumor cell migration, metastatic spread, tumor relapse and worse overall survival (Heyking *et al.* 2016; Jin *et al.* 2012; Pedersen *et al.* 2016; Pridgeon *et al.* 2017). As DKK2 is over-expressed in ES, it was interesting to investigate a possible interaction with posterior *HOXD* genes. DKK2 can act as agonist or as antagonist of the Wnt/ß-catenin pathway, depending on different factors such as binding with the co-receptor LRP6 (LDL receptor related protein 6) or presence of the cofactor Kremen-2 (Mao *et al.* 2002). Studies demonstrated that DKK2 induces terminal osteoblast differentiation on the one hand, but on the other hand also affects the activity of osteoclasts. Accordingly, loss of DKK2 leads to osteopenia and mineralization defects, as shown *in vivo* (Glass & Karsenty 2007; Li *et al.* 2005). In ES, DKK2 acts as agonist of the Wnt/ß-catenin signaling pathway and promotes bone infiltration, osteolysis and metastasis (Hauer *et al.* 2013). Even though transient EWS-FLI1 knock down in ES cells did not affect the expression of DKK2, it was demonstrated that transduction of EWS-FLI1 to NC-MSC leads to acute up-regulation of DKK2. Similar to HOXD13, exposure of EWS-FLI1^{+} NC-MSC to differentiation medium for 6 weeks further enhanced the expression of DKK2 (Hauer *et al.* 2013; Heyking *et al.* 2016). As shown in this study, suppression of DKK2 resulted in reduced expression of all of the three analyzed *HOXD* genes (see Figure 5), indicating posterior *HOXD* genes to be downstream targets of DKK2 in ES. HOXD13 knock down, in turn, decreased the gene expression level of *DKK2* (see Figure 13). Thus, there seems to exist a reciprocal influence

of HOXD13 and DKK2. Subsequent analyses in our laboratory further revealed that WNT3a (Wnt family member 3A), WNT5a (Wnt family member 5A), WNT11 (Wnt family member 11) and a combination of these three Wnt family members increase the expression of posterior *HOXD* genes and LEF1 (lymphoid enhancer binding factor 1), a known Wnt/β-catenin target gene (Heyking *et al.* 2016). Together, these findings indicate that active Wnt signaling induces posterior *HOXD* genes in ES. It could be a promising approach to further elucidate the interactions between posterior *HOXD* genes and Wnt signaling in ES, since the precise mechanisms are still not clear today.

5.3 Diverse impact of posterior *HOXD* genes on neuronal differentiation ability of ES cell lines

Early on, a relationship between malignant peripheral neuroectodermal tumors of childhood and adolescents and ES was discovered by their similar histology. In the past, it was therefore hard to distinguish ES from other pediatric small round blue cell tumors (Schmidt *et al.* 1985). Nowadays, NCSC are still considered as most probable cells of origin of ES besides MSC. Interestingly, transduction of EWS-FLI1 in neuro-mesenchymal stem cells induced a neural crest stem cell phenotype (Levetzow *et al.* 2011). Furthermore, EWS-FLI1 transduced MSC exhibited an increased expression of neuronal marker genes or genes involved in neuronal differentiation, such as *NGFR*, *neuropeptide Y receptor Y1 (NPY1R)*, *gastrin releasing peptide* (*GRP)*, *msh homeobox 1* (*MSX1*), *NK2 homeobox 2* (*NKX2-2*) and others (Riggi *et al.* 2008). Overall, these findings emphasize the association of ES with neuronal differentiation patterns. In addition, 89 % of the list of over-expressed genes in ES are known to be expressed in neuronal tissue or during neuronal differentiation, including *HOX* genes (Staege *et al.* 2004). *HOX* genes are well-known for their key role in neuronal differentiation during embryogenesis. They are as well required for the organization, differentiation and connectivity of motoneuron subtypes, as they are needed in other neuronal classes to form synaptic specificity (Philippidou & Dasen 2013). As demonstrated in a study, individual induction of several *HOXD* genes by retinoic acid in neuroblastoma cells initiated neuronal differentiation associated with up-regulation of neuronal differentiation genes such as *neurofilament medium* (*NEFM*) (Zha *et al.* 2012). To analyze a potential impact of posterior *HOXD* genes on the neuronal differentiation capacity in ES, neuronal differentiation was induced by BHA in two ES cell lines with posterior HOXD suppression. Morphologic changes towards neurogenic differentiation recognizable by

typical neurogenic cell fibers were obvious in all transfected A673 cells grown in differentiation medium. On protein level, neuronal differentiation was measured by immunofluorescence against GFAP. GFAP is an intermediate filament protein with specifity for mature astrocytes of the central nervous system, exclusively expressed in neural tissue, and therefore works as prototype antigen to identify neural tissue (Choi & Kim 1984; Eng *et al.* 2000; Hol & Pekny 2015; Reeves *et al.* 1989). All A673 infectants grown in differentiation medium fully differentiated and expressed GFAP, though to a varying extent. HOXD11 knock down showed limited expression of GFAP, whereas HOXD13 suppression significantly enhanced the expression (see Figure 9). Additionally, gene expression analyses of the three neuronal marker genes *GAP43*, *NGFR* and *SLIT2* were performed. GAP43 is a protein with specific expression in the nervous system that plays a crucial role in the development of axon terminals and synaptic growth (Aigner *et al.* 1995; Grasselli & Strata 2013; Benowitz & Routtenberg 1997). NGFR is important for the differentiation and survival of sympathetic and sensory neurons and nerve growth by binding the neurotrophic factor NGF (nerve growth factor) (Chao *et al.* 1986; Johnson *et al.* 1986; Matsushima & Bogenmann 1990). The last analyzed gene *SLIT2* encodes a protein involved in axon guidance and neural cell migration by interaction with roundabout guidance receptors (Brose *et al.* 1999; Marillat *et al.* 2002; Wang *et al.* 1999). The results of the gene expression analyses differed between the two ES cell lines, possibly due to beginning apoptosis in SK-N-MC cells caused by the treatment with differentiation medium. In A673 cells, HOXD10 seems to have hardly any influence on the neurogenic differentiation ability. HOXD11 expression, in contrast, could induce neuronal differentiation in A673 cells, since HOXD11 RNA interference led to reduced expression of GFAP, *NGFR* and *SLIT2,* even though the induction of *GAP43* is inconsistent with this hypothesis. However, HOXD13 knock down clearly increased the expression of GFAP, *GAP43* and *NGFR*. Thus, over-expression of HOXD13 may contribute to the immature phenotype of ES by inhibiting neuronal differentiation. In SK-N-MC cells, in contrast, all of the three neuronal genes presented decreased expression after posterior HOXD suppression. Presumably, the pre-apoptotic state of the cells could have caused this noticeable difference. This may be improved by the use of a higher cell number. Furthermore, the neuronal differentiation assay could additionally be conducted in other ES cell lines, such as in EW-7 or TC-71 cells, to enhance the reliability.

5.4 Role of HOXD10, HOXD11 and HOXD13 in ES pathology

ES is a highly malignant tumor of bone and soft tissue that tends to form early metastasis predominantly in lung, bone or bone marrow. Even today, the exact molecular mechanisms of its osteotropism, osteolytic behavior, invasiveness and metastatic spread remain partly elusive. In the last decades, major key players of ES malignancy have been detected, primarily the pathognomical *EWS-FLI1* fusion gene. But also EWS-FLI1 independent genes and pathways (Wnt/ß-catenin signaling, IGF1 or RB/p53 pathway) were shown to have great influence (Kim & Park 2016; Pridgeon *et al.* 2017). However, little is yet known about the contribution of posterior *HOXD* genes to ES malignancy, but a number of studies already investigated the impact of HOXD10, HOXD11 and HOXD13 on other malignancies. HOXD10 was shown to act as tumor suppressor in breast cancer, gastric cancer or cholangiocellular carcinoma (Vardhini *et al.* 2014; Yang *et al.* 2015; Wang *et al.* 2012). Similar to HOXD10, HOXD13 has tumor suppressive properties in some tumor types, such as in pancreatic or breast cancer where low HOXD13 expression levels are associated with poor outcome (Joo *et al.* 2016; Zhong *et al.* 2015). In contrast, over-expression of HOXD11 and HOXD13 typically has pro-cancerogenic effects, as shown in laryngeal squamous cell carcinoma and head/ neck cancer (HOXD11), in Kaposi sarcoma, adenocarcinoma of colon and pleomorphic adenoma of the salivary glands (HOXD13) or in acute myeloid leukemia and myelodysplastic syndrome (by gene fusion of *HOXD11* or *HOXD13* with *NUP98*), for instance (de Barros E Lima Bueno, R. *et al.* 2016; Cantile *et al.* 2009; Sharpe *et al.* 2014; Pineault *et al.* 2003; Slape *et al.* 2008; Taketani *et al.* 2002).

5.4.1 Influence of posterior *HOXD* genes on bone-associated genes and osteotropic tumor growth

Due to the immature phenotype of ES maintained by EZH2 (Richter *et al.* 2009), the ability of ES cells to differentiate into different lineages is an interesting topic of research. It has already been demonstrated that ES cells are able to differentiate into the chondrogenic and osteogenic lineage, suggesting ES to originate from MSC or NCSC in transition to a more differentiated phenotype of the chondro-osseous lineage (Hauer *et al.* 2013; Heyking *et al.* 2016; Schmidt *et al.* 1985). To evaluate the impact of posterior *HOXD* genes on the chondrogenic and osteogenic differentiation capacity of ES cells, differentiation assays were previously performed in the laboratory (see doctoral thesis of M. Ertl, (Heyking *et al.* 2016)). In the chondrogenic differentiation assay of SK-N-MC cells, knock down of HOXD10

and HOXD11 resulted in a decrease of two early chondrogenic marker genes (*Indian hedgehog signaling molecule (IHH)*; *SRY-box 9 (SOX9)*), whereas a late chondrogenic marker gene (*collagen type X alpha 1 chain* (*COL10A1)*) was not affected. Thus, HOXD10 and HOXD11 seem to contribute to the early chondrogenic differentiation potential of ES. Surprisingly, no impact of posterior *HOXD* genes on the osteogenic differentiation potential of ES cells could be determined in the osteogenic differentiation assay, since neither changes of osteogenic marker genes, nor differences in the Alzian Red S staining were observed. Thus, the question arose whether and in what manner posterior *HOXD* genes could, nevertheless, contribute to osteotropic tumor growth. A study of our laboratory previously demonstrated that DKK2 induces a number of bone-associated and osteolytic genes (namely *CXCR4*, *PTHLH*, *RUNX2*, *TGFB1*, *HIF1A*, *IL6*, *JAG1* and *FLT1*) (Hauer *et al.* 2013). By this study, a series of genes possibly contributing to osteotropism and osteolysis in ES was identified. Subsequently, gene expression analyses of these genes were made in transiently and constitutively transfected posterior HOXD knock down cells to gain knowledge on potential posterior HOXD downstream targets.

5.4.1.1 Enhancement of osteotropic tumor growth mediated by RUNX2

RUNX2 is part of the RUNX family of transcription factors, including RUNX1, RUNX2 and RUNX3 (Ito *et al.* 2015). It plays a crucial role in osteoblast differentiation and bone formation (Bruderer *et al.* 2014; Liu & Lee 2013). The so-called master transcription factor of osteogenesis affects the expression of a large number of osteogenic genes, and thus regulates early osteoblast differentiation, matrix production, mineralization of bone during development, but also chondrocyte maturation (Liu & Lee 2013; Vimalraj *et al.* 2015). During bone development, its function depends on multiple factors as cofactors, the cellular context and the interaction with main developmental signaling pathways (Ito *et al.* 2015; Komori 2011; Bruderer *et al.* 2014). Also *HOX* genes interact with RUNX2 during ossification and chondrocyte differentiation. A study published by Villavicencio-Lorini *et al.* demonstrated that synpolydactyly homolog (*spdh*) mice with a polyalanine expansion in *HOXD13* and mice with triple gene inactivation of *HOXD11*, *HOXD12* and *HOXD13* developed polydactyly, abnormal ossification and missing joints in the autopod. Mice with single *HOXD13* inactivation (with or without additional *HOXA13* inactivation) presented similar phenotypes with delay of ossification, ossification defects or abnormal joint formation. Furthermore, *spdh* mice exhibited significantly decreased RUNX2 expression. Subsequent

analyses showed that HOXA13 and HOXD11-13 directly regulate RUNX2 by activation of the *RUNX2* promotor with the strongest induction by HOXD13 (Villavicencio-Lorini *et al.* 2010). Another study confirmed that HOXA11 and HOXD11 act upstream RUNX2 and SHOX2 (short stature homeobox 2) in early chondrocyte differentiation of the zeugopod. *HOXA11* and *HOXD11* deficient mice presented severe chondrocyte differentiation defects in radius and ulna resulting in shortened bones. Moreover, no RUNX2 and SHOX2 expression could be detected in chondrocytes of the ulna of *HOXA11* / *HOXD11* mutant mice, suggesting RUNX2 and SHOX2 as downstream targets of HOXA11 and HOXD11 (Gross *et al.* 2012). Besides its major contribution to bone development, RUNX2 has impact on the tumorigenesis of different malignancies, such as breast, prostate and pancreatic cancer or malignant melanoma, to name only a few. In most cases, up-regulation of RUNX2 can be found (Ferrari *et al.* 2013; Sun *et al.* 2015). In breast cancer, for instance, over-expression of RUNX2 is associated with a more invasive phenotype and increased bone metastases (Chimge & Frenkel 2013; Ferrari *et al.* 2013). In ES, alterations of RUNX2 expression may contribute to pathology, since EWS-FLI1 seems to impair osteoblast differentiation by suppressing RUNX2 (Li *et al.* 2010a). In this doctoral thesis, it was investigated whether RUNX2 could act downstream posterior *HOXD* genes in ES, even though HOXD expression was shown to be independent of EWS-FLI1 in ES. As demonstrated, suppression of single posterior *HOXD* genes did not affect RUNX2 consistently. However, it is known that *HOX* genes also interact with each other and influence their mutual gene expression as restricted expression of *HOX* genes is required for their special regional functions (Mallo & Alonso 2013). There seems to exist a “self-regulation” mechanism among activation or repression of individual *HOX* genes during embryogenesis. For instance, it was shown that disrupted expression of HOXA13 leads to ectopic expression of diverse *HOXD* genes in vertebrate limb development (Sheth *et al.* 2014). Therefore, it was evaluated whether there is an interaction between posterior *HOXD* genes in ES cells which could lead to increased impact on the expression of RUNX2. Interestingly, simultaneous suppression of posterior *HOXD* genes significantly decreased the gene expression of *RUNX2* in both ES cell lines. Thus, posterior *HOXD* genes seem to interact here with each other in a mutually reinforcing way. These interactions may affect osteolysis and osteotropic tumor growth in ES mediated by RUNX2.

Subsequently, the influence of posterior HOXD suppression on four osteolytic genes (*HIF1A*, *FLT1*, *JAG1* and *IL6*) was analyzed. HIF1A, a transcription factor induced in a hypoxic microenvironment, increases the expression of numerous gene products involved

in bone invasion or angiogenesis like CXCR4 and VEGFA (Ke & Costa 2006; Mimeault & Batra 2013). Thus, it plays a critical role in bone tumor development and metastatic spread of different malignancies by strong contribution to bone destruction (Guan *et al.* 2015; Knowles *et al.* 2010; Storti *et al.* 2013; Zhong *et al.* 1999). FLT1, a member of the vascular endothelial growth factor receptor family, promotes tumor growth via pro-angiogenesis, metastasis and lymph angiogenesis. In bone tumors, FLT1 expression is associated with increased malignant potential, tumor angiogenesis and osteolysis (Dimova *et al.* 2014; Ohba *et al.* 2014; Shibuya 2015). The canonical Notch ligand JAG1 is an important mediator of bone metastasis by activating the Notch pathway in bone cells. Notch activation leads to maintenance of cancer stem cell populations, inhibits apoptosis and promotes cell proliferation (Li *et al.* 2014a). JAG1 further stimulates IL6 release from osteoblasts and directly activates osteoclast differentiation (Sethi *et al.* 2011). Secreted IL6 induces inflammatory responses, enhances proliferation, inhibits apoptosis and has profound effects on the tumor microenvironment and the pre-metastatic niche (Chang *et al.* 2014; Rattigan *et al.* 2010). In ES, it contributes to tumor progression by increasing resistance to apoptosis and promoting metastasis (Lissat *et al.* 2015). As shown, transient HOXD10 suppression in A673 cells and constitutive and transient HOXD10 suppression in SK-N-MC cells reduced the gene expression of *HIF1A*. Furthermore, a clear tendency towards *FLT1* reduction was observed after HOXD10 knock down in both cell lines. *IL6* was significantly down-regulated by HOXD10 suppression in all analyzed cells. HOXD11 knock down, on the contrary, had only little impact on osteolytic genes and barely revealed consistent results. However, transient and constitutive HOXD13 knock down in SK-N-MC cells and transient knock down in A673 cells significantly reduced the gene expression of *JAG1* and *IL6* (see Figure 14). Apart from genes involved in osteolytic tumor growth, genes associated with bone colonization contribute to bone tumor development and bone metastases, as well. CXCR4, a chemokine receptor, is known to play a key role in cancer cell proliferation, invasion and metastatic spread in several human malignancies (Burger & Kipps 2006; Cojoc *et al.* 2013; Domanska *et al.* 2013). Increased expression of CXCR4 contributes to metastasis to lung and bone in ES and is associated with poor outcome (Bennani-Baiti *et al.* 2010; Krook *et al.* 2014). PTHLH, a member of the parathyroid hormone family, has physiologically central roles in endochondral bone formation and bone remodeling, but it is also produced by tumor cells metastasizing to bone (Nishihara *et al.* 2007). In cancer, PTHLH is responsible for humoral hypercalcemia and acts as important factor for osteolysis, since it inhibits osteoblast differentiation, activates osteoclasts and thus, promotes bone tumor cell colonization, invasion and bone destruction (Li *et al.* 2014b; Mak, Isabella W Y *et al.* 2013;

Sottnik & Keller 2013; Zheng *et al.* 2013). TGFB1 can either act as tumor suppressor by inhibiting growth and inducing apoptosis, or as tumor promoter, since secreted TGFB1 stimulates the release of osteolytic cytokines, and thereby functions as major contributor to bone metastases and metastatic spread (Bachman & Park 2005; Tan *et al.* 2009; Zarzynska 2014). However, gene expression analyses of A673 and SK-N-MC cells with posterior HOXD10 and HOXD11 suppression revealed no definite impact on *CXCR4* and *TGFB1*. In contrast, *PTHLH* could be a downstream target of HOXD10 and HOXD11, since constitutive knock down of stably transfected A673 and SK-N-MC cells and transiently transfected A673 cells exhibited down-regulation of *PTHLH*. HOXD13 did not to affect *TGFB1* or *PTHLH*, whereas it seems to reduce the expression of *CXCR4* (see Figure 15). Overall, posterior *HOXD* gene suppression had differential impact on bone-associated genes, in addition to the regulation of RUNX2 mentioned above. HOXD10 could affect osteolytic tumor growth and bone invasion by induction of IL6, HIF1A, FLT1 and PTHLH. HOXD11 and HOXD13 have influence on JAG1, IL6 and CXCR4 (HOXD13) or PTHLH (HOXD11). Subsequent investigations of our laboratory further demonstrated that posterior *HOXD* genes additionally promote the gene expression of osteoblast-specific *BGLAP* (*bone gamma-carboxyglutamate protein*) and pre-/osteoclast-specific *PDGFB* (*platelet derived growth factor subunit B*) which are both known to be important for ossification and endochondral bone development in ES (Donovan *et al.* 2013; Heyking *et al.* 2016; Komori 2010).

5.4.1.2 Promotion of bone marrow invasiveness and osteolysis in tumor tissue *in vivo*

Since posterior *HOXD* genes are likely to affect osteotropic tumor growth by inducing bone-associated genes such as *RUNX2*, *BGLAP*, *PDGFB* or *IL6*, their impact on bone colonization, invasion into bone / bone marrow and osteolysis *in vivo* was of great interest. A673 cells with stable HOXD10, HOXD11, HOXD13 down-regulation and sh.control infectants were directly injected into the medullary cavity behind the proximal tibia plateau of immunodeficient $Rag2^{-/-}\gamma c^{-/-}$ mice. However, no significant difference between the numbers of mice exhibiting invasion into cortical bone was detected. Consistent with this observation, posterior *HOXD* genes only partially affected bone-associated genes with the exception of *RUNX2*, *BGLAP* and *PDGFB*, as mentioned above. Moreover, it was demonstrated that posterior HOXD suppression had no impact on the number of TRAP positive osteoclasts in bone tissue. Therefore, other osteolytic genes such as *DKK2* or $VEGFA_{165}$ (*vascular endothelial growth factor A165*) seem to play a greater role in cortical bone destruction of

ES. *In vivo* studies demonstrated significantly less cortical bone lesions after down-regulation of DKK2 in A673 cells, suggesting DKK2 to be a key player of osteolysis in ES (Hauer *et al.* 2013). Another study showed reduced cortical bone destruction by inhibition of $VEGFA_{165}$ in TC-71 cells, presumably mediated by RANKL (Guan *et al.* 2009). A potential influence of posterior *HOXD* genes on $VEGFA_{165}$ has not been analyzed in this study, but they had no significant effect on FLT1, another member of the vascular endothelial growth factor receptor family. Though, tumors developed from sh.HOXD10 and sh.HOXD11 transfected A673 cells presented less bone marrow invasiveness, as demonstrated by X-ray radiography and H&E staining. A lower release of IL6 in A673 cells with stable HOXD10 and HOXD11 suppression could contribute to the observed reduced bone marrow invasiveness, since IL6 was shown to promote ES cell migration, dissemination and tumor progression (Lissat et al. 2015). Furthermore, especially hypoxic tumor sites like bone marrow exhibit enhanced secretion of IL6. This, in turn, promotes tumor cell expansion by preparing a pro-cancerogenic micro environment (Catalano *et al.* 2013; Chang *et al.* 2014). But not only HOXD10 and HOXD11 contributed to bone marrow invasiveness. The relative invasion into bone marrow was even reduced after HOXD13 knock down. Hence, posterior *HOXD* genes seem to increase subsequent bone marrow invasion, whereas other genes have greater impact on early destruction of cortical bone. Furthermore, additional analyses showed that posterior HOXD suppression significantly reduced the number of TRAP positive osteoclasts in tumor tissue. This may be caused by a posterior HOXD dependent regulation of PTHLH and PDGFB, since both are known to promote osteoclast activation (Keller 2002; Kusumbe & Adams 2014; Mak *et al.* 2013; Zhang *et al.* 1998). In addition, it supports the critical role of posterior *HOXD* gene mediated induction of RUNX2 and subsequent increased osteolytic capacity of ES, as RUNX2 contributes to osteoclastogenesis substantially (Enomoto *et al.* 2003). Altogether, these findings indicate that posterior *HOXD* genes mimic an immature endochondral developmental transcription program in ES and thereby contribute to osteolytic tumor growth. The analysis of a potential impact of posterior *HOXD* genes on other mediators of osteoclastic activity, like RANKL/RANK signaling or *TNFRSF11B* (*TNF receptor superfamily member 11b*, known as *OPG*) could provide further insight here (Goswami & Sharma-Walia 2016; Park *et al.* 2017).

5.4.2 Influence of posterior *HOXD* genes on ES growth and invasiveness *in vitro*

After evaluating the effect of posterior *HOXD* gene over-expression on osteotropism and osteolytic tumor growth, the impact on other characteristic features of ES pathology was investigated. The development and growth of tumor tissue clearly differs from normal tissue as cancer cells exhibit defects in control circuits regulating cell proliferation and homeostasis. Hanahan and Weinberg designated six “hallmarks of cancer” characterizing the exceptional ability of cancer cells found in most human tumors: self-sufficiency in growth signals, insensitivity to antigrowth signals, evading apoptosis, limitless replicative potential, sustained angiogenesis, and tissue invasion and metastasis (Hanahan & Weinberg 2000). Since these mechanisms may also count for ES cells, *in vitro* experiments related to some of these hallmarks were performed. Specifically, the proliferative capacity, the contact dependent and independent growth behavior and the invasive potential of ES cells with posterior HOXD knock down were analyzed and compared to control cells.

To gain knowledge of posterior *HOXD* gene mediated changes in the proliferation behavior, the impedance-based instrument xCELLigence system was utilized. The analysis of A673 cells demonstrated distinct differences in doubling time and slope of posterior HOXD knock down cells compared to control cells. As demonstrated, the growth curve of sh.HOXD10 and sh.HOXD13 infectants exhibited a significantly decreased slope and an increased doubling time. HOXD11 suppression showed analogous, but not significant effects. Interestingly, the exponential growth of cells with HOXD13 suppression began only after about sixty hours, while all other cell lines reached the exponential phase within the first twenty hours. The growth curve of sh.HOXD13 infectants further never attained a cell index over 4 before apoptosis, whereas all other curves achieved cell indices in a range of 4.8 to 5.9. Thus, HOXD13 suppression seemed to lead to a lower tolerance for contact dependent growth. Therefore, it can be presumed that HOXD10 and especially HOXD13 enhance the proliferative capacity of ES cells. HOXD13 could further be a reinforcing factor for an early begin of tumor proliferation. However, these results could not be confirmed in SK-N-MC cells, because SK-N-MC infectants did not enter a phase of exponential growth under the given conditions, independent of HOXD suppression. Though inserting a higher number of cells in comparison to A673, this assay could not be performed successfully. Thus, SK-N-MC cells do not seem to tolerate contact dependent growth in the way demonstrated for A673 cells.

Similarly, in contact independent growth the number of colonies were most prominently reduced after suppression of HOXD13. In sh.HOXD10 and sh.HOXD11 infectants, the results differed from the observations made in the proliferation assay. While HOXD10 suppression reduced contact dependent growth, it had no reproducible effect on anchorage independent growth. However, HOXD11 knock down significantly reduced the number of colonies, but to a lesser extent than HOXD13 (see Figure 19). Interestingly, HOXD10 and HOXD11 seem to influence the ability to form colonies in other tumor types, too. As in ES, HOXD10 and HOXD11 are over-expressed in laryngeal squamous cell carcinoma. Here, it was shown that knock down of HOXD10 and HOXD11 clearly inhibited colony formation in cell lines from human head and neck squamous cell carcinomas (FADU and UMSCC14 cells) (de Barros E Lima Bueno, R. *et al.* 2016). In contrast, HOXD10 expression significantly reduced colony formation in different cell lines of hepatocellular carcinomas (Guo *et al.* 2017). Thus, the impact of posterior *HOXD* genes on anchorage independent growth seems to depend on the tumor and cell type. In ES, HOXD11 and HOXD13 may contribute to tumor proliferation, since they significantly enhanced anchorage independent growth *in vitro*.

The invasive potential of A673 and SK-N-MC cells with HOXD10, HOXD11 and HOXD13 suppression and control cells was investigated by detecting cells which were able to migrate through Matrigel matrix. Both ES cell lines presented invasiveness, but SK-N-MC cells exhibited less invasive potential in general as demonstrated by fewer and smaller invasions (compare Figure 20 and 21). Independently of this, however, a strong reduction of invasions was recognized after HOXD10 and HOXD13 knock down in both ES cell lines. Furthermore, suppression of HOXD11 significantly decreased the invasive capacity in A673 cells. In SK-N-MC cells, invasions developed from sh.HOXD11 infectants were much smaller than those of sh.control cells, but the numerical reduction of invasions did not reach statistical significance. However, studies in other cancer cell lines have come to similar conclusions. In FADU and UMSCC14 cells of human head and neck squamous cell carcinomas, the transwell cell migration was clearly inhibited after HOXD10 and HOXD11 suppression (de Barros E Lima Bueno, R. *et al.* 2016). Moreover, HOXD10 and HOXD11 knock down significantly reduced the invasion through Matrigel in H357 cells, another cell line of head and neck squamous cell carcinoma (Sharpe *et al.* 2014).

Overall, the investigations *in vitro* strongly indicated a contribution of posterior *HOXD* genes to proliferation, contact independent growth and invasiveness of ES cells. In all of the three *in vitro* experiments the strongest influence was observed after HOXD13 knock down,

suggesting that the over-expression of HOXD13 has the greatest impact on ES pathology amongst the analyzed posterior *HOXD* genes.

5.4.3 MMP1 as posterior HOXD downstream target and key player of invasion and metastatic spread in ES

Once it has been established that posterior *HOXD* genes significantly affect ES cell invasion *in vitro*, the question of the underlying mechanisms arose. As proven in many studies, matrix metallopeptidases (MMPs), members of multifunctional family of zinc dependent endopeptidases, contribute to metastatic spread in various cancer types. MMPs are proteolytic enzymes which are able to degrade the extracellular matrix. They play an important role in physiological processes like fetal tissue development or tissue repair, but also in oncogenesis (Johansson *et al.* 2000; Tauro *et al.* 2014; Wieczorek *et al.* 2015). As modulators of the tumor microenvironment and key regulators of the interaction between stroma und tumor tissue, MMPs promote proteolysis and consequently enhance invasion, angiogenesis, inflammation and metastasis (Kessenbrock *et al.* 2010). Studies of our laboratory already demonstrated a strong involvement of MMP1 to invasion and metastasis of ES. It was demonstrated that MMP1 expression can be affected by different genes and pathways, such as by DKK2, ADGRG2 (adhesion G protein-coupled receptor G2, formerly known as G protein-coupled receptor 64) or STEAP1 (STEAP family member 1) (Grünewald *et al.* 2012a; Hauer *et al.* 2013; Richter *et al.* 2013). Suppression of MMP1 significantly inhibited invasion and metastatic spread *in vitro* and *in vivo* in ES cell lines. Moreover, knock down of MMP1 significantly reduced the number of lung metastases in $Rag2^{-/-}\gamma c^{-/-}$ mice (Richter *et al.* 2013). As demonstrated by gene expression analyses, MMP1 can also be induced by posterior *HOXD* genes. Single suppression of HOXD11 and HOXD13 significantly inhibited MMP1. Interestingly, also simultaneous knock down of all of the three *HOXD* genes reduced the gene expression of *MMP1* significantly. Therefore, the effect of posterior *HOXD* gene suppression on MMP1 seems to be strengthened by mutual interference, similar to the effect on RUNX2. The strongest correlation between MMP1 and *HOXD* genes can be presumed for HOXD13, since HOXD13 down-regulation suppressed MMP1 clearly in both ES cell lines as it led to a significant reduction of invasion *in vitro* and to a decrease of pulmonary metastasis (see 5.4.4). Furthermore, this study confirmed the contribution of MMP1 to lung metastasis in ES once again, as shown by a significant reduction of lung metastasis developed from sh.HOD11 and sh.HOXD13 infectants (see 5.4.4). Less dependency on HOXD10 may explain why the number of lung metastasis

formed by sh.HOXD10 infectants only marginally deviated from control cells. It was thus possible to show that MMP1 functions as key player of invasion and metastatic spread in ES, in parts regulated by HOXD11 and HOXD13, but the exact pathway remains elusive at this time. Apart from MMP1, however, the reduced invasiveness observed *in vitro* after HOXD10 down-regulation seems to be influenced by other mediators, too. For this reason, additional MMPs were investigated concerning their dependence on posterior *HOXD* genes. MMP7 is involved in angiogenesis and invasion. It inhibits apoptosis in malignant tissue and further promotes osteolysis and bone metastasis by inducing RANKL (Kessenbrock *et al.* 2010; Rodríguez *et al.* 2010). However, no valid statement can be made about the influence of posterior *HOXD* genes on *MMP7* due to low gene expression in the tested cell lines. Another potent stimulator of angiogenesis is MMP9. It increases the release of VEGFA, the most important factor in tumor angiogenesis (Bergers *et al.* 2000; Kessenbrock *et al.* 2010; Rodríguez *et al.* 2010). As demonstrated, HOXD13 seems to induce the expression of *MMP9*, but further analyses are necessary to confirm this thesis. MMP14 is involved in angiogenesis, as well. Furthermore, it is a key regulator of cell migration and invasion (Itoh 2006; Kessenbrock *et al.* 2010; Rodríguez *et al.* 2010). Interestingly, HOXD10 suppression significantly reduced the expression of *MMP14* in A673 and SK-N-MC cells. Thus, decreased MMP14 expression could explain the reduced invasiveness of sh.HOXD10 infectants presented *in vitro*. Moreover, a regulation of MMP14 via HOXD10 has already been detected in endothelial cells, where HOXD10 suppressed MMP14 and thereby inhibited migration and angiogenesis, contradictory to the results of this study (Myers *et al.* 2002). Therefore, HOXD10 may regulate MMP14, but the effect can either be suppressive or inductive, depending on the tumor type.

5.4.4 Reduction of metastatic spread after HOXD11 and HOXD13 knock down *in vivo*

ES is characterized by early metastatic spread to lung, bone or bone marrow. Even today, the formation of metastases usually constitutes the life-limiting event. Despite a wide range of therapeutic approaches, the disseminated disease still has dismal survival rates (Biswas & Bakhshi 2016; Burdach *et al.* 2003; Burdach *et al.* 2010; Ladenstein *et al.* 2010; Thiel *et al.* 2016). Therefore, investigations regarding the development and spread of metastases are of great importance. Again, the pathognomonical fusion gene *EWS-FLI1* seems to play a key role in tumor cell dissemination and metastatic spread, but the exact mechanisms are at present unclear (Chaturvedi *et al.* 2012; Knott *et al.* 2016; Franzetti *et al.* 2017).

Moreover, others factors and pathways were identified to be promote metastasis (Lawlor & Sorensen 2015). An involvement of DKK2, CXCR4 and ERBB4 (erb-b2 receptor tyrosine kinase 4) was demonstrated in different studies, for instance (Hauer *et al.* 2013; Krook *et al.* 2014; Mendoza-Naranjo *et al.* 2013). To assess the potential impact of posterior *HOXD* genes, metastatic spread was analyzed in a xeno-transplantation model. A673 cells with posterior HOXD suppression and respective controls were injected into the tail vein of immunodeficient Rag2$^{-/-}$γc$^{-/-}$ mice and all apparent metastases were counted. Overall, the most metastases developed in lung tissue, which fits to the general metastasis pattern of ES. Interestingly, no metastases were detected in bone or bone marrow, other typical locations of metastasis of ES. This result was already observed in other studies of our laboratory with similar experimental setup (Hauer *et al.* 2013; Heyking *et al.* 2017; Richter *et al.* 2009). In contrast, other studies demonstrated bone metastasis after intravenous injection of ES cells in other mouse strains, such as in Crl/nu/nu (CD-1) BR mice or NOD/scid mice (Franzius *et al.* 2006; Manara *et al.* 2007; Scotlandi *et al.* 2000b). But pre-treatments were carried out in some of these experimental setups and could thereby facilitate invasion into bone. NOD/scid mice were irradiated with 3.5 Gy before transplantation (Franzius *et al.* 2006), whereas Crl/nu/nu (CD-1) BR mice received anti-asialo GM1 antiserum to decrease natural killer cells (Manara *et al.* 2007). Thus, the use of other mouse strains or different pre-treatments could cause the differing metastasis pattern. A further difference between the results of this study and the most frequent pattern of metastasis in humans is the development of liver metastases in some Rag2$^{-/-}$γc$^{-/-}$ mice, since liver metastases of ES hardly occur in humans (Siemers 2013). Thus, the utilized mouse model is not able to mimic the natural distribution of metastases observed in humans completely. Nevertheless, it is a valuable tool to compare metastatic spread of wildtype and knock down cells, apart from bone lesions. In this study, a few liver metastases developed in all groups, but the highest number were formed by sh.HOXD10 infectants. As shown in many studies, HOXD10 often functions as tumor suppressor, such as in cholangiocellular carcinoma, ovarian cancer or gastric cancer (Nakayama *et al.* 2013; Wang *et al.* 2012; Yang *et al.* 2015). It has further been demonstrated that HOXD10 inhibits progression of hepatocellular carcinoma depending on promoter region methylation (Guo *et al.* 2017). Another study presented that high expression levels of miR-10b significantly enhance cell migration and invasion in hepatocellular carcinoma and clearly reduce HOXD10 expression (Liao *et al.* 2014). Thus, HOXD10 could have tumor suppressive properties in liver tissue. As HOXD10 can either work tumor suppressive or pro-cancerogenic, the effect of HOXD10 dysregulation may therefore depend on a number of factors, like tumor type, active

regulation mechanisms as negative regulation by miR-10b or epigenetic alterations. However, at this point there is no sufficient explanation why HOXD10 suppresses liver metastases, but enhances lung metastases in this study. Thus, additional studies are necessary to clarify this contradictory result. Concerning lung metastases, the impact of posterior *HOXD* gene suppression was unequivocal: in line with the result *in vitro* posterior HOXD knock down significantly reduced the invasive potential by a reduction of lung metastases. HOXD10 suppression led to a slight decrease down to 69 %, whereas HOXD11 and HOXD13 knock down reduced the number of metastases down to 15 - 17 %. The histological analyses further demonstrated differences in the tumor nodule size and the rate of necrosis. Sh.control and sh.HOXD10 infectants formed big tumor nodules with a high rate of necrosis. In contrast, sh.HOXD11 and sh.HOXD13 infectants built smaller, less necrotic lesions. Following this study, the same experiment was performed in SK-N-MC cells. A significant reduction of lung metastasis was detected after knock down of all of the three posterior *HOXD* genes (Heyking *et al.* 2016). It can be concluded that at least HOXD11 and HOXD13 play an important role in the regulation of pulmonary metastasis of ES, presumably mediated by an induction of MMP1.

5.5 Clinical relevance and future perspectives

The knowledge of fundamental mechanisms on tumor pathology can offer new therapeutic approaches and thereby complement the usual therapeutic treatments. As in many other cancer entities, research on specific target genes plays a central role today with the aim to develop more effective, but less toxic drugs. In addition to its contribution to targeted therapy, basic research can lead to the identification of tumor specific marker genes, which can provide information regarding the differentiation of tumor subtypes or the prediction of clinical outcome. In ES, most studies focused on the gene fusion EWS-FLI1 as starting point of targeted therapy. But due to pharmacokinetic properties or emergence of drug resistance, most studies on targeting EWS-FLI1 are still in their preclinical phase (Pishas & Lessnick 2016; Weidenbusch *et al.* 2018; Yu *et al.* 2017). Current promising approaches of targeted therapy in ES are, inter alia, the application of PARP-, LSD1-, or HDAC inhibitors or IGF1R monoclonal antibodies, some of which are already being tested in clinical trials (Pishas & Lessnick 2016; Weidenbusch *et al.* 2018; Yu *et al.* 2017). Despite this great scientific progress, there are still unknown mechanisms and pathways in ES, which require basic research. Especially the over-expression of a number of genes in ES raises the

question, how these genes contribute to ES pathology and if their over-expression has clinical relevance. In this study, the over-expressed genes *HOXD10*, *HOXD11* and *HOXD13* were selected for investigations concerning their contribution to ES malignancy. For many years, research on *HOX* genes focused on their involvement in embryonic development, but during the last decades there are increasingly more studies that tackle the issue of their role in cancer. Due to their differential expression in cancer, they can function as diagnostic marker genes (Morgan & El-Tanani 2016; Morgan *et al.* 2017). In prostate cancer, for instance, *HOXC6* can be used as marker gene for early diagnosis of aggressive prostate cancer in patients with low serum PSA levels as part of a urinary three-gene panel (Leyten *et al.* 2015). Furthermore, studies showed that altered expression levels of *HOX* genes are associated with changed clinical outcomes in various tumor types (Morgan *et al.* 2017). In most cases, elevated *HOX* RNA levels are associated with worse prognosis, as in AML (HOXA9) (Gao *et al.* 2016), ovarian cancer (HOXA13) (Kelly *et al.* 2016), or gastric cancer (HOXC6) (Zhang *et al.* 2013). In addition, HOX protein interactions have already been successfully used as specific therapy targets in some malignancies. It is difficult to directly target HOX proteins, but studies demonstrated that inhibition of the interaction of HOX and PBX proteins is a rational approach. PBX (Pre-B-cell Leukemia Homeobox) proteins work as co-factors of HOX proteins. By interaction with HOX proteins they enhance the DNA binding specifity, strengthen the binding and influence subsequent key transcriptional events (Morgan *et al.* 2017). This HOX/PBX dimer formation can be inhibited by a specifically developed peptide, HXR9. HXR9 disrupts HOX/PBX binding by competitive antagonism and thus prevents HOX/PBX dimers from binding to DNA (Alharbi *et al.* 2017; Morgan *et al.* 2017; Morgan *et al.* 2007). It was shown that disruption of the HOX/PBX binding with HRX9 induced apoptosis in various malignancies such as in AML, malignant melanoma, prostate cancer, mesothelioma or ovarian cancer (Alharbi *et al.* 2017; Kelly *et al.* 2016; Morgan *et al.* 2014; Morgan *et al.* 2007; Morgan *et al.* 2016). However, there are even more opportunities to affect altered HOX expression in cancer. In breast, gastric, colorectal, bladder and ovarian cancer, HOXD10 has tumor-suppressive properties. Studies demonstrated that HOXD10 is suppressed by miR-10b, a small molecular non-coding regulatory RNA associated with invasion and metastasis (An *et al.* 2017; Ma *et al.* 2015; Nakayama *et al.* 2013; Wang *et al.* 2016; Xiao *et al.* 2014). Therefore, targeting miR10-b could be another approach in tumor targeted therapy. Liang *et. al* already developed a specific miRNA-10b sponge which suppresses the expression level of miRNA-10b and thereby significantly reduces proliferation, invasion and metastasis of breast cancer cells *in vitro* (Liang *et al.* 2016). In conclusion, *HOX* genes were shown to have

potential as diagnostic or prognostic marker genes, or even as therapy targets in various malignancies. But to date, there a no studies regarding these functions in ES. This could possibly due to the fact that there is still a lack of profound knowledge of their involvement in the ES pathology. In this study, it was demonstrated that posterior *HOXD* are regulated by the Wnt/ß-catenin agonist DKK2 and, in turn, affect the expression of bone-associated genes like *RUNX2*. A contribution of HOXD10, HOXD11 and HOXD13 to osteolytic tumor growth was demonstrated in a xenograft mouse-model. Moreover, HOXD10 enhanced the proliferation and invasiveness of ES cells *in vitro*, whereas HOXD11 increased colony formation, metastatic spread and probably also *in vitro* invasiveness. Furthermore, it was proven that HOXD13, in particular, has great impact on the malignant behavior of ES cells, as it promoted proliferation, colony formation and invasiveness *in vitro* as well as invasion and metastasis *in vivo*. In addition, this study confirmed that MMP1 is a key player of metastatic spread in ES and a downstream target of posterior *HOXD* genes. These results demonstrate a major contribution of HOXD10, HOXD11 and HOXD13 to ES pathology, but there are yet no studies addressing posterior *HOXD* genes as possible target genes in ES. Thus, this study can serve as basis to further analyze their ability to function as marker genes or even as ES-specific therapeutic targets. To facilitate this, further investigations are necessary, as there are still unresolved issues. In particular, more research is needed to clarify the ambiguous role of HOXD10 in cancer. Interestingly, this study demonstrated a pro-cancerogenic effect of HOXD10 in ES, contradictory to published literature in other tumor types. Although it was demonstrated that posterior *HOXD* genes are regulated by DKK2, the issue of other HOXD regulators could offer further information on ES signaling pathways. Another interesting aspect would be the exploration of additional HOXD downstream targets, since the results of this study do not completely explain the contribution of posterior *HOXD* genes to osteotropism and osteolysis. To further elucidate this question, the development of another *in vivo* mouse model could be relevant, since no statement regarding bone metastasis was obtained by the performed *in vivo* experiment. In conclusion, further research on the contribution of posterior *HOXD* genes on ES pathology may still provide new insights into the molecular mechanisms of ES. Thus, it is still an interesting and promising topic of research, although critical findings were already obtained in this study.

6. Summary

Ewing sarcomas (ES) are highly malignant bone or soft tissue tumors with an immature stemness phenotype, characterized by early metastasis to lung and bone. In children and adolescents, ES is the second most frequent form of bone cancer. Despite a variety of therapeutic approaches, the prognosis of metastasized ES is still poor. However, accurate knowledge of tumor promoting molecular mechanisms may offer new therapeutic strategies. DNA microarray analyses demonstrated three genes of the posterior *HOXD* locus, *HOXD10*, *HOXD11* and *HOXD13*, to be over-expressed in ES. *HOX* genes contain a characteristic DNA sequence, the homeobox, which encodes the evolutionary highly-conserved DNA-binding homeodomain. They are known as key regulators of embryonic development as they determine the anterior-posterior body axis. In vertebrates, posterior *HOX* genes are involved in limb development by patterning the proximo-distal axis and directly contributing to bone formation and ossification patterns, in parts mediated by RUNX2. Though, *HOX* genes are also implicated in the tumorigenesis of different malignancies due to their influence on cell proliferation, differentiation and apoptosis. In this doctoral thesis, it was investigated how HOXD10, HOXD11 and HOXD13 contribute to the malignancy of ES. By gene expression analyses, it was demonstrated that posterior *HOXD* genes are neither regulated by the pathognomonical fusion gene *EWS-FLI1*, nor by EZH2, an important epigenetic regulator in ES. However, suppression of DKK2, an agonist of the Wnt/ß-catenin signaling pathway in ES, significantly reduced posterior HOXD expression, indicating active Wnt signaling to induce posterior *HOXD* gene expression in ES. As NCSC are considered as presumable cells of origin of ES, the impact of posterior *HOXD* genes on the neuronal differentiation ability was analyzed. While HOXD10 and HOXD11 exhibited only sporadic effects on neuronal marker genes, HOXD13 knock down significantly increased the expression of three neuronal marker gene, suggesting HOXD13 to contribute to the immature phenotype of ES by inhibiting neuronal differentiation. To evaluate the effect of posterior *HOXD* genes on osteotropic tumor growth, gene expression analyses of bone-associated genes were conducted in ES cells with posterior HOXD suppression. Simultaneous knock down of HOXD10, HOXD11 and HOXD13 significantly decreased the expression of RUNX2, a key factor of osteoblast differentiation and bone formation. Individual posterior *HOXD* gene inhibition further revealed a HOXD10 dependent regulation of IL6. Subsequent *in vivo* analyses demonstrated that posterior HOXD suppression has no influence on cortical bone infiltration, but decreases bone marrow invasiveness and the number of $TRAP^+$ osteoclasts within the tumor tissue, presumably mediated by RUNX2. To

examine the impact of posterior *HOXD* genes on the invasive and metastatic phenotype of ES, proliferation, anchorage independent growth and invasiveness were investigated in posterior HOXD knock down cells *in vitro*. While anchorage independent growth was promoted by HOXD11 and HOXD13, proliferation and invasiveness were dependent on HOXD10 and HOXD13. The observed effect on the invasive behavior may be in parts mediated by MMP1, a key factor of metastasis in ES, since it was demonstrated that individual inhibition of HOXD11 and HOXD13 and triple HOXD knock down decreased the expression of MMP1. In line with these results, suppression of HOXD11 and HOXD13 significantly reduced the number of lung metastases *in vivo*. These findings indicate a major contribution of HOXD10, HOXD11 and HOXD13 to the malignancy of ES and may therefore serve as basis for further investigations on their suitability as ES-specific therapeutic target genes.

7. Zusammenfassung

Ewing Sarkome (ES) sind hoch maligne Knochen- und Weichteiltumore mit einem unreifen stammzellähnlichen Phänotyp, die durch frühe Lungen- und Knochenmetastasierung gekennzeichnet sind. Bei Kindern und Jugendlichen ist das ES die zweithäufigste Form des Knochenkrebses. Trotz einer Vielzahl therapeutischer Möglichkeiten ist die Prognose des metastasierten ES immer noch schlecht. Die genaue Kenntnis der tumorfördernden molekularen Mechanismen könnte jedoch neue therapeutische Strategien ermöglichen. DNS-Microarray-Analysen zeigten, dass drei Gene des posterioren *HOXD*-Lokus, *HOXD10*, *HOXD11* und *HOXD13*, im ES überexprimiert sind. *HOX* Gene beinhalten eine charakteristische DNS-Sequenz, die Homöobox, die die evolutionär hoch-konservierte DNS-bindende Homöodomäne kodiert. Sie sind als Hauptregulatoren der embryonalen Entwicklung bekannt, da sie unter anderem die anterior-posteriore Körperachse bestimmen. Bei Wirbeltieren sind die posterioren *HOX* Gene außerdem an der Extremitäten-Entwicklung beteiligt, indem sie die proximo-distale Körperachse gliedern, und tragen direkt zur Knochenbildung und zur Ossifikation bei, was teilweise durch RUNX2 vermittelt wird. Jedoch sind die *HOX* Gene aufgrund ihres Einflusses auf Zellproliferation, Differenzierung und Apoptose auch an der Entstehung unterschiedlicher Malignitäten beteiligt. In dieser Doktorarbeit wurde untersucht, wie HOXD10, HOXD11 und HOXD13 zu der Malignität des ES beitragen. Durch Genexpressionsanalysen wurde gezeigt, dass die posterioren *HOXD* Gene weder durch das pathognomonische Fusionsgen *EWS-FLI1*, noch durch EZH2, einem wichtigen epigenetischen Regulator im ES, reguliert werden. Die Suppression von DKK2, einem Agonisten des Wnt/ß-catenin Signalwegs im ES, reduzierte die Expression der posterioren *HOXD* Gene signifikant, was darauf hindeutet, dass aktive Wnt Signale die Expression der posterioren *HOXD* Gene im ES induzieren. Da NCSC als mutmaßliche Ursprungszellen des ES gelten, wurde die Wirkung der posterioren *HOXD* Gene auf die Fähigkeit zur neuronalen Differenzierung untersucht. Während HOXD10 und HOXD11 nur vereinzelte Effekte auf neuronale Markergene hatten, verstärkte die Herunterregulierung von HOXD13 die Expression von drei neuronalen Markergenen. Dies weist darauf hin, dass HOXD13 durch Hemmung der neuronalen Differenzierung zu dem unreifen Phänotyp des ES beitragen könnte. Um die Wirkung der posterioren *HOXD* Gene auf das osteotrope Tumorwachstum zu beurteilen, wurden Genexpressionsanalysen knochenassoziierter Gene in ES-Zellen mit HOXD Suppression durchgeführt. Die simultane Herrunterregulierung von HOXD10, HOXD11 und HOXD13 führte zu einer signifikanten Verringerung der Expression von RUNX2, einem Schlüsselfaktor der

Osteoblastendifferenzierung und Knochenbildung. Die Hemmung einzelner *HOXD* Gene zeigte darüber hinaus, dass die Regulierung von IL6 von HOXD10 abhängt. Nachfolgende *in vivo* Untersuchungen ergaben, dass die posteriore HOXD Suppression keinen Einfluss auf die Infiltration des kortikalen Knochens hat, aber die Invasivität ins Knochenmark und die Anzahl der $TRAP^+$ Osteoklasten verringert, was vermutlich durch RUNX2 vermittelt wird. Um die Wirkung der posterioren *HOXD* Gene auf den invasiven und metastasierenden Phänotyp des ES zu überprüfen, wurde die Proliferation, das kontakt-unabhängige Wachstum und die Invasivität in Zellen nach HOXD Suppression *in vitro* untersucht. Während das kontakt-unabhängige Wachstum von HOXD11 und HOXD13 gefördert wurde, waren die Proliferation und die Invasivität von HOXD10 und HOXD13 abhängig. Der beobachtete Effekt auf das invasive Verhalten wird wahrscheinlich zum Teil von MMP1, einem Hauptfaktor der Metastasierung beim ES, vermittelt, da gezeigt wurde, dass die einzelne Hemmung von HOXD11 und HOXD13 als auch die gleichzeitige Herrunterregulierung aller drei *HOXD* Gene die Expression von MMP1 maßgeblich reduzierten. In Übereinstimmung mit diesen Resultaten verringerte die Suppression von HOXD11 und HOXD13 auch die Anzahl der Lungenmetastasen *in vivo* signifikant. Diese Ergebnisse weisen auf eine deutliche Beteiligung von HOXD10, HOXD11 und HOXD13 an der Malignität des ES hin und könnten deshalb als Grundlage für weitere Untersuchungen bezüglich ihrer Eignung als ES-spezifische therapeutische Zielgene dienen.

8. References

Abate-Shen, C. (2002): Deregulated homeobox gene expression in cancer: cause or consequence? In: *Nature reviews. Cancer* 2 (10), S. 777–785.

Abdelmaksoud-Dammak, R.; Chamtouri, N.; Triki, M.; Saadallah-Kallel, A.; Ayadi, W.; Charfi, S.; Khabir, A.; Ayadi, L.; Sallemi-Boudawara, T.; Mokdad-Gargouri, R. (2017): Overexpression of miR-10b in colorectal cancer patients: Correlation with TWIST-1 and E-cadherin expression. In: *Tumour biology : the journal of the International Society for Oncodevelopmental Biology and Medicine* 39 (3), 1010428317695916.

ACEA Biosciences: The xCELLigence Real-Time Cell Analysis (RTCA) assay principle (2017). Online verfügbar unter https://www.aceabio.com/xcelligence-real-time-cell-analysis-rtca-assay-principle/, zuletzt aktualisiert am 8/14/2017, zuletzt geprüft am 12/1/2018.

Ahmed, A. A.; Sherman, A. K.; Pawel, B. R. (2012): Expression of therapeutic targets in Ewing sarcoma family tumors. In: *Human pathology* 43 (7), S. 1077–1083.

Aigner, L.; Arber, S.; Kapfhammer, J. P.; Laux, T.; Schneider, C.; Botteri, F.; Brenner, H. R.; Caroni, P. (1995): Overexpression of the neural growth-associated protein GAP-43 induces nerve sprouting in the adult nervous system of transgenic mice. In: *Cell* 83 (2), S. 269–278.

Akarsu, A. N.; Stoilov, I.; Yilmaz, E.; Sayli, B. S.; Sarfarazi, M. (1996): Genomic structure of HOXD13 gene: a nine polyalanine duplication causes synpolydactyly in two unrelated families. In: *Human molecular genetics* 5 (7), S. 945–952.

Alava, E. de; Kawai, A.; Healey, J. H.; Fligman, I.; Meyers, P. A.; Huvos, A. G.; Gerald, W. L.; Jhanwar, S. C.; Argani, P.; Antonescu, C. R.; Pardo-Mindan, F. J.; Ginsberg, J.; Womer, R.; Lawlor, E. R.; Wunder, J.; Andrulis, I.; Sorensen, P. H.; Barr, F. G.; Ladanyi, M. (1998): EWS-FLI1 fusion transcript structure is an independent determinant of prognosis in Ewing's sarcoma. In: *Journal of clinical oncology : official journal of the American Society of Clinical Oncology* 16 (4), S. 1248–1255.

Alharbi, R. A.; Pandha, H. S.; Simpson, G. R.; Pettengell, R.; Poterlowicz, K.; Thompson, A.; Harrington, K.; El-Tanani, M.; Morgan, R. (2017): Inhibition of HOX/PBX dimer formation leads to necroptosis in acute myeloid leukemia cells. In: *Oncotarget* 8 (52), S. 89566–89579.

Alharbi, R. A.; Pettengell, R.; Pandha, H. S.; Morgan, R. (2013): The role of HOX genes in normal hematopoiesis and acute leukemia. In: *Leukemia* 27 (5), S. 1000–1008.

Ambros, I. M.; Ambros, P. F.; Strehl, S.; Kovar, H.; Gadner, H.; Salzer-Kuntschik, M. (1991): MIC2 is a specific marker for Ewing's sarcoma and peripheral primitive neuroectodermal tumors. Evidence for a common histogenesis of Ewing's sarcoma and peripheral primitive neuroectodermal tumors from MIC2 expression and specific chromosome aberration. In: *Cancer* 67 (7), S. 1886–1893.

An, N.; Luo, X.; Zhang, M.; Yu, R. (2017): MicroRNA-376b promotes breast cancer metastasis by targeting Hoxd10 directly. In: *Experimental and therapeutic medicine* 13 (1), S. 79–84.

Arnaldez, F. I.; Helman, L. J. (2014): New strategies in ewing sarcoma: lost in translation? In: *Clinical cancer research : an official journal of the American Association for Cancer Research* 20 (12), S. 3050–3056.

Bachman, K. E.; Park, B. H. (2005): Duel nature of TGF-beta signaling: tumor suppressor vs. tumor promoter. In: *Current opinion in oncology* 17 (1), S. 49–54.

Bais, M.; McLean, J.; Sebastiani, P.; Young, M.; Wigner, N.; Smith, T.; Kotton, D. N.; Einhorn, T. A.; Gerstenfeld, L. C. (2009): Transcriptional analysis of fracture healing and the induction of embryonic stem cell-related genes. In: *PloS one* 4 (5), e5393.

Ban, J.; Bennani-Baiti, I. M.; Kauer, M.; Schaefer, K.-L.; Poremba, C.; Jug, G.; Schwentner, R.; Smrzka, O.; Muehlbacher, K.; Aryee, Dave N T; Kovar, H. (2008): EWS-FLI1 suppresses NOTCH-activated p53 in Ewing's sarcoma. In: *Cancer research* 68 (17), S. 7100–7109.

Bateson, W. (1894). Materials for the study of variation. In: *London: MacMillan*.

Beh, C. Y.; El-Sharnouby, S.; Chatzipli, A.; Russell, S.; Choo, S. W.; White, R. (2016): Roles of cofactors and chromatin accessibility in Hox protein target specificity. In: *Epigenetics & chromatin* 9, S. 1.

Bennani-Baiti, I. M.; Cooper, A.; Lawlor, E. R.; Kauer, M.; Ban, J.; Aryee, Dave N T; Kovar, H. (2010): Intercohort gene expression co-analysis reveals chemokine receptors as prognostic indicators in Ewing's sarcoma. In: *Clinical cancer research : an official journal of the American Association for Cancer Research* 16 (14), S. 3769–3778.

Benowitz, L. I.; Routtenberg, A. (1997): GAP-43: an intrinsic determinant of neuronal development and plasticity. In: *Trends in Neurosciences* 20 (2), S. 84–91.

Bergers, G.; Brekken, R.; McMahon, G.; Vu, T. H.; Itoh, T.; Tamaki, K.; Tanzawa, K.; Thorpe, P.; Itohara, S.; Werb, Z.; Hanahan, D. (2000): Matrix metalloproteinase-9 triggers the angiogenic switch during carcinogenesis. In: *Nature cell biology* 2 (10), S. 737–744.

Bernstein, M.; Kovar, H.; Paulussen, M.; Randall, R. L.; Schuck, A.; Teot, L. A.; Juergens, H. (2006): Ewing's sarcoma family of tumors: current management. In: *The oncologist* 11 (5), S. 503–519.

Biermann, J. S.; Chow, W.; Reed, D. R.; Lucas, D.; Adkins, D. R.; Agulnik, M.; Benjamin, R. S.; Brigman, B.; Budd, G. T.; Curry, W. T.; Didwania, A.; Fabbri, N.; Hornicek, F. J.; Kuechle, J. B.; Lindskog, D.; Mayerson, J.; McGarry, S. V.; Million, L.; Morris, C. D.; Movva, S.; O'Donnell, R. J.; Randall, R. L.; Rose, P.; Santana, V. M.; Satcher, R. L.; Schwartz, H.; Siegel, H. J.; Thornton, K.; Villalobos, V.; Bergman, M. A.; Scavone, J. L.

(2017): NCCN Guidelines Insights: Bone Cancer, Version 2.2017. In: *Journal of the National Comprehensive Cancer Network : JNCCN* 15 (2), S. 155–167.

Biswas, B.; Bakhshi, S. (2016): Management of Ewing sarcoma family of tumors: Current scenario and unmet need. In: *World journal of orthopedics* 7 (9), S. 527–538.

Blaeschke, F.; Thiel, U.; Kirschner, A.; Thiede, M.; Rubio, R. A.; Schirmer, D.; Kirchner, T.; Richter, Günther H S; Mall, S.; Klar, R.; Riddell, S.; Busch, D. H.; Krackhardt, A.; Grunewald, Thomas G P; Burdach, S. (2016): Human HLA-A*02:01/CHM1+ allo-restricted T cell receptor transgenic CD8+ T cells specifically inhibit Ewing sarcoma growth in vitro and in vivo. In: *Oncotarget* 7 (28), S. 43267–43280.

Boncinelli, E. (1997): Homeobox genes and disease. In: *Current opinion in genetics & development* 7 (3), S. 331–337.

Bonewald, L. F.; Johnson, M. L. (2008): Osteocytes, mechanosensing and Wnt signaling. In: *Bone* 42 (4), S. 606–615.

Boulet, A. M.; Capecchi, M. R. (2002): Duplication of the Hoxd11 gene causes alterations in the axial and appendicular skeleton of the mouse. In: *Developmental biology* 249 (1), S. 96–107.

Boulet, A. M.; Capecchi, M. R. (2004): Multiple roles of Hoxa11 and Hoxd11 in the formation of the mammalian forelimb zeugopod. In: *Development (Cambridge, England)* 131 (2), S. 299–309.

Breau, M. A.; Wilkinson, D. G.; Xu, Q. (2013): A Hox gene controls lateral line cell migration by regulating chemokine receptor expression downstream of Wnt signaling. In: *Proceedings of the National Academy of Sciences of the United States of America* 110 (42), S. 16892–16897.

Brenner, J. C.; Feng, F. Y.; Han, S.; Patel, S.; Goyal, S. V.; Bou-Maroun, L. M.; Liu, M.; Lonigro, R.; Prensner, J. R.; Tomlins, S. A.; Chinnaiyan, A. M. (2012): PARP-1 inhibition as a targeted strategy to treat Ewing's sarcoma. In: *Cancer research* 72 (7), S. 1608–1613.

Bridges, C. B. (1921): Genetical and Cytological Proof of Non-disjunction of the Fourth Chromosome of Drosophila Melanogaster. In: *Proceedings of the National Academy of Sciences of the United States of America* 7 (7), S. 186–192.

Brose, K.; Bland, K. S.; Wang, K. H.; Arnott, D.; Henzel, W.; Goodman, C. S.; Tessier-Lavigne, M.; Kidd, T. (1999): Slit proteins bind Robo receptors and have an evolutionarily conserved role in repulsive axon guidance. In: *Cell* 96 (6), S. 795–806.

Bruderer, M.; Richards, R. G.; Alini, M.; Stoddart, M. J. (2014): Role and regulation of RUNX2 in osteogenesis. In: *European cells & materials* 28, S. 269–286.

Bruneau, S.; Johnson, K. R.; Yamamoto, M.; Kuroiwa, A.; Duboule, D. (2001): The mouse Hoxd13(spdh) mutation, a polyalanine expansion similar to human type II

synpolydactyly (SPD), disrupts the function but not the expression of other Hoxd genes. In: *Developmental biology* 237 (2), S. 345–353.

Burchill, S. A. (2008): Molecular abnormalities in Ewing's sarcoma. In: *Expert review of anticancer therapy* 8 (10), S. 1675–1687.

Burdach, S. (2004): Treatment of advanced Ewing tumors by combined radiochemotherapy and engineered cellular transplants. In: *Pediatric transplantation* 8 Suppl 5, S. 67–82.

Burdach, S.; Jürgens, H. (2002): High-dose chemoradiotherapy (HDC) in the Ewing family of tumors (EFT). In: *Critical Reviews in Oncology/Hematology* 41 (2), S. 169–189.

Burdach, S.; Meyer-Bahlburg, A.; Laws, H. J.; Haase, R.; van Kaik, B.; Metzner, B.; Wawer, A.; Finke, R.; Göbel, U.; Haerting, J.; Pape, H.; Gadner, H.; Dunst, J.; Juergens, H. (2003): High-dose therapy for patients with primary multifocal and early relapsed Ewing's tumors: results of two consecutive regimens assessing the role of total-body irradiation. In: *Journal of clinical oncology : official journal of the American Society of Clinical Oncology* 21 (16), S. 3072–3078.

Burdach, S.; Plehm, S.; Unland, R.; Borkhardt, A.; Staege, M. S.; Müller-Tidow, C.; Richter, G. H.S. (2009): Epigenetic maintenance of stemness and malignancy in peripheral neuroectodermal tumors by EZH2. In: *Cell Cycle* 8 (13), S. 1991–1996.

Burdach, S.; Thiel, U.; Schöniger, M.; Haase, R.; Wawer, A.; Nathrath, M.; Kabisch, H.; Urban, C.; Laws, H. J.; Dirksen, U.; Steinborn, M.; Dunst, J.; Jürgens, H. (2010): Total body MRI-governed involved compartment irradiation combined with high-dose chemotherapy and stem cell rescue improves long-term survival in Ewing tumor patients with multiple primary bone metastases. In: *Bone marrow transplantation* 45 (3), S. 483–489.

Burdach, S.; van Kaick, B.; Laws, H. J.; Ahrens, S.; Haase, R.; Körholz, D.; Pape, H.; Dunst, J.; Kahn, T.; Willers, R.; Engel, B.; Dirksen, U.; Kramm, C.; Nürnberger, W.; Heyll, A.; Ladenstein, R.; Gadner, H.; Jürgens, H.; Go el, U. (2000): Allogeneic and autologous stem-cell transplantation in advanced Ewing tumors. An update after long-term follow-up from two centers of the European Intergroup study EICESS. Stem-Cell Transplant Programs at Düsseldorf University Medical Center, Germany and St. Anna Kinderspital, Vienna, Austria. In: *Annals of oncology : official journal of the European Society for Medical Oncology* 11 (11), S. 1451–1462.

Burdach, S. E. G.; Westhoff, M.-A.; Steinhauser, M. F.; Debatin, K.-M. (2018): Precision medicine in pediatric oncology. In: *Molecular and cellular pediatrics* 5 (1), S. 6.

Burger, J. A.; Kipps, T. J. (2006): CXCR4: a key receptor in the crosstalk between tumor cells and their microenvironment. In: *Blood* 107 (5), S. 1761–1767.

Bürglin, T. R.; Affolter, M. (2016): Homeodomain proteins: an update. In: *Chromosoma* 125 (3), S. 497–521.

Cai, L.-y.; Abe, M.; Izumi, S.-i.; Imura, M.; Yasugi, T.; Ushijima, T. (2007): Identification of PRTFDC1 silencing and aberrant promoter methylation of GPR150, ITGA8 and HOXD11 in ovarian cancers. In: *Life sciences* 80 (16), S. 1458–1465.

Cantile, M.; Franco, R.; Tschan, A.; Baumhoer, D.; Zlobec, I.; Schiavo, G.; Forte, I.; Bihl, M.; Liguori, G.; Botti, G.; Tornillo, L.; Karamitopoulou-Diamantis, E.; Terracciano, L.; Cillo, C. (2009): HOX D13 expression across 79 tumor tissue types. In: *International journal of cancer* 125 (7), S. 1532–1541.

Carrillo, J.; Agra, N.; Fernández, N.; Pestaña, A.; Alonso, J. (2009): Devazepide, a nonpeptide antagonist of CCK receptors, induces apoptosis and inhibits Ewing tumor growth. In: *Anti-cancer drugs* 20 (7), S. 527–533.

Carrillo, J.; García-Aragoncillo, E.; Azorín, D.; Agra, N.; Sastre, A.; González-Mediero, I.; García-Miguel, P.; Pestaña, A.; Gallego, S.; Segura, D.; Alonso, J. (2007): Cholecystokinin down-regulation by RNA interference impairs Ewing tumor growth. In: *Clinical cancer research : an official journal of the American Association for Cancer Research* 13 (8), S. 2429–2440.

Carrio, M.; Arderiu, G.; Myers, C.; Boudreau, N. J. (2005): Homeobox D10 induces phenotypic reversion of breast tumor cells in a three-dimensional culture model. In: *Cancer research* 65 (16), S. 7177–7185.

Casey, D. L.; Wexler, L. H.; Meyers, P. A.; Magnan, H.; Chou, A. J.; Wolden, S. L. (2015): Radiation for bone metastases in Ewing sarcoma and rhabdomyosarcoma. In: *Pediatric blood & cancer* 62 (3), S. 445–449.

Catalano, V.; Turdo, A.; Di Franco, S.; Dieli, F.; Todaro, M.; Stassi, G. (2013): Tumor and its microenvironment: a synergistic interplay. In: *Seminars in cancer biology* 23 (6 Pt B), S. 522–532.

Chang, Q.; Daly, L.; Bromberg, J. (2014): The IL-6 feed-forward loop: a driver of tumorigenesis. In: *Seminars in immunology* 26 (1), S. 48–53.

Chao, M. V.; Bothwell, M. A.; Ross, A. H.; Koprowski, H.; Lanahan, A. A.; Buck, C. R.; Sehgal, A. (1986): Gene transfer and molecular cloning of the human NGF receptor. In: *Science (New York, N.Y.)* 232 (4749), S. 518–521.

Chaturvedi, A.; Hoffman, L. M.; Welm, A. L.; Lessnick, S. L.; Beckerle, M. C. (2012): The EWS/FLI Oncogene Drives Changes in Cellular Morphology, Adhesion, and Migration in Ewing Sarcoma. In: *Genes & cancer* 3 (2), S. 102–116.

Cheng, W.; Liu, J.; Yoshida, H.; Rosen, D.; Naora, H. (2005): Lineage infidelity of epithelial ovarian cancers is controlled by HOX genes that specify regional identity in the reproductive tract. In: *Nature medicine* 11 (5), S. 531–537.

Chimge, N.-O.; Frenkel, B. (2013): The RUNX family in breast cancer: relationships with estrogen signaling. In: *Oncogene* 32 (17), S. 2121–2130.

Choe, A.; Phun, H. Q.; Tieu, D. D.; Hu, Y. H.; Carpenter, E. M. (2006): Expression patterns of Hox10 paralogous genes during lumbar spinal cord development. In: *Gene expression patterns : GEP* 6 (7), S. 730–737.

Choi, B. H.; Kim, R. C. (1984): Expression of glial fibrillary acidic protein in immature oligodendroglia. In: *Science (New York, N.Y.)* 223 (4634), S. 407–409.

Cidre-Aranaz, F.; Alonso, J. (2015): EWS/FLI1 Target Genes and Therapeutic Opportunities in Ewing Sarcoma. In: *Frontiers in oncology* 5, S. 162.

Cojoc, M.; Peitzsch, C.; Trautmann, F.; Polishchuk, L.; Telegeev, G. D.; Dubrovska, A. (2013): Emerging targets in cancer management: role of the CXCL12/CXCR4 axis. In: *OncoTargets and therapy* 6, S. 1347–1361.

Coleman, R. E. (2001): Metastatic bone disease: clinical features, pathophysiology and treatment strategies. In: *Cancer treatment reviews* 27 (3), S. 165–176.

Condie, B. G.; Capecchi, M. R. (1993): Mice homozygous for a targeted disruption of Hoxd-3 (Hox-4.1) exhibit anterior transformations of the first and second cervical vertebrae, the atlas and the axis. In: *Development (Cambridge, England)* 119 (3), S. 579–595.

Corey, E.; Quinn, J. E.; Bladou, F.; Brown, L. G.; Roudier, M. P.; Brown, J. M.; Buhler, K. R.; Vessella, R. L. (2002): Establishment and characterization of osseous prostate cancer models: intra-tibial injection of human prostate cancer cells. In: *The Prostate* 52 (1), S. 20–33.

Cowherd, R. M.; Lyle, R. E.; Miller, C. P.; Mcgehee, R. E. (1997): Developmental profile of homeobox gene expression during 3T3-L1 adipogenesis. In: *Biochemical and biophysical research communications* 237 (2), S. 470–475.

Daftary, G. S.; Taylor, H. S. (2006): Endocrine regulation of HOX genes. In: *Endocrine reviews* 27 (4), S. 331–355.

Dancey, J. E. (2006): Therapeutic targets: MTOR and related pathways. In: *Cancer biology & therapy* 5 (9), S. 1065–1073.

Davis, A. P.; Capecchi, M. R. (1994): Axial homeosis and appendicular skeleton defects in mice with a targeted disruption of hoxd-11. In: *Development (Cambridge, England)* 120 (8), S. 2187–2198.

Davis, A. P.; Witte, D. P.; Hsieh-Li, H. M.; Potter, S. S.; Capecchi, M. R. (1995): Absence of radius and ulna in mice lacking hoxa-11 and hoxd-11. In: *Nature* 375 (6534), S. 791–795.

Daw, N. C.; Laack, N. N.; McIlvaine, E. J.; Krailo, M.; Womer, R. B.; Granowetter, L.; Grier, H. E.; Marina, N. M.; Bernstein, M. L.; Gebhardt, M. C.; Marcus, K. J.; Advani, S. M.; Healey, J. H.; Letson, G. D.; Gorlick, R. G.; Randall, R. L. (2016): Local Control Modality and Outcome for Ewing Sarcoma of the Femur: A Report From the Children's Oncology Group. In: *Annals of surgical oncology* 23 (11), S. 3541–3547.

de Barros E Lima Bueno, R.; Ramão, A.; Pinheiro, D. G.; Alves, C. P.; Kannen, V.; Jungbluth, A. A.; Araújo, L. F. de; Muys, B. R.; Fonseca, A. S.; Plaça, J. R.; Panepucci, R. A.; Neder, L.; Saggioro, F. P.; Mamede, R. C. M.; Figueiredo, D. L. A.; Silva, W. A. (2016): HOX genes: potential candidates for the progression of laryngeal squamous cell carcinoma. In: *Tumour biology : the journal of the International Society for Oncodevelopmental Biology and Medicine* 37 (11), S. 15087–15096.

Delattre, O.; Zucman, J.; Plougastel, B.; Desmaze, C.; Melot, T.; Peter, M.; Kovar, H.; Joubert, I.; Jong, P. de; Rouleau, G. (1992): Gene fusion with an ETS DNA-binding domain caused by chromosome translocation in human tumours. In: *Nature* 359 (6391), S. 162–165.

Dimova, I.; Popivanov, G.; Djonov, V. (2014): Angiogenesis in cancer - general pathways and their therapeutic implications. In: *Journal of B.U.ON. : official journal of the Balkan Union of Oncology* 19 (1), S. 15–21.

Dobbs, M. B.; Gurnett, C. A.; Pierce, B.; Exner, G. U.; Robarge, J.; Morcuende, J. A.; Cole, W. G.; Templeton, P. A.; Foster, B.; Bowcock, A. M. (2006): HOXD10 M319K mutation in a family with isolated congenital vertical talus. In: *Journal of orthopaedic research : official publication of the Orthopaedic Research Society* 24 (3), S. 448–453.

Dohjima, T.; Lee, N. S.; Li, H.; Ohno, T.; Rossi, J. J. (2003): Small interfering RNAs expressed from a Pol III promoter suppress the EWS/Fli-1 transcript in an Ewing sarcoma cell line. In: *Molecular therapy : the journal of the American Society of Gene Therapy* 7 (6), S. 811–816.

Domanska, U. M.; Kruizinga, R. C.; Nagengast, W. B.; Timmer-Bosscha, H.; Huls, G.; de Vries, Elisabeth G E; Walenkamp, Annemiek M E (2013): A review on CXCR4/CXCL12 axis in oncology: no place to hide. In: *European journal of cancer (Oxford, England : 1990)* 49 (1), S. 219–230.

Donovan, J.; Abraham, D.; Norman, J. (2013): Platelet-derived growth factor signaling in mesenchymal cells. In: *Frontiers in bioscience (Landmark edition)* 18, S. 106–119.

Duan, P.; Bonewald, L. F. (2016): The role of the wnt/β-catenin signaling pathway in formation and maintenance of bone and teeth. In: *The international journal of biochemistry & cell biology* 77 (Pt A), S. 23–29.

DuBois, S. G.; Krailo, M. D.; Gebhardt, M. C.; Donaldson, S. S.; Marcus, K. J.; Dormans, J.; Shamberger, R. C.; Sailer, S.; Nicholas, R. W.; Healey, J. H.; Tarbell, N. J.; Randall, R. L.; Devidas, M.; Meyer, J. S.; Granowetter, L.; Womer, R. B.; Bernstein, M.; Marina, N.; Grier, H. E. (2015): Comparative evaluation of local control strategies in localized Ewing sarcoma of bone: a report from the Children's Oncology Group. In: *Cancer* 121 (3), S. 467–475.

Duboule, D. (1992): The vertebrate limb: a model system to study the Hox/HOM gene network during development and evolution. In: *BioEssays : news and reviews in molecular, cellular and developmental biology* 14 (6), S. 375–384.

Dunn, T.; Praissman, L.; Hagag, N.; Viola, M. V. (1994): ERG gene is translocated in an Ewing's sarcoma cell line. In: *Cancer Genetics and Cytogenetics* 76 (1), S. 19–22.

Eng, L. F.; Ghirnikar, R. S.; Lee, Y. L. (2000): Glial fibrillary acidic protein: GFAP-thirty-one years (1969-2000). In: *Neurochemical research* 25 (9-10), S. 1439–1451.

Engert, F.; Schneider, C.; Weiβ, L. M.; Probst, M.; Fulda, S. (2015): PARP Inhibitors Sensitize Ewing Sarcoma Cells to Temozolomide-Induced Apoptosis via the Mitochondrial Pathway. In: *Molecular cancer therapeutics* 14 (12), S. 2818–2830.

Enomoto, H.; Shiojiri, S.; Hoshi, K.; Furuichi, T.; Fukuyama, R.; Yoshida, C. A.; Kanatani, N.; Nakamura, R.; Mizuno, A.; Zanma, A.; Yano, K.; Yasuda, H.; Higashio, K.; Takada, K.; Komori, T. (2003): Induction of osteoclast differentiation by Runx2 through receptor activator of nuclear factor-kappa B ligand (RANKL) and osteoprotegerin regulation and partial rescue of osteoclastogenesis in Runx2-/- mice by RANKL transgene. In: *Journal of Biological Chemistry* 278 (26), S. 23971–23977.

Esiashvili, N.; Goodman, M.; Marcus, R. B. (2008): Changes in incidence and survival of Ewing sarcoma patients over the past 3 decades: Surveillance Epidemiology and End Results data. In: *Journal of pediatric hematology/oncology* 30 (6), S. 425–430.

Ewing, J. (1972): Classics in oncology. Diffuse endothelioma of bone. James Ewing. Proceedings of the New York Pathological Society, 1921. In: *CA: a cancer journal for clinicians* 22 (2), S. 95–98.

Fassel, H.; Tracy, D.; Louer, K.; Klement, G. L. (2016): Insulin-like Growth Factor Receptor Inhibition as Maintenance Therapy for Metastatic Ewing Sarcoma. In: *Journal of pediatric hematology/oncology* 38 (7), S. 563–569.

Fellinger, E. J.; Garin-Chesa, P.; Su, S. L.; DeAngelis, P.; Lane, J. M.; Rettig, W. J. (1991): Biochemical and genetic characterization of the HBA71 Ewing's sarcoma cell surface antigen. In: *Cancer research* 51 (1), S. 336–340.

Ferrari, N.; McDonald, L.; Morris, J. S.; Cameron, E. R.; Blyth, K. (2013): RUNX2 in mammary gland development and breast cancer. In: *Journal of cellular physiology* 228 (6), S. 1137–1142.

Franzetti, G.-A.; Laud-Duval, K.; van der Ent, W.; Brisac, A.; Irondelle, M.; Aubert, S.; Dirksen, U.; Bouvier, C.; Pinieux, G. de; Snaar-Jagalska, E.; Chavrier, P.; Delattre, O. (2017): Cell-to-cell heterogeneity of EWSR1-FLI1 activity determines proliferation/migration choices in Ewing sarcoma cells. In: *Oncogene* 36 (25), S. 3505–3514.

Franzius, C.; Hotfilder, M.; Poremba, C.; Hermann, S.; Schäfers, K.; Gabbert, H. E.; Jürgens, H.; Schober, O.; Schäfers, M.; Vormoor, J. (2006): Successful high-resolution animal positron emission tomography of human Ewing tumours and their metastases in a murine xenograft model. In: *European journal of nuclear medicine and molecular imaging* 33 (12), S. 1432–1441.

Fröhling, S.; Scholl, C.; Bansal, D.; Huntly, Brian J P (2007): HOX gene regulation in acute myeloid leukemia: CDX marks the spot? In: *Cell cycle (Georgetown, Tex.)* 6 (18), S. 2241–2245.

Gao, L.; Sun, J.; Liu, F.; Zhang, H.; Ma, Y. (2016): Higher expression levels of the HOXA9 gene, closely associated with MLL-PTD and EZH2 mutations, predict inferior outcome in acute myeloid leukemia. In: *OncoTargets and therapy* 9, S. 711–722.

Garber, R. L.; Kuroiwa, A.; Gehring, W. J. (1983): Genomic and cDNA clones of the homeotic locus Antennapedia in Drosophila. In: *The EMBO journal* 2 (11), S. 2027–2036.

García-Aragoncillo, E.; Carrillo, J.; Lalli, E.; Agra, N.; Gómez-López, G.; Pestaña, A.; Alonso, J. (2008): DAX1, a direct target of EWS/FLI1 oncoprotein, is a principal regulator of cell-cycle progression in Ewing's tumor cells. In: *Oncogene* 27 (46), S. 6034–6043.

Gaspar, N.; Hawkins, D. S.; Dirksen, U.; Lewis, I. J.; Ferrari, S.; Le Deley, M.-C.; Kovar, H.; Grimer, R.; Whelan, J.; Claude, L.; Delattre, O.; Paulussen, M.; Picci, P.; Sundby Hall, K.; van den Berg, Hendrik; Ladenstein, R.; Michon, J.; Hjorth, L.; Judson, I.; Luksch, R.; Bernstein, M. L.; Marec-Bérard, P.; Brennan, B.; Craft, A. W.; Womer, R. B.; Juergens, H.; Oberlin, O. (2015): Ewing Sarcoma: Current Management and Future Approaches Through Collaboration. In: *Journal of clinical oncology : official journal of the American Society of Clinical Oncology* 33 (27), S. 3036–3046.

Gehring, W. J.; Affolter, M.; Bürglin, T. (1994): Homeodomain proteins. In: *Annual review of biochemistry* 63, S. 487–526.

Gehring, W. J.; Hiromi, Y. (1986): Homeotic genes and the homeobox. In: *Annual review of genetics* 20, S. 147–173.

Gersch, R. P.; Lombardo, F.; McGovern, S. C.; Hadjiargyrou, M. (2005): Reactivation of Hox gene expression during bone regeneration. In: *Journal of orthopaedic research : official publication of the Orthopaedic Research Society* 23 (4), S. 882–890.

Giard, D. J.; Aaronson, S. A.; Todaro, G. J.; Arnstein, P.; Kersey, J. H.; Dosik, H.; Parks, W. P. (1973): In vitro cultivation of human tumors: establishment of cell lines derived from a series of solid tumors. In: *Journal of the National Cancer Institute* 51 (5), S. 1417–1423.

Glass, D. A.; Karsenty, G. (2007): In vivo analysis of Wnt signaling in bone. In: *Endocrinology* 148 (6), S. 2630–2634.

Goldman, J. P.; Blundell, M. P.; Lopes, L.; Kinnon, C.; Di Santo, J P; Thrasher, A. J. (1998): Enhanced human cell engraftment in mice deficient in RAG2 and the common cytokine receptor gamma chain. In: *British journal of haematology* 103 (2), S. 335–342.

Goodman, F. R.; Scambler, P. J. (2001): Human HOX gene mutations. In: *Clinical genetics* 59 (1), S. 1–11.

Gorski, D. H.; Walsh, K. (2000): The role of homeobox genes in vascular remodeling and angiogenesis. In: *Circulation research* 87 (10), S. 865–872.

Goswami, S.; Sharma-Walia, N. (2016): Osteoprotegerin rich tumor microenvironment: implications in breast cancer. In: *Oncotarget* 7 (27), S. 42777–42791.

Grasselli, G.; Strata, P. (2013): Structural plasticity of climbing fibers and the growth-associated protein GAP-43. In: *Frontiers in neural circuits* 7, S. 25.

Grier, D. G.; Thompson, A.; Kwasniewska, A.; McGonigle, G. J.; Halliday, H. L.; Lappin, T. R. (2005): The pathophysiology of HOX genes and their role in cancer. In: *The Journal of pathology* 205 (2), S. 154–171.

Grier, H. E.; Krailo, M. D.; Tarbell, N. J.; Link, M. P.; Fryer, Christopher J H; Pritchard, D. J.; Gebhardt, M. C.; Dickman, P. S.; Perlman, E. J.; Meyers, P. A.; Donaldson, S. S.; Moore, S.; Rausen, A. R.; Vietti, T. J.; Miser, J. S. (2003): Addition of ifosfamide and etoposide to standard chemotherapy for Ewing's sarcoma and primitive neuroectodermal tumor of bone. In: *The New England journal of medicine* 348 (8), S. 694–701.

Gröbner, S. N.; Worst, B. C.; Weischenfeldt, J.; Buchhalter, I.; Kleinheinz, K.; Rudneva, V. A.; Johann, P. D.; Balasubramanian, G. P.; Segura-Wang, M.; Brabetz, S.; Bender, S.; Hutter, B.; Sturm, D.; Pfaff, E.; Hübschmann, D.; Zipprich, G.; Heinold, M.; Eils, J.; Lawerenz, C.; Erkek, S.; Lambo, S.; Waszak, S.; Blattmann, C.; Borkhardt, A.; Kuhlen, M.; Eggert, A.; Fulda, S.; Gessler, M.; Wegert, J.; Kappler, R.; Baumhoer, D.; Burdach, S.; Kirschner-Schwabe, R.; Kontny, U.; Kulozik, A. E.; Lohmann, D.; Hettmer, S.; Eckert, C.; Bielack, S.; Nathrath, M.; Niemeyer, C.; Richter, G. H.; Schulte, J.; Siebert, R.; Westermann, F.; Molenaar, J. J.; Vassal, G.; Witt, H.; Burkhardt, B.; Kratz, C. P.; Witt, O.; van Tilburg, C. M.; Kramm, C. M.; Fleischhack, G.; Dirksen, U.; Rutkowski, S.; Frühwald, M.; Hoff, K. von; Wolf, S.; Klingebiel, T.; Koscielniak, E.; Landgraf, P.; Koster, J.; Resnick, A. C.; Zhang, J.; Liu, Y.; Zhou, X.; Waanders, A. J.; Zwijnenburg, D. A.; Raman, P.; Brors, B.; Weber, U. D.; Northcott, P. A.; Pajtler, K. W.; Kool, M.; Piro, R. M.; Korbel, J. O.; Schlesner, M.; Eils, R.; Jones, D. T. W.; Lichter, P.; Chavez, L.; Zapatka, M.; Pfister, S. M. (2018): The landscape of genomic alterations across childhood cancers. In: *Nature* 555 (7696), S. 321–327.

Gross, S.; Krause, Y.; Wuelling, M.; Vortkamp, A. (2012): Hoxa11 and Hoxd11 regulate chondrocyte differentiation upstream of Runx2 and Shox2 in mice. In: *PloS one* 7 (8), e43553.

Grünewald, T. G. P.; Bernard, V.; Gilardi-Hebenstreit, P.; Raynal, V.; Surdez, D.r.; Aynaud, M.; Mirabeau, O.; Cidre-Aranaz, F.; Tirode, F.; Zaidi, S.; Perot, G.; Jonker, A. H.; Lucchesi, C.; Le Deley, M.; Oberlin, O.; Marec-Bérard, P.; Véron, A. S.; Reynaud, S.; Lapouble, E.; Boeva, V.; Rio Frio, T.; Alonso, J.; Bhatia, S.; Pierron, G.; Cancel-Tassin, G.; Cussenot, O.; Cox, D. G.; Morton, L. M.; Machiela, M. J.; Chanock, S. J.; Charnay, P.; Delattre, O. (2015): Chimeric EWSR1-FLI1 regulates the Ewing sarcoma susceptibility gene EGR2 via a GGAA microsatellite. In: *Nature genetics* 47 (9), S. 1073–1078.

Grünewald, T. G. P.; Diebold, I.; Esposito, I.; Plehm, S.; Hauer, K.; Thiel, U.; da Silva-Buttkus, P.; Neff, F.; Unland, R.; Müller-Tidow, C.; Zobywalski, C.; Lohrig, K.; Lewandrowski, U.; Sickmann, A.; Prazeres da Costa, O.; Görlach, A.; Cossarizza, A.; Butt, E.; Richter, G. H. S.; Burdach, S. (2012a): STEAP1 is associated with the invasive and oxidative stress phenotype of Ewing tumors. In: *Molecular cancer research : MCR* 10 (1), S. 52–65.

Grünewald, T. G. P.; Ranft, A.; Esposito, I.; da Silva-Buttkus, P.; Aichler, M.; Baumhoer, D.; Schaefer, K. L.; Ottaviano, L.; Poremba, C.; Jundt, G.; Jürgens, H.; Dirksen, U.; Richter, G. H. S.; Burdach, S. (2012b): High STEAP1 expression is associated with improved outcome of Ewing's sarcoma patients. In: *Annals of oncology : official journal of the European Society for Medical Oncology* 23 (8), S. 2185–2190.

Guan, G.; Zhang, Y.; Lu, Y.; Liu, L.; Shi, D.; Wen, Y.; Yang, L.; Ma, Q.; Liu, T.; Zhu, X.; Qiu, X.; Zhou, Y. (2015): The HIF-1α/CXCR4 pathway supports hypoxia-induced metastasis of human osteosarcoma cells. In: *Cancer letters* 357 (1), S. 254–264.

Guan, H.; Zhou, Z.; Cao, Y.; Duan, X.; Kleinerman, E. S. (2009): VEGF165 promotes the osteolytic bone destruction of Ewing's sarcoma tumors by upregulating RANKL. In: *Oncology research* 18 (2-3), S. 117–125.

Guerzoni, C.; Fiori, V.; Terracciano, M.; Manara, M. C.; Moricoli, D.; Pasello, M.; Sciandra, M.; Nicoletti, G.; Gellini, M.; Dominici, S.; Chiodoni, C.; Fornasari, P. M.; Lollini, P.-L.; Colombo, M. P.; Picci, P.; Cianfriglia, M.; Magnani, M.; Scotlandi, K. (2015): CD99 triggering in Ewing sarcoma delivers a lethal signal through p53 pathway reactivation and cooperates with doxorubicin. In: *Clinical cancer research : an official journal of the American Association for Cancer Research* 21 (1), S. 146–156.

Guo, Y.; Peng, Y.; Gao, D.; Zhang, M.; Yang, W.; Linghu, E.; Herman, J. G.; Fuks, F.; Dong, G.; Guo, M. (2017): Silencing HOXD10 by promoter region hypermethylation activates ERK signaling in hepatocellular carcinoma. In: *Clinical Epigenetics* 9.

Haeusler, J.; Ranft, A.; Boelling, T.; Gosheger, G.; Braun-Munzinger, G.; Vieth, V.; Burdach, S.; van den Berg, Henk; Juergens, H.; Dirksen, U. (2010): The value of local treatment in patients with primary, disseminated, multifocal Ewing sarcoma (PDMES). In: *Cancer* 116 (2), S. 443–450.

Hahm, K. B.; Cho, K.; Lee, C.; Im, Y. H.; Chang, J.; Choi, S. G.; Sorensen, P. H.; Thiele, C. J.; Kim, S. J. (1999): Repression of the gene encoding the TGF-beta type II receptor is a major target of the EWS-FLI1 oncoprotein. In: *Nature genetics* 23 (2), S. 222–227.

Hanahan, D.; Weinberg, R. A. (2000): The hallmarks of cancer. In: *Cell* 100 (1), S. 57–70.

Hauer, K.; Calzada-Wack, J.; Steiger, K.; Grunewald, T. G. P.; Baumhoer, D.; Plehm, S.; Buch, T.; Prazeres da Costa, O.; Esposito, I.; Burdach, S.; Richter, G. H. S. (2013): DKK2 mediates osteolysis, invasiveness, and metastatic spread in Ewing sarcoma. In: *Cancer research* 73 (2), S. 967–977.

Hayano, T.; Matsui, H.; Nakaoka, H.; Ohtake, N.; Hosomichi, K.; Suzuki, K.; Inoue, I. (2016): Germline Variants of Prostate Cancer in Japanese Families. In: *PloS one* 11 (10), e0164233.

Hedlund, E.; Karsten, S. L.; Kudo, L.; Geschwind, D. H.; Carpenter, E. M. (2004): Identification of a Hoxd10-regulated transcriptional network and combinatorial interactions with Hoxa10 during spinal cord development. In: *Journal of neuroscience research* 75 (3), S. 307–319.

Hensel, T.; Giorgi, C.; Schmidt, O.; Calzada-Wack, J.; Neff, F.; Buch, T.; Niggli, F. K.; Schäfer, B. W.; Burdach, S.; Richter, G. H. S. (2016): Targeting the EWS-ETS transcriptional program by BET bromodomain inhibition in Ewing sarcoma. In: *Oncotarget* 7 (2), S. 1451–1463.

Heyking, K. v.; Calzada-Wack, J.; Göllner, S.; Neff, F.; Schmidt, O.; Hensel, T.; Schirmer, D.; Fasan, A.; Esposito, I.; Müller-Tidow, C.; Sorensen, P. H.; Burdach, S.; Richter, G. H. S. (2017): The endochondral bone protein CHM1 sustains an undifferentiated, invasive phenotype, promoting lung metastasis in Ewing sarcoma. In: *Molecular oncology* 11 (9), S. 1288–1301.

Heyking, K. v.; Fasan, A.; Burdach, S.; Richter, G. H. S. (2014): BRICHOS genes CHM1 and ITM2A maintain an undifferentiated, invasive phenotype in Ewing sarcoma. In: *Cancer Res* 74 (19 Supplement), S. 3973.

Heyking, K. v.; Roth, L.; Ertl, M.; Schmidt, O.; Calzada-Wack, J.; Neff, F.; Lawlor, E. R.; Burdach, S.; Richter, G. H. S. (2016): The posterior HOXD locus. Its contribution to phenotype and malignancy of Ewing sarcoma. In: *Oncotarget* 7 (27), S. 41767–41780.

Hol, E. M.; Pekny, M. (2015): Glial fibrillary acidic protein (GFAP) and the astrocyte intermediate filament system in diseases of the central nervous system. In: *Current opinion in cell biology* 32, S. 121–130.

Holland, P. W. H. (2013): Evolution of homeobox genes. In: *Wiley interdisciplinary reviews. Developmental biology* 2 (1), S. 31–45.

Holland, P. W. H.; Booth, H. A. F.; Bruford, E. A. (2007): Classification and nomenclature of all human homeobox genes. In: *BMC biology* 5, S. 47.

Hong, C.-S.; Jeong, O.; Piao, Z.; Guo, C.; Jung, M.-R.; Choi, C.; Park, Y.-K. (2015): HOXB5 induces invasion and migration through direct transcriptional up-regulation of β-catenin in human gastric carcinoma. In: *The Biochemical journal* 472 (3), S. 393–403.

Horton, S. J.; Grier, D. G.; McGonigle, G. J.; Thompson, A.; Morrow, M.; Silva, I. de; Moulding, D. A.; Kioussis, D.; Lappin, Terence R J; Brady, Hugh J M; Williams, O. (2005): Continuous MLL-ENL expression is necessary to establish a "Hox Code" and maintain immortalization of hematopoietic progenitor cells. In: *Cancer research* 65 (20), S. 9245–9252.

Hu, J.; Gray, C. A.; Spencer, T. E. (2004): Gene expression profiling of neonatal mouse uterine development. In: *Biology of reproduction* 70 (6), S. 1870–1876.

Huang, L.; Pu, Y.; Hepps, D.; Danielpour, D.; Prins, G. S. (2007): Posterior Hox gene expression and differential androgen regulation in the developing and adult rat prostate lobes. In: *Endocrinology* 148 (3), S. 1235–1245.

Human Methylcellulose Base Media: R&D Systems. Online verfügbar unter https://www.rndsystems.com/products/human-methylcellulose-base-media_hsc002#product-datasheets, zuletzt geprüft am 12/1/2018.

Im, Y. H.; Kim, H. T.; Lee, C.; Poulin, D.; Welford, S.; Sorensen, P. H.; Denny, C. T.; Kim, S. J. (2000): EWS-FLI1, EWS-ERG, and EWS-ETV1 oncoproteins of Ewing tumor family all suppress transcription of transforming growth factor beta type II receptor gene. In: *Cancer research* 60 (6), S. 1536–1540.

Ito, Y.; Bae, S.-C.; Chuang, L. S. H. (2015): The RUNX family: developmental regulators in cancer. In: *Nature reviews. Cancer* 15 (2), S. 81–95.

Itoh, Y. (2006): MT1-MMP: a key regulator of cell migration in tissue. In: *IUBMB life* 58 (10), S. 589–596.

Iwamoto, Y. (2007): Diagnosis and treatment of Ewing's sarcoma. In: *Japanese journal of clinical oncology* 37 (2), S. 79–89.

Jacques, C.; Lamoureux, F.; Baud'huin, M.; Rodriguez Calleja, L.; Quillard, T.; Amiaud, J.; Tirode, F.; Rédini, F.; Bradner, J. E.; Heymann, D.; Ory, B. (2016): Targeting the epigenetic readers in Ewing sarcoma inhibits the oncogenic transcription factor EWS/Fli1. In: *Oncotarget* 7 (17), S. 24125–24140.

Javaheri, T.; Kazemi, Z.; Pencik, J.; Pham, H. T.; Kauer, M.; Noorizadeh, R.; Sax, B.; Nivarthi, H.; Schlederer, M.; Maurer, B.; Hofbauer, M.; Aryee, D. N.; Wiedner, M.; Tomazou, E. M.; Logan, M.; Hartmann, C.; Tuckermann, J. P.; Kenner, L.; Mikula, M.; Dolznig, H.; Üren, A.; Richter, G. H.; Grebien, F.; Kovar, H.; Moriggl, R. (2016): Increased survival and cell cycle progression pathways are required for EWS/FLI1-induced malignant transformation. In: *Cell death & disease* 7 (10), e2419.

Jawad, M. U.; Cheung, M. C.; Min, E. S.; Schneiderbauer, M. M.; Koniaris, L. G.; Scully, S. P. (2009): Ewing sarcoma demonstrates racial disparities in incidence-related and sex-related differences in outcome: an analysis of 1631 cases from the SEER database, 1973-2005. In: *Cancer* 115 (15), S. 3526–3536.

Jiang, Y.; Ludwig, J.; Janku, F. (2015): Targeted therapies for advanced Ewing sarcoma family of tumors. In: *Cancer treatment reviews* 41 (5), S. 391–400.

Jin, Z.; Zhao, C.; Han, X.; Han, Y. (2012): Wnt5a promotes ewing sarcoma cell migration through upregulating CXCR4 expression. In: *BMC cancer* 12, S. 480.

Johansson, N.; Ahonen, M.; Kähäri, V. M. (2000): Matrix metalloproteinases in tumor invasion. In: *Cellular and molecular life sciences : CMLS* 57 (1), S. 5–15.

Johnson, D.; Kan, S.-H.; Oldridge, M.; Trembath, R. C.; Roche, P.; Esnouf, R. M.; Giele, H.; Wilkie, A. O. M. (2003): Missense mutations in the homeodomain of HOXD13 are associated with brachydactyly types D and E. In: *American journal of human genetics* 72 (4), S. 984–997.

Johnson, D.; Lanahan, A.; Buck, C. R.; Sehgal, A.; Morgan, C.; Mercer, E.; Bothwell, M.; Chao, M. (1986): Expression and structure of the human NGF receptor. In: *Cell* 47 (4), S. 545–554.

Joo, M. K.; Park, J.-J.; Chun, H. J. (2016): Impact of homeobox genes in gastrointestinal cancer. In: *World journal of gastroenterology* 22 (37), S. 8247–8256.

Juergens, C.; Weston, C.; Lewis, I.; Whelan, J.; Paulussen, M.; Oberlin, O.; Michon, J.; Zoubek, A.; Juergens, H.; Craft, A. (2006): Safety assessment of intensive induction with vincristine, ifosfamide, doxorubicin, and etoposide (VIDE) in the treatment of Ewing tumors in the EURO-E.W.I.N.G. 99 clinical trial. In: *Pediatric blood & cancer* 47 (1), S. 22–29.

Juergens, H.; Daw, N. C.; Geoerger, B.; Ferrari, S.; Villarroel, M.; Aerts, I.; Whelan, J.; Dirksen, U.; Hixon, M. L.; Yin, D.; Wang, T.; Green, S.; Paccagnella, L.; Gualberto, A. (2011): Preliminary efficacy of the anti-insulin-like growth factor type 1 receptor antibody figitumumab in patients with refractory Ewing sarcoma. In: *Journal of clinical oncology : official journal of the American Society of Clinical Oncology* 29 (34), S. 4534–4540.

Kachgal, S.; Mace, K. A.; Boudreau, N. J. (2012): The dual roles of homeobox genes in vascularization and wound healing. In: *Cell adhesion & migration* 6 (6), S. 457–470.

Kajdaniuk, D.; Marek, B.; Borgiel-Marek, H.; Kos-Kudła, B. (2013): Transforming growth factor β1 (TGFβ1) in physiology and pathology. In: *Endokrynologia Polska* 64 (5), S. 384–396.

Kauer, M.; Ban, J.; Kofler, R.; Walker, B.; Davis, S.; Meltzer, P.; Kovar, H. (2009): A molecular function map of Ewing's sarcoma. In: *PloS one* 4 (4), e5415.

Ke, Q.; Costa, M. (2006): Hypoxia-inducible factor-1 (HIF-1). In: *Molecular pharmacology* 70 (5), S. 1469–1480.

Keller, E. T. (2002): The role of osteoclastic activity in prostate cancer skeletal metastases. In: *Drugs of today (Barcelona, Spain : 1998)* 38 (2), S. 91–102.

Kelly, Z.; Moller-Levet, C.; McGrath, S.; Butler-Manuel, S.; Kavitha Madhuri, T.; Kierzek, A. M.; Pandha, H.; Morgan, R.; Michael, A. (2016): The prognostic significance of specific HOX gene expression patterns in ovarian cancer. In: *International journal of cancer* 139 (7), S. 1608–1617.

Kennedy, A. L.; Vallurupalli, M.; Chen, L.; Crompton, B.; Cowley, G.; Vazquez, F.; Weir, B. A.; Tsherniak, A.; Parasuraman, S.; Kim, S.; Alexe, G.; Stegmaier, K. (2015): Functional, chemical genomic, and super-enhancer screening identify sensitivity to

cyclin D1/CDK4 pathway inhibition in Ewing sarcoma. In: *Oncotarget* 6 (30), S. 30178–30193.

Kessenbrock, K.; Plaks, V.; Werb, Z. (2010): Matrix metalloproteinases: regulators of the tumor microenvironment. In: *Cell* 141 (1), S. 52–67.

Kim, C.; Nielsen, H. C. (2000): Hoxa-5 in mouse developing lung: cell-specific expression and retinoic acid regulation. In: *American journal of physiology. Lung cellular and molecular physiology* 279 (5), L863-71.

Kim, S. K.; Park, Y.-K. (2016): Ewing sarcoma: a chronicle of molecular pathogenesis. In: *Human pathology* 55, S. 91–100.

Kinsey, M.; Smith, R.; Iyer, A. K.; McCabe, Edward R B; Lessnick, S. L. (2009): EWS/FLI and its downstream target NR0B1 interact directly to modulate transcription and oncogenesis in Ewing's sarcoma. In: *Cancer research* 69 (23), S. 9047–9055.

Kirschner, A.; Thiede, M.; Grünewald, T. G. P.; Alba Rubio, R.; Richter, G. H. S.; Kirchner, T.; Busch, D. H.; Burdach, S.; Thiel, U. (2017): Pappalysin-1 T cell receptor transgenic allo-restricted T cells kill Ewing sarcoma in vitro and in vivo. In: *Oncoimmunology* 6 (2), e1273301.

Kmita, M.; Duboule, D. (2003): Organizing axes in time and space; 25 years of colinear tinkering. In: *Science (New York, N.Y.)* 301 (5631), S. 331–333.

Kmita, M.; Fraudeau, N.; Hérault, Y.; Duboule, D. (2002): Serial deletions and duplications suggest a mechanism for the collinearity of Hoxd genes in limbs. In: *Nature* 420 (6912), S. 145–150.

Knott, M. M. L.; Dallmayer, M.; Grünewald, T. G. P. (2016): Next steps in preventing Ewing sarcoma progression. In: *Future oncology (London, England)* 12 (1), S. 1–4.

Knowles, H. J.; Schaefer, K.-L.; Dirksen, U.; Athanasou, N. A. (2010): Hypoxia and hypoglycaemia in Ewing's sarcoma and osteosarcoma: regulation and phenotypic effects of Hypoxia-Inducible Factor. In: *BMC cancer* 10, S. 372.

Komori, T. (2010): Regulation of bone development and extracellular matrix protein genes by RUNX2. In: *Cell and tissue research* 339 (1), S. 189–195.

Komori, T. (2011): Signaling networks in RUNX2-dependent bone development. In: *Journal of cellular biochemistry* 112 (3), S. 750–755.

Kovar, H. (2005): Context matters: the hen or egg problem in Ewing's sarcoma. In: *Seminars in cancer biology* 15 (3), S. 189–196.

Kovar, H.; Amatruda, J.; Brunet, E.; Burdach, S.; Cidre-Aranaz, F.; Alava, E. de; Dirksen, U.; van der Ent, Wietske; Grohar, P.; Grünewald, Thomas G P; Helman, L.; Houghton, P.; Iljin, K.; Korsching, E.; Ladanyi, M.; Lawlor, E.; Lessnick, S.; Ludwig, J.; Meltzer, P.; Metzler, M.; Mora, J.; Moriggl, R.; Nakamura, T.; Papamarkou, T.; Radic Sarikas, B.; Rédini, F.; Richter, Guenther H S; Rossig, C.; Schadler, K.; Schäfer, B. W.; Scotlandi,

K.; Sheffield, N. C.; Shelat, A.; Snaar-Jagalska, E.; Sorensen, P.; Stegmaier, K.; Stewart, E.; Sweet-Cordero, A.; Szuhai, K.; Tirado, O. M.; Tirode, F.; Toretsky, J.; Tsafou, K.; Üren, A.; Zinovyev, A.; Delattre, O. (2016): The second European interdisciplinary Ewing sarcoma research summit--A joint effort to deconstructing the multiple layers of a complex disease. In: *Oncotarget* 7 (8), S. 8613–8624.

Kovar, H.; Dworzak, M.; Strehl, S.; Schnell, E.; Ambros, I. M.; Ambros, P. F.; Gadner, H. (1990): Overexpression of the pseudoautosomal gene MIC2 in Ewing's sarcoma and peripheral primitive neuroectodermal tumor. In: *Oncogene* 5 (7), S. 1067–1070.

Krishnamurthy, N.; Kurzrock, R. (2018): Targeting the Wnt/beta-catenin pathway in cancer: Update on effectors and inhibitors. In: *Cancer treatment reviews* 62, S. 50–60.

Krook, M. A.; Nicholls, L. A.; Scannell, C. A.; Chugh, R.; Thomas, D. G.; Lawlor, E. R. (2014): Stress-induced CXCR4 promotes migration and invasion of ewing sarcoma. In: *Molecular cancer research : MCR* 12 (6), S. 953–964.

Krumlauf, R. (1994): Hox genes in vertebrate development. In: *Cell* 78 (2), S. 191–201.

Kumar, B. de; Parker, H. J.; Paulson, A.; Parrish, M. E.; Zeitlinger, J.; Krumlauf, R. (2017): Hoxa1 targets signaling pathways during neural differentiation of ES cells and mouse embryogenesis. In: *Developmental biology* 432 (1), S. 151–164.

Kuss, P.; Kraft, K.; Stumm, J.; Ibrahim, D.; Vallecillo-Garcia, P.; Mundlos, S.; Stricker, S. (2014): Regulation of cell polarity in the cartilage growth plate and perichondrium of metacarpal elements by HOXD13 and WNT5A. In: *Developmental biology* 385 (1), S. 83–93.

Kusumbe, A. P.; Adams, R. H. (2014): Osteoclast progenitors promote bone vascularization and osteogenesis. In: *Nature medicine* 20 (11), S. 1238–1240.

Ladenstein, R.; Pötschger, U.; Le Deley, Marie Cécile; Whelan, J.; Paulussen, M.; Oberlin, O.; van den Berg, Henk; Dirksen, U.; Hjorth, L.; Michon, J.; Lewis, I.; Craft, A.; Jürgens, H. (2010): Primary disseminated multifocal Ewing sarcoma: results of the Euro-EWING 99 trial. In: *Journal of clinical oncology : official journal of the American Society of Clinical Oncology* 28 (20), S. 3284–3291.

Lance-Jones, C.; Omelchenko, N.; Bailis, A.; Lynch, S.; Sharma, K. (2001): Hoxd10 induction and regionalization in the developing lumbosacral spinal cord. In: *Development (Cambridge, England)* 128 (12), S. 2255–2268.

Lappin, T. R. J.; Grier, D. G.; Thompson, A.; Halliday, H. L. (2006): HOX genes: seductive science, mysterious mechanisms. In: *The Ulster medical journal* 75 (1), S. 23–31.

Lawlor, E. R.; Sorensen, P. H. (2015): Twenty Years on: What Do We Really Know about Ewing Sarcoma and What Is the Path Forward? In: *Critical reviews in oncogenesis* 20 (3-4), S. 155–171.

Le Deley, M.-C.; Paulussen, M.; Lewis, I.; Brennan, B.; Ranft, A.; Whelan, J.; Le Teuff, G.; Michon, J.; Ladenstein, R.; Marec-Bérard, P.; van den Berg, Henk; Hjorth, L.;

Wheatley, K.; Judson, I.; Juergens, H.; Craft, A.; Oberlin, O.; Dirksen, U. (2014): Cyclophosphamide compared with ifosfamide in consolidation treatment of standard-risk Ewing sarcoma: results of the randomized noninferiority Euro-EWING99-R1 trial. In: *Journal of clinical oncology : official journal of the American Society of Clinical Oncology* 32 (23), S. 2440–2448.

Leavey, P. J.; Collier, A. B. (2008): Ewing sarcoma: prognostic criteria, outcomes and future treatment. In: *Expert review of anticancer therapy* 8 (4), S. 617–624.

Lessnick, S. L.; Dacwag, C. S.; Golub, T. R. (2002): The Ewing's sarcoma oncoprotein EWS/FLI induces a p53-dependent growth arrest in primary human fibroblasts. In: *Cancer cell* 1 (4), S. 393–401.

Levetzow, C. von; Jiang, X.; Gwye, Y.; Levetzow, G. von; Hung, L.; Cooper, A.; Hsu, J. H.-R.; Lawlor, E. R. (2011): Modeling initiation of Ewing sarcoma in human neural crest cells. In: *PloS one* 6 (4), e19305.

Lewis, E. B. (1978): A gene complex controlling segmentation in Drosophila. In: *Nature* 276 (5688), S. 565–570.

Leyten, G. H. J. M.; Hessels, D.; Smit, F. P.; Jannink, S. A.; Jong, H. de; Melchers, W. J. G.; Cornel, E. B.; Reijke, T. M. de; Vergunst, H.; Kil, P.; Knipscheer, B. C.; Hulsbergen-van de Kaa, C. A.; Mulders, P. F. A.; van Oort, I. M.; Schalken, J. A. (2015): Identification of a Candidate Gene Panel for the Early Diagnosis of Prostate Cancer. In: *Clinical cancer research : an official journal of the American Association for Cancer Research* 21 (13), S. 3061–3070.

Li, D.; Masiero, M.; Banham, A. H.; Harris, A. L. (2014a): The notch ligand JAGGED1 as a target for anti-tumor therapy. In: *Frontiers in oncology* 4, S. 254.

Li, S.; Siegal, G. P. (2010): Small cell tumors of bone. In: *Advances in anatomic pathology* 17 (1), S. 1–11.

Li, X.; Liu, P.; Liu, W.; Maye, P.; Zhang, J.; Zhang, Y.; Hurley, M.; Guo, C.; Boskey, A.; Le Sun; Harris, S. E.; Rowe, D. W.; Ke, H. Z.; Wu, D. (2005): Dkk2 has a role in terminal osteoblast differentiation and mineralized matrix formation. In: *Nature genetics* 37 (9), S. 945–952.

Li, X.; McGee-Lawrence, M. E.; Decker, M.; Westendorf, J. J. (2010a): The Ewing's sarcoma fusion protein, EWS-FLI, binds Runx2 and blocks osteoblast differentiation. In: *Journal of cellular biochemistry* 111 (4), S. 933–943.

Li, Y.; Guo, L.; Lu, S.; Han, Z. (2014b): [Role of parathyroid hormone-like hormone during embryonic development]. In: *Yi chuan = Hereditas / Zhongguo yi chuan xue hui bian ji* 36 (9), S. 871–878.

Li, Y.; Tanaka, K.; Fan, X.; Nakatani, F.; Li, X.; Nakamura, T.; Takasaki, M.; Yamamoto, S.; Iwamoto, Y. (2010b): Inhibition of the transcriptional function of p53 by EWS-Fli1 chimeric protein in Ewing Family Tumors. In: *Cancer letters* 294 (1), S. 57–65.

Liang, A.-L.; Zhang, T.-T.; Zhou, N.; Wu, C. Y.; Lin, M.-H.; Liu, Y.-J. (2016): MiRNA-10b sponge: An anti-breast cancer study in vitro. In: *Oncology reports* 35 (4), S. 1950–1958.

Liao, C.-g.; Kong, L.-m.; Zhou, P.; Yang, X.-l.; Huang, J.-g.; Zhang, H.-l.; Lu, N. (2014): miR-10b is overexpressed in hepatocellular carcinoma and promotes cell proliferation, migration and invasion through RhoC, uPAR and MMPs. In: *Journal of Translational Medicine* 12.

Lin, A. W.; Carpenter, E. M. (2003): Hoxa10 and Hoxd10 coordinately regulate lumbar motor neuron patterning. In: *Journal of neurobiology* 56 (4), S. 328–337.

Lissat, A.; Joerschke, M.; Shinde, D. A.; Braunschweig, T.; Meier, A.; Makowska, A.; Bortnick, R.; Henneke, P.; Herget, G.; Gorr, T. A.; Kontny, U. (2015): IL6 secreted by Ewing sarcoma tumor microenvironment confers anti-apoptotic and cell-disseminating paracrine responses in Ewing sarcoma cells. In: *BMC cancer* 15 (1), S. 552.

Liu, A. K.; Stinauer, M.; Albano, E.; Greffe, B.; Tello, T.; Maloney, K. (2011): Local control of metastatic sites with radiation therapy in metastatic Ewing sarcoma and rhabdomyosarcoma. In: *Pediatric blood & cancer* 57 (1), S. 169–171.

Liu, T. M.; Lee, E. H. (2013): Transcriptional regulatory cascades in Runx2-dependent bone development. In: *Tissue engineering. Part B, Reviews* 19 (3), S. 254–263.

Llombart-Bosch, A.; Navarro, S. (2001): Immunohistochemical detection of EWS and FLI-1 proteinss in Ewing sarcoma and primitive neuroectodermal tumors: comparative analysis with CD99 (MIC-2) expression. In: *Applied immunohistochemistry & molecular morphology : AIMM* 9 (3), S. 255–260.

Ma, Z.; Chen, Y.; Min, L.; Li, L.; Huang, H.; Li, J.; Yan, Q.; Song, P.; Dai, L.; Yao, X. (2015): Augmented miR-10b expression associated with depressed expression of its target gene KLF4 involved in gastric carcinoma. In: *International journal of clinical and experimental pathology* 8 (5), S. 5071–5079.

Mak, I. W. Y.; Turcotte, R. E.; Ghert, M. (2013): Parathyroid hormone-related protein (PTHrP) modulates adhesion, migration and invasion in bone tumor cells. In: *Bone* 55 (1), S. 198–207.

Mallo, M.; Alonso, C. R. (2013): The regulation of Hox gene expression during animal development. In: *Development (Cambridge, England)* 140 (19), S. 3951–3963.

Manara, M. C.; Landuzzi, L.; Nanni, P.; Nicoletti, G.; Zambelli, D.; Lollini, P. L.; Nanni, C.; Hofmann, F.; García-Echeverría, C.; Picci, P.; Scotlandi, K. (2007): Preclinical in vivo study of new insulin-like growth factor-I receptor--specific inhibitor in Ewing's sarcoma. In: *Clinical cancer research : an official journal of the American Association for Cancer Research* 13 (4), S. 1322–1330.

Manara, M. C.; Terracciano, M.; Mancarella, C.; Sciandra, M.; Guerzoni, C.; Pasello, M.; Grilli, A.; Zini, N.; Picci, P.; Colombo, M. P.; Morrione, A.; Scotlandi, K. (2016): CD99

triggering induces methuosis of Ewing sarcoma cells through IGF-1R/RAS/Rac1 signaling. In: *Oncotarget* 7 (48), S. 79925–79942.

Mann, R. S.; Lelli, K. M.; Joshi, R. (2009): Hox specificity unique roles for cofactors and collaborators. In: *Current topics in developmental biology* 88, S. 63–101.

Mao, B.; Wu, W.; Davidson, G.; Marhold, J.; Li, M.; Mechler, B. M.; Delius, H.; Hoppe, D.; Stannek, P.; Walter, C.; Glinka, A.; Niehrs, C. (2002): Kremen proteins are Dickkopf receptors that regulate Wnt/beta-catenin signalling. In: *Nature* 417 (6889), S. 664–667.

Marillat, V.; Cases, O.; Nguyen-Ba-Charvet, K. T.; Tessier-Lavigne, M.; Sotelo, C.; Chédotal, A. (2002): Spatiotemporal expression patterns of slit and robo genes in the rat brain. In: *The Journal of comparative neurology* 442 (2), S. 130–155.

Marina, N. M.; Liu, Q.; Donaldson, S. S.; Sklar, C. A.; Armstrong, G. T.; Oeffinger, K. C.; Leisenring, W. M.; Ginsberg, J. P.; Henderson, T. O.; Neglia, J. P.; Stovall, M. A.; Yasui, Y.; Randall, R. L.; Geller, D. S.; Robison, L. L.; Ness, K. K. (2017): Longitudinal follow-up of adult survivors of Ewing sarcoma: A report from the Childhood Cancer Survivor Study. In: *Cancer*.

Matsumoto, Y.; Tanaka, K.; Nakatani, F.; Matsunobu, T.; Matsuda, S.; Iwamoto, Y. (2001): Downregulation and forced expression of EWS-Fli1 fusion gene results in changes in the expression of G(1)regulatory genes. In: *British journal of cancer* 84 (6), S. 768–775.

Matsushima, H.; Bogenmann, E. (1990): Nerve growth factor (NGF) induces neuronal differentiation in neuroblastoma cells transfected with the NGF receptor cDNA. In: *Molecular and cellular biology* 10 (9), S. 5015–5020.

McGinnis, W.; Krumlauf, R. (1992): Homeobox genes and axial patterning. In: *Cell* 68 (2), S. 283–302.

Mendoza-Naranjo, A.; El-Naggar, A.; Wai, D. H.; Mistry, P.; Lazic, N.; Ayala, F. R. R.; da Cunha, I. W.; Rodriguez-Viciana, P.; Cheng, H.; Tavares Guerreiro Fregnani, J. H.; Reynolds, P.; Arceci, R. J.; Nicholson, A.; Triche, T. J.; Soares, F. A.; Flanagan, A. M.; Wang, Y. Z.; Strauss, S. J.; Sorensen, P. H. (2013): ERBB4 confers metastatic capacity in Ewing sarcoma. In: *EMBO molecular medicine* 5 (7), S. 1087–1102.

Merchant, M. S.; Bernstein, D.; Amoako, M.; Baird, K.; Fleisher, T. A.; Morre, M.; Steinberg, S. M.; Sabatino, M.; Stroncek, D. F.; Venkatasan, A. M.; Wood, B. J.; Wright, M.; Zhang, H.; Mackall, C. L. (2016): Adjuvant Immunotherapy to Improve Outcome in High-Risk Pediatric Sarcomas. In: *Clinical cancer research : an official journal of the American Association for Cancer Research* 22 (13), S. 3182–3191.

Mimeault, M.; Batra, S. K. (2013): Hypoxia-inducing factors as master regulators of stemness properties and altered metabolism of cancer- and metastasis-initiating cells. In: *Journal of cellular and molecular medicine* 17 (1), S. 30–54.

Misra, M.; Shah, V.; Carpenter, E.; McCaffery, P.; Lance-Jones, C. (2009): Restricted patterns of Hoxd10 and Hoxd11 set segmental differences in motoneuron subtype

complement in the lumbosacral spinal cord. In: *Developmental biology* 330 (1), S. 54–72.

Miyagawa, Y.; Okita, H.; Nakaijima, H.; Horiuchi, Y.; Sato, B.; Taguchi, T.; Toyoda, M.; Katagiri, Y. U.; Fujimoto, J.; Hata, J.-I.; Umezawa, A.; Kiyokawa, N. (2008): Inducible expression of chimeric EWS/ETS proteins confers Ewing's family tumor-like phenotypes to human mesenchymal progenitor cells. In: *Molecular and cellular biology* 28 (7), S. 2125–2137.

Mollard, R.; Dziadek, M. (1997): Homeobox genes from clusters A and B demonstrate characteristics of temporal colinearity and differential restrictions in spatial expression domains in the branching mouse lung. In: *The International journal of developmental biology* 41 (5), S. 655–666.

Montavon, T.; Soshnikova, N. (2014): Hox gene regulation and timing in embryogenesis. In: *Seminars in cell & developmental biology* 34, S. 76–84.

Moon, R. T.; Bowerman, B.; Boutros, M.; Perrimon, N. (2002): The promise and perils of Wnt signaling through beta-catenin. In: *Science (New York, N.Y.)* 296 (5573), S. 1644–1646.

Moore, D. D.; Haydon, R. C. (2014): Ewing's sarcoma of bone. In: *Cancer treatment and research* 162, S. 93–115.

Morgan, R.; Boxall, A.; Harrington, K. J.; Simpson, G. R.; Michael, A.; Pandha, H. S. (2014): Targeting HOX transcription factors in prostate cancer. In: *BMC urology* 14, S. 17.

Morgan, R.; El-Tanani, M. (2016): HOX Genes as Potential Markers of Circulating Tumour Cells. In: *Current molecular medicine* 16 (4), S. 322–327.

Morgan, R.; El-Tanani, M.; Hunter, K. D.; Harrington, K. J.; Pandha, H. S. (2017): Targeting HOX/PBX dimers in cancer. In: *Oncotarget* 8 (19), S. 32322–32331.

Morgan, R.; Pirard, P. M.; Shears, L.; Sohal, J.; Pettengell, R.; Pandha, H. S. (2007): Antagonism of HOX/PBX dimer formation blocks the in vivo proliferation of melanoma. In: *Cancer Res* 67 (12), S. 5806–5813.

Morgan, R.; Simpson, G.; Gray, S.; Gillett, C.; Tabi, Z.; Spicer, J.; Harrington, K. J.; Pandha, H. S. (2016): HOX transcription factors are potential targets and markers in malignant mesothelioma. In: *BMC cancer* 16, S. 85.

Mugford, J. W.; Sipilä, P.; Kobayashi, A.; Behringer, R. R.; McMahon, A. P. (2008): Hoxd11 specifies a program of metanephric kidney development within the intermediate mesoderm of the mouse embryo. In: *Developmental biology* 319 (2), S. 396–405.

Myers, C.; Charboneau, A.; Cheung, I.; Hanks, D.; Boudreau, N. (2002): Sustained expression of homeobox D10 inhibits angiogenesis. In: *The American journal of pathology* 161 (6), S. 2099–2109.

Naing, A.; LoRusso, P.; Fu, S.; Hong, D. S.; Anderson, P.; Benjamin, R. S.; Ludwig, J.; Chen, H. X.; Doyle, L. A.; Kurzrock, R. (2012): Insulin growth factor-receptor (IGF-1R) antibody cixutumumab combined with the mTOR inhibitor temsirolimus in patients with refractory Ewing's sarcoma family tumors. In: *Clinical cancer research : an official journal of the American Association for Cancer Research* 18 (9), S. 2625–2631.

Nakayama, I.; Shibazaki, M.; Yashima-Abo, A.; Miura, F.; Sugiyama, T.; Masuda, T.; Maesawa, C. (2013): Loss of HOXD10 expression induced by upregulation of miR-10b accelerates the migration and invasion activities of ovarian cancer cells. In: *International journal of oncology* 43 (1), S. 63–71.

Neijts, R.; Amin, S.; van Rooijen, C.; Tan, S.; Creyghton, M. P.; Laat, W. de; Deschamps, J. (2016): Polarized regulatory landscape and Wnt responsiveness underlie Hox activation in embryos. In: *Genes & development* 30 (17), S. 1937–1942.

Neilsen, P. M.; Pishas, K. I.; Callen, D. F.; Thomas, D. M. (2011): Targeting the p53 Pathway in Ewing Sarcoma. In: *Sarcoma* 2011, S. 746939.

Ning, M. S.; Perkins, S. M.; Borinstein, S. C.; Holt, G. E.; Stavas, M. J.; Shinohara, E. T. (2016): Role of radiation in the treatment of non-metastatic osseous Ewing sarcoma. In: *Journal of medical imaging and radiation oncology* 60 (1), S. 119–128.

Nishihara, M.; Kanematsu, T.; Taguchi, T.; Razzaque, M. S. (2007): PTHrP and tumorigenesis: is there a role in prognosis? In: *Annals of the New York Academy of Sciences* 1117, S. 385–392.

Ohba, T.; Cates, Justin M M; Cole, H. A.; Slosky, D. A.; Haro, H.; Ando, T.; Schwartz, H. S.; Schoenecker, J. G. (2014): Autocrine VEGF/VEGFR1 signaling in a subpopulation of cells associates with aggressive osteosarcoma. In: *Molecular cancer research : MCR* 12 (8), S. 1100–1111.

Osborne, J.; Hu, C.; Hawley, C.; Underwood, L. J.; O'Brien, T. J.; Baker, V. V. (1998): Expression of HOXD10 gene in normal endometrium and endometrial adenocarcinoma. In: *Journal of the Society for Gynecologic Investigation* 5 (5), S. 277–280.

Ozaki, T. (2015): Diagnosis and treatment of Ewing sarcoma of the bone: a review article. In: *Journal of orthopaedic science : official journal of the Japanese Orthopaedic Association* 20 (2), S. 250–263.

Park, J. H.; Lee, N. K.; Lee, S. Y. (2017): Current Understanding of RANK Signaling in Osteoclast Differentiation and Maturation. In: *Molecules and cells* 40 (10), S. 706–713.

Paronetto, M. P. (2013): Ewing sarcoma protein: a key player in human cancer. In: *International journal of cell biology* 2013, S. 642853.

Paulino, A. C.; Mai, W. Y.; Teh, B. S. (2013): Radiotherapy in metastatic ewing sarcoma. In: *American journal of clinical oncology* 36 (3), S. 283–286.

Paulussen, M.; Craft, A. W.; Lewis, I.; Hackshaw, A.; Douglas, C.; Dunst, J.; Schuck, A.; Winkelmann, W.; Köhler, G.; Poremba, C.; Zoubek, A.; Ladenstein, R.; van den Berg, Henk; Hunold, A.; Cassoni, A.; Spooner, D.; Grimer, R.; Whelan, J.; McTiernan, A.; Jürgens, H. (2008): Results of the EICESS-92 Study: two randomized trials of Ewing's sarcoma treatment--cyclophosphamide compared with ifosfamide in standard-risk patients and assessment of benefit of etoposide added to standard treatment in high-risk patients. In: *Journal of clinical oncology : official journal of the American Society of Clinical Oncology* 26 (27), S. 4385–4393.

PDQ Pediatric Treatment Editorial Board (2018): PDQ Pediatric Treatment Editorial Board. Ewing Sarcoma Treatment (PDQ®): Health Professional Version. In: *PDQ Cancer Information Summaries* 2018 Nov 21. Online verfügbar unter https://www.ncbi.nlm.nih.gov/pubmed/?term=26389480.

PDQ Pediatric Treatment Editorial Board (2019): Ewing Sarcoma Treatment (PDQ®): Health Professional Version: National Cancer Institute (US), 1/31/2019.

Pearson, J. C.; Lemons, D.; McGinnis, W. (2005): Modulating Hox gene functions during animal body patterning. In: *Nature reviews. Genetics* 6 (12), S. 893–904.

Pedersen, E. A.; Menon, R.; Bailey, K. M.; Thomas, D. G.; van Noord, R. A.; Tran, J.; Wang, H.; Qu, P. P.; Hoering, A.; Fearon, E. R.; Chugh, R.; Lawlor, E. R. (2016): Activation of Wnt/β-Catenin in Ewing Sarcoma Cells Antagonizes EWS/ETS Function and Promotes Phenotypic Transition to More Metastatic Cell States. In: *Cancer research* 76 (17), S. 5040–5053.

Peter, M.; Couturier, J.; Pacquement, H.; Michon, J.; Thomas, G.; Magdelenat, H.; Delattre, O. (1997): A new member of the ETS family fused to EWS in Ewing tumors. In: *Oncogene* 14 (10), S. 1159–1164.

Philippidou, P.; Dasen, J. S. (2013): Hox genes: choreographers in neural development, architects of circuit organization. In: *Neuron* 80 (1), S. 12–34.

Pilato, B.; Pinto, R.; Summa, S. de; Lambo, R.; Paradiso, A.; Tommasi, S. (2013): HOX gene methylation status analysis in patients with hereditary breast cancer. In: *Journal of human genetics* 58 (1), S. 51–53.

Pineault, K. M.; Swinehart, I. T.; Garthus, K. N.; Ho, E.; Yao, Q.; Schipani, E.; Kozloff, K. M.; Wellik, D. M. (2015): Hox11 genes regulate postnatal longitudinal bone growth and growth plate proliferation. In: *Biology open* 4 (11), S. 1538–1548.

Pineault, K. M.; Wellik, D. M. (2014): Hox genes and limb musculoskeletal development. In: *Current osteoporosis reports* 12 (4), S. 420–427.

Pineault, N.; Buske, C.; Feuring-Buske, M.; Abramovich, C.; Rosten, P.; Hogge, D. E.; Aplan, P. D.; Humphries, R. K. (2003): Induction of acute myeloid leukemia in mice by the human leukemia-specific fusion gene NUP98-HOXD13 in concert with Meis1. In: *Blood* 101 (11), S. 4529–4538.

Pishas, K. I.; Lessnick, S. L. (2016): Recent advances in targeted therapy for Ewing sarcoma. In: *F1000Research* 5.

Podlasek, C. A.; Duboule, D.; Bushman, W. (1997): Male accessory sex organ morphogenesis is altered by loss of function of Hoxd-13. In: *Developmental dynamics : an official publication of the American Association of Anatomists* 208 (4), S. 454–465.

Polakis, P. (2012): Wnt Signaling in Cancer. In: *Cold Spring Harbor Perspectives in Biology* 4 (5).

Pridgeon, M. G.; Grohar, P. J.; Steensma, M. R.; Williams, B. O. (2017): Wnt Signaling in Ewing Sarcoma, Osteosarcoma, and Malignant Peripheral Nerve Sheath Tumors. In: *Current osteoporosis reports* 15 (4), S. 239–246.

Procino, A.; Cillo, C. (2013): The HOX genes network in metabolic diseases. In: *Cell biology international* 37 (11), S. 1145–1148.

Quinonez, S. C.; Innis, J. W. (2014): Human HOX gene disorders. In: *Molecular genetics and metabolism* 111 (1), S. 4–15.

Raney, R. B.; Asmar, L.; Newton, W. A.; Bagwell, C.; Breneman, J. C.; Crist, W.; Gehan, E. A.; Webber, B.; Wharam, M.; Wiener, E. S.; Anderson, J. R.; Maurer, H. M. (1997): Ewing's sarcoma of soft tissues in childhood: a report from the Intergroup Rhabdomyosarcoma Study, 1972 to 1991. In: *Journal of clinical oncology : official journal of the American Society of Clinical Oncology* 15 (2), S. 574–582.

Rattigan, Y.; Hsu, J.-M.; Mishra, P. J.; Glod, J.; Banerjee, D. (2010): Interleukin 6 mediated recruitment of mesenchymal stem cells to the hypoxic tumor milieu. In: *Experimental cell research* 316 (20), S. 3417–3424.

Redline, R. W.; Williams, A. J.; Patterson, P.; Collins, T. (1992): Human HOX4E: a gene strongly expressed in the adult male and female urogenital tracts. In: *Genomics* 13 (2), S. 425–430.

Reeves, S. A.; Helman, L. J.; Allison, A.; Israel, M. A. (1989): Molecular cloning and primary structure of human glial fibrillary acidic protein. In: *Proceedings of the National Academy of Sciences of the United States of America* 86 (13), S. 5178–5182.

Richter, G. H. S.; Fasan, A.; Hauer, K.; Grünewald, T. G. P.; Berns, C.; Rössler, S.; Naumann, I.; Staege, M. S.; Fulda, S.; Esposito, I.; Burdach, S. (2013): G-Protein coupled receptor 64 promotes invasiveness and metastasis in Ewing sarcomas through PGF and MMP1. In: *The Journal of pathology* 230 (1), S. 70–81.

Richter, G. H. S.; Plehm, S.; Fasan, A.; Rössler, S.; Unland, R.; Bennani-Baiti, I. M.; Hotfilder, M.; Löwel, D.; Luettichau, I. von; Mossbrugger, I.; Quintanilla-Martinez, L.; Kovar, H.; Staege, M. S.; Müller-Tidow, C.; Burdach, S. (2009): EZH2 is a mediator of EWS/FLI1 driven tumor growth and metastasis blocking endothelial and neuro-ectodermal differentiation. In: *Proceedings of the National Academy of Sciences of the United States of America* 106 (13), S. 5324–5329.

Riggi, N.; Knoechel, B.; Gillespie, S. M.; Rheinbay, E.; Boulay, G.; Suvà, M. L.; Rossetti, N. E.; Boonseng, W. E.; Oksuz, O.; Cook, E. B.; Formey, A.; Patel, A.; Gymrek, M.; Thapar, V.; Deshpande, V.; Ting, D. T.; Hornicek, F. J.; Nielsen, G. P.; Stamenkovic, I.; Aryee, M. J.; Bernstein, B. E.; Rivera, M. N. (2014): EWS-FLI1 utilizes divergent chromatin remodeling mechanisms to directly activate or repress enhancer elements in Ewing sarcoma. In: *Cancer cell* 26 (5), S. 668–681.

Riggi, N.; Suvà, M.-L.; Suvà, D.; Cironi, L.; Provero, P.; Tercier, S.; Joseph, J.-M.; Stehle, J.-C.; Baumer, K.; Kindler, V.; Stamenkovic, I. (2008): EWS-FLI-1 expression triggers a Ewing's sarcoma initiation program in primary human mesenchymal stem cells. In: *Cancer research* 68 (7), S. 2176–2185.

Riggi, N.; Suvà, M.-L.; Vito, C. de; Provero, P.; Stehle, J.-C.; Baumer, K.; Cironi, L.; Janiszewska, M.; Petricevic, T.; Suvà, D.; Tercier, S.; Joseph, J.-M.; Guillou, L.; Stamenkovic, I. (2010): EWS-FLI-1 modulates miRNA145 and SOX2 expression to initiate mesenchymal stem cell reprogramming toward Ewing sarcoma cancer stem cells. In: *Genes & development* 24 (9), S. 916–932.

Rinn, J. L.; Kertesz, M.; Wang, J. K.; Squazzo, S. L.; Xu, X.; Brugmann, S. A.; Goodnough, L. H.; Helms, J. A.; Farnham, P. J.; Segal, E.; Chang, H. Y. (2007): Functional demarcation of active and silent chromatin domains in human HOX loci by noncoding RNAs. In: *Cell* 129 (7), S. 1311–1323.

Rodrigues, M. F. S. D.; Esteves, C. M.; Xavier, F. C. A.; Nunes, F. D. (2016): Methylation status of homeobox genes in common human cancers. In: *Genomics* 108 (5-6), S. 185–193.

Rodríguez, D.; Morrison, C. J.; Overall, C. M. (2010): Matrix metalloproteinases: what do they not do? New substrates and biological roles identified by murine models and proteomics. In: *Biochimica et biophysica acta* 1803 (1), S. 39–54.

Roessner, A.; Jürgens, H. (1993): Round cell tumours of bone. In: *Pathology, research and practice* 189 (10), S. 111–136.

Rorie, C. J.; Thomas, V. D.; Chen, P.; Pierce, H. H.; O'Bryan, J. P.; Weissman, B. E. (2004): The Ews/Fli-1 fusion gene switches the differentiation program of neuroblastomas to Ewing sarcoma/peripheral primitive neuroectodermal tumors. In: *Cancer research* 64 (4), S. 1266–1277.

Rubock, M. J.; Larin, Z.; Cook, M.; Papalopulu, N.; Krumlauf, R.; Lehrach, H. (1990): A yeast artificial chromosome containing the mouse homeobox cluster Hox-2. In: *Proceedings of the National Academy of Sciences of the United States of America* 87 (12), S. 4751–4755.

Rux, D. R.; Wellik, D. M. (2016): Hox genes in the adult skeleton: Novel functions beyond embryonic development. In: *Developmental dynamics : an official publication of the American Association of Anatomists*.

Safford, K. M.; Hicok, K. C.; Safford, S. D.; Halvorsen, Y.-D. C.; Wilkison, W. O.; Gimble, J. M.; Rice, H. E. (2002): Neurogenic differentiation of murine and human adipose-derived stromal cells. In: *Biochemical and biophysical research communications* 294 (2), S. 371–379.

Sarfarazi, M.; Akarsu, A. N.; Sayli, B. S. (1995): Localization of the syndactyly type II (synpolydactyly) locus to 2q31 region and identification of tight linkage to HOXD8 intragenic marker. In: *Human molecular genetics* 4 (8), S. 1453–1458.

Sayli, B. S.; Akarsu, A. N.; Sayli, U.; Akhan, O.; Ceylaner, S.; Sarfarazi, M. (1995): A large Turkish kindred with syndactyly type II (synpolydactyly). 1. Field investigation, clinical and pedigree data. In: *Journal of medical genetics* 32 (6), S. 421–434.

Schirmer, D.; Grünewald, T. G. P.; Klar, R.; Schmidt, O.; Wohlleber, D.; Rubío, R. A.; Uckert, W.; Thiel, U.; Bohne, F.; Busch, D. H.; Krackhardt, A. M.; Burdach, S.; Richter, G. H. S. (2016): Transgenic antigen-specific, HLA-A*02:01-allo-restricted cytotoxic T cells recognize tumor-associated target antigen STEAP1 with high specificity. In: *Oncoimmunology* 5 (6), e1175795.

Schmidt, D.; Harms, D.; Burdach, S. (1985): Malignant peripheral neuroectodermal tumours of childhood and adolescence. In: *Virchows Archiv. A, Pathological anatomy and histopathology* 406 (3), S. 351–365.

Schuck, A.; Ahrens, S.; Paulussen, M.; Kuhlen, M.; Könemann, S.; Rübe, C.; Winkelmann, W.; Kotz, R.; Dunst, J.; Willich, N.; Jürgens, H. (2003): Local therapy in localized Ewing tumors: results of 1058 patients treated in the CESS 81, CESS 86, and EICESS 92 trials. In: *International journal of radiation oncology, biology, physics* 55 (1), S. 168–177.

Schwab, K.; Hartman, H. A.; Liang, H.-C.; Aronow, B. J.; Patterson, L. T.; Potter, S. S. (2006): Comprehensive microarray analysis of Hoxa11/Hoxd11 mutant kidney development. In: *Developmental biology* 293 (2), S. 540–554.

Scotlandi, K.; Baldini, N.; Cerisano, V.; Manara, M. C.; Benini, S.; Serra, M.; Lollini, P. L.; Nanni, P.; Nicoletti, G.; Bernard, G.; Bernard, A.; Picci, P. (2000a): CD99 engagement: an effective therapeutic strategy for Ewing tumors. In: *Cancer research* 60 (18), S. 5134–5142.

Scotlandi, K.; Benini, S.; Manara, M. C.; Serra, M.; Nanni, P.; Lollini, P. L.; Nicoletti, G.; Landuzzi, L.; Chano, T.; Picci, P.; Baldini, N. (2000b): Murine model for skeletal metastases of Ewing's sarcoma. In: *Journal of orthopaedic research : official publication of the Orthopaedic Research Society* 18 (6), S. 959–966.

Scott, M. P. (1992): Vertebrate homeobox gene nomenclature. In: *Cell* 71 (4), S. 551–553.

Seifert, A.; Werheid, D. F.; Knapp, S. M.; Tobiasch, E. (2015): Role of Hox genes in stem cell differentiation. In: *World journal of stem cells* 7 (3), S. 583–595.

Sethi, N.; Dai, X.; Winter, C. G.; Kang, Y. (2011): Tumor-derived JAGGED1 promotes osteolytic bone metastasis of breast cancer by engaging notch signaling in bone cells. In: *Cancer cell* 19 (2), S. 192–205.

Shah, N.; Sukumar, S. (2010): The Hox genes and their roles in oncogenesis. In: *Nature reviews. Cancer* 10 (5), S. 361–371.

Sharkey, M.; Graba, Y.; Scott, M. P. (1997): Hox genes in evolution: protein surfaces and paralog groups. In: *Trends in genetics : TIG* 13 (4), S. 145–151.

Sharpe, D. J.; Orr, K. S.; Moran, M.; White, S. J.; McQuaid, S.; Lappin, T. R.; Thompson, A.; James, J. A. (2014): POU2F1 activity regulates HOXD10 and HOXD11 promoting a proliferative and invasive phenotype in head and neck cancer. In: *Oncotarget* 5 (18), S. 8803–8815.

Sheth, R.; Bastida, M. F.; Kmita, M.; Ros, M. (2014): \"Self-regulation,\" a new facet of Hox genes' function. In: *Developmental dynamics : an official publication of the American Association of Anatomists* 243 (1), S. 182–191.

Shibuya, M. (2015): VEGF-VEGFR System as a Target for Suppressing Inflammation and other Diseases. In: *Endocrine, metabolic & immune disorders drug targets* 15 (2), S. 135–144.

Shrimpton, A. E.; Levinsohn, E. M.; Yozawitz, J. M.; Packard, D. S.; Cady, R. B.; Middleton, F. A.; Persico, A. M.; Hootnick, D. R. (2004): A HOX gene mutation in a family with isolated congenital vertical talus and Charcot-Marie-Tooth disease. In: *American journal of human genetics* 75 (1), S. 92–96.

Siemers, F. (2013): Weichteilsarkome im Bereich der Extremitäten – Teil 1. Die Rolle der Plastischen Chirurgie im Rahmen eines interdisziplinären Behandlungskonzeptes. Hg. v. Ärzteblatt Sachsen-Anhalt. Online verfügbar unter https://www.aerzteblatt-sachsen-anhalt.de/ausgabe/fachartikel/106-fachartikel-09-2013/340-weichteilsarkome-im-bereich-der-extremitaeten-teil-1.html, zuletzt geprüft am 12/1/2018.

Slape, C.; Liu, L. Y.; Beachy, S.; Aplan, P. D. (2008): Leukemic transformation in mice expressing a NUP98-HOXD13 transgene is accompanied by spontaneous mutations in Nras, Kras, and Cbl. In: *Blood* 112 (5), S. 2017–2019.

Sorensen, P. H.; Lessnick, S. L.; Lopez-Terrada, D.; Liu, X. F.; Triche, T. J.; Denny, C. T. (1994): A second Ewing's sarcoma translocation, t(21;22), fuses the EWS gene to another ETS-family transcription factor, ERG. In: *Nature genetics* 6 (2), S. 146–151.

Soshnikova, N.; Duboule, D. (2009): Epigenetic temporal control of mouse Hox genes in vivo. In: *Science (New York, N.Y.)* 324 (5932), S. 1320–1323.

Sottnik, J. L.; Keller, E. T. (2013): Understanding and targeting osteoclastic activity in prostate cancer bone metastases. In: *Current molecular medicine* 13 (4), S. 626–639.

Srivastava, S.; Dhawan, J.; Mishra, R. K. (2015): Epigenetic mechanisms and boundaries in the regulation of mammalian Hox clusters. In: *Mechanisms of development* 138 Pt 2, S. 160–169.

Staege, M. S.; Hutter, C.; Neumann, I.; Foja, S.; Hattenhorst, U. E.; Hansen, G.; Afar, D.; Burdach, Stefan E G (2004): DNA microarrays reveal relationship of Ewing family tumors to both endothelial and fetal neural crest-derived cells and define novel targets. In: *Cancer research* 64 (22), S. 8213–8221.

Stahl, M.; Ranft, A.; Paulussen, M.; Bölling, T.; Vieth, V.; Bielack, S.; Görtitz, I.; Braun-Munzinger, G.; Hardes, J.; Jürgens, H.; Dirksen, U. (2011): Risk of recurrence and survival after relapse in patients with Ewing sarcoma. In: *Pediatric blood & cancer* 57 (4), S. 549–553.

Stewart, E.; Goshorn, R.; Bradley, C.; Griffiths, L. M.; Benavente, C.; Twarog, N. R.; Miller, G. M.; Caufield, W.; Freeman, B. B.; Bahrami, A.; Pappo, A.; Wu, J.; Loh, A.; Karlström, Å.; Calabrese, C.; Gordon, B.; Tsurkan, L.; Hatfield, M. J.; Potter, P. M.; Snyder, S. E.; Thiagarajan, S.; Shirinifard, A.; Sablauer, A.; Shelat, A. A.; Dyer, M. A. (2014): Targeting the DNA repair pathway in Ewing sarcoma. In: *Cell reports* 9 (3), S. 829–841.

Storti, P.; Bolzoni, M.; Donofrio, G.; Airoldi, I.; Guasco, D.; Toscani, D.; Martella, E.; Lazzaretti, M.; Mancini, C.; Agnelli, L.; Patrene, K.; Maïga, S.; Franceschi, V.; Colla, S.; Anderson, J.; Neri, A.; Amiot, M.; Aversa, F.; David Roodman, G.; Giuliani, N. (2013): Hypoxia-inducible factor (HIF)-1α suppression in myeloma cells blocks tumoral growth in vivo inhibiting angiogenesis and bone destruction. In: *Leukemia* 27 (8), S. 1697–1706.

Sun, S.-S.; Zhang, L.; Yang, J.; Zhou, X. (2015): Role of runt-related transcription factor 2 in signal network of tumors as an inter-mediator. In: *Cancer letters* 361 (1), S. 1–7.

Svoboda, L. K.; Harris, A.; Bailey, N. J.; Schwentner, R.; Tomazou, E.; Levetzow, C. von; Magnuson, B.; Ljungman, M.; Kovar, H.; Lawlor, E. R. (2014): Overexpression of HOX genes is prevalent in Ewing sarcoma and is associated with altered epigenetic regulation of developmental transcription programs. In: *Epigenetics : official journal of the DNA Methylation Society* 9 (12), S. 1613–1625.

Tai, D.; Wells, K.; Arcaroli, J.; Vanderbilt, C.; Aisner, D. L.; Messersmith, W. A.; Lieu, C. H. (2015): Targeting the WNT Signaling Pathway in Cancer Therapeutics. In: *The oncologist* 20 (10), S. 1189–1198.

Taketani, T.; Taki, T.; Shibuya, N.; Ito, E.; Kitazawa, J.; Terui, K.; Hayashi, Y. (2002): The HOXD11 gene is fused to the NUP98 gene in acute myeloid leukemia with t(2;11)(q31;p15). In: *Cancer research* 62 (1), S. 33–37.

Tan, A. R.; Alexe, G.; Reiss, M. (2009): Transforming growth factor-beta signaling: emerging stem cell target in metastatic breast cancer? In: *Breast cancer research and treatment* 115 (3), S. 453–495.

Tanaka, M.; Yamazaki, Y.; Kanno, Y.; Igarashi, K.; Aisaki, K.-i.; Kanno, J.; Nakamura, T. (2014): Ewing's sarcoma precursors are highly enriched in embryonic osteochondrogenic progenitors. In: *The Journal of clinical investigation* 124 (7), S. 3061–3074.

Tap, W. D.; Demetri, G.; Barnette, P.; Desai, J.; Kavan, P.; Tozer, R.; Benedetto, P. W.; Friberg, G.; Deng, H.; McCaffery, I.; Leitch, I.; Badola, S.; Chang, S.; Zhu, M.; Tolcher, A. (2012): Phase II study of ganitumab, a fully human anti-type-1 insulin-like growth factor receptor antibody, in patients with metastatic Ewing family tumors or desmoplastic small round cell tumors. In: *Journal of clinical oncology : official journal of the American Society of Clinical Oncology* 30 (15), S. 1849–1856.

Tauro, M.; McGuire, J.; Lynch, C. C. (2014): New approaches to selectively target cancer-associated matrix metalloproteinase activity. In: *Cancer metastasis reviews* 33 (4), S. 1043–1057.

Terui, K.; Kitazawa, J.; Takahashi, Y.; Tohno, C.; Hayashi, Y.; Taketani, T.; Taki, T.; Ito, E. (2003): Successful treatment of acute myelomonocytic leukaemia with NUP98-HOXD11 fusion transcripts and monitoring of minimal residual disease. In: *British journal of haematology* 120 (2), S. 274–276.

Theisen, E. R.; Pishas, K. I.; Saund, R. S.; Lessnick, S. L. (2016): Therapeutic opportunities in Ewing sarcoma: EWS-FLI inhibition via LSD1 targeting. In: *Oncotarget* 7 (14), S. 17616–17630.

Thiel, U.; Pirson, S.; Müller-Spahn, C.; Conrad, H.; Busch, D. H.; Bernhard, H.; Burdach, S.; Richter, G H S (2011): Specific recognition and inhibition of Ewing tumour growth by antigen-specific allo-restricted cytotoxic T cells. In: *British journal of cancer* 104 (6), S. 948–956.

Thiel, U.; Schober, S. J.; Einspieler, I.; Kirschner, A.; Thiede, M.; Schirmer, D.; Gall, K.; Blaeschke, F.; Schmidt, O.; Jabar, S.; Ranft, A.; Alba Rubío, R.; Dirksen, U.; Grunewald, T. G. P.; Sorensen, P. H.; Richter, G. H. S.; Lüttichau, I. T. von; Busch, D. H.; Burdach, S. E. G. (2017): Ewing sarcoma partial regression without GvHD by chondromodulin-I/HLA-A*02:01-specific allorestricted T cell receptor transgenic T cells. In: *Oncoimmunology* 6 (5), e1312239.

Thiel, U.; Wawer, A.; Luettichau, I. von; Bender, H.-U.; Blaeschke, F.; Grunewald, T. G. P.; Steinborn, M.; Röper, B.; Bonig, H.; Klingebiel, T.; Bader, P.; Koscielniak, E.; Paulussen, M.; Dirksen, U.; Juergens, H.; Kolb, H.-J.; Burdach, S. E. G. (2016): Bone marrow involvement identifies a subgroup of advanced Ewing sarcoma patients with fatal outcome irrespective of therapy in contrast to curable patients with multiple bone metastases but unaffected marrow. In: *Oncotarget* 7 (43), S. 70959–70968.

Tirado, O. M.; Mateo-Lozano, S.; Villar, J.; Dettin, L. E.; Llort, A.; Gallego, S.; Ban, J.; Kovar, H.; Notario, V. (2006): Caveolin-1 (CAV1) is a target of EWS/FLI-1 and a key determinant of the oncogenic phenotype and tumorigenicity of Ewing's sarcoma cells. In: *Cancer research* 66 (20), S. 9937–9947.

Tirode, F.; Laud-Duval, K.; Prieur, A.; Delorme, B.; Charbord, P.; Delattre, O. (2007): Mesenchymal stem cell features of Ewing tumors. In: *Cancer cell* 11 (5), S. 421–429.

Todorova, R. (2014): Ewing's sarcoma cancer stem cell targeted therapy. In: *Current stem cell research & therapy* 9 (1), S. 46–62.

Truong, M.; Yang, B.; Wagner, J.; Kobayashi, Y.; Rajamanickam, V.; Brooks, J.; Jarrard, D. F. (2012): Even-skipped homeobox 1 is frequently hypermethylated in prostate cancer and predicts PSA recurrence. In: *British journal of cancer* 107 (1), S. 100–107.

van Driel, M.; van Leeuwen, J. (2014): Cancer and bone: a complex complex. In: *Archives of biochemistry and biophysics* 561, S. 159–166.

Vardhini, N. V.; Rao, P Jagan Mohan; Murthy, P. B.; Sudhakar, G. (2014): HOXD10 expression in human breast cancer. In: *Tumour biology : the journal of the International Society for Oncodevelopmental Biology and Medicine* 35 (11), S. 10855–10860.

Villavicencio-Lorini, P.; Kuss, P.; Friedrich, J.; Haupt, J.; Farooq, M.; Türkmen, S.; Duboule, D.; Hecht, J.; Mundlos, S. (2010): Homeobox genes d11-d13 and a13 control mouse autopod cortical bone and joint formation. In: *The Journal of clinical investigation* 120 (6), S. 1994–2004.

Vimalraj, S.; Arumugam, B.; Miranda, P. J.; Selvamurugan, N. (2015): Runx2: Structure, function, and phosphorylation in osteoblast differentiation. In: *International journal of biological macromolecules* 78, S. 202–208.

Vormoor, B.; Curtin, N. J. (2014): Poly(ADP-ribose) polymerase inhibitors in Ewing sarcoma. In: *Current opinion in oncology* 26 (4), S. 428–433.

Vornicova, O.; Bar-Sela, G. (2016): Investigational therapies for Ewing sarcoma: a search without a clear finding. In: *Expert opinion on investigational drugs* 25 (6), S. 679–686.

Wagner, L. M.; Fouladi, M.; Ahmed, A.; Krailo, M. D.; Weigel, B.; DuBois, S. G.; Doyle, L. A.; Chen, H.; Blaney, S. M. (2015): Phase II study of cixutumumab in combination with temsirolimus in pediatric patients and young adults with recurrent or refractory sarcoma: a report from the Children's Oncology Group. In: *Pediatric blood & cancer* 62 (3), S. 440–444.

Wang, K. H.; Brose, K.; Arnott, D.; Kidd, T.; Goodman, C. S.; Henzel, W.; Tessier-Lavigne, M. (1999): Biochemical purification of a mammalian slit protein as a positive regulator of sensory axon elongation and branching. In: *Cell* 96 (6), S. 771–784.

Wang, L.; Chen, S.; Xue, M.; Zhong, J.; Wang, X.; Gan, L.; Lam, Emily K Y; Liu, X.; Zhang, J.; Zhou, T.; Yu, J.; Jin, H.; Si, J. (2012): Homeobox D10 gene, a candidate tumor suppressor, is downregulated through promoter hypermethylation and associated with gastric carcinogenesis. In: *Molecular medicine (Cambridge, Mass.)* 18, S. 389–400.

Wang, X.; Choi, J.-H.; Ding, J.; Yang, L.; Ngoka, L. C.; Lee, E. J.; Zha, Y.; Mao, L.; Jin, B.; Ren, M.; Cowell, J.; Huang, S.; Shi, H.; Cui, H.; Ding, H.-F. (2013): HOXC9 directly

regulates distinct sets of genes to coordinate diverse cellular processes during neuronal differentiation. In: *BMC genomics* 14, S. 830.

Wang, Y.; Li, Z.; Zhao, X.; Zuo, X.; Peng, Z. (2016): miR-10b promotes invasion by targeting HOXD10 in colorectal cancer. In: *Oncology letters* 12 (1), S. 488–494.

Ward, E.; DeSantis, C.; Robbins, A.; Kohler, B.; Jemal, A. (2014): Childhood and adolescent cancer statistics, 2014. In: *CA: a cancer journal for clinicians* 64 (2), S. 83–103.

Warot, X.; Fromental-Ramain, C.; Fraulob, V.; Chambon, P.; Dollé, P. (1997): Gene dosage-dependent effects of the Hoxa-13 and Hoxd-13 mutations on morphogenesis of the terminal parts of the digestive and urogenital tracts. In: *Development (Cambridge, England)* 124 (23), S. 4781–4791.

Warren, M.; Weindel, M.; Ringrose, J.; Venable, C.; Reyes, A.; Terashima, K.; Rao, P.; Chintagumpala, M.; Hicks, M. J.; Lopez-Terrada, D.; Lu, X.-Y. (2013): Integrated multimodal genetic testing of Ewing sarcoma--a single-institution experience. In: *Human pathology* 44 (10), S. 2010–2019.

Weidenbusch, B.; Richter, G. H. S.; Kesper, M. S.; Guggemoos, M.; Gall, K.; Prexler, C.; Kazantsev, I.; Sipol, A.; Lindner, L.; Nathrath, M.; Witt, O.; Specht, K.; Beitinger, F.; Knebel, C.; Hosie, S.; Eisenhardt-Rothe, R. von; Weichert, W.; Luettichau, I. T.-v.; Burdach, S. (2018): Transcriptome based individualized therapy of refractory pediatric sarcomas: feasibility, tolerability and efficacy. In: *Oncotarget* 9 (29), S. 20747–20760.

Weilbaecher, K. N.; Guise, T. A.; McCauley, L. K. (2011): Cancer to bone: a fatal attraction. In: *Nature reviews. Cancer* 11 (6), S. 411–425.

Wellik, D. M. (2007): Hox patterning of the vertebrate axial skeleton. In: *Developmental dynamics : an official publication of the American Association of Anatomists* 236 (9), S. 2454–2463.

Wieczorek, E.; Jablonska, E.; Wasowicz, W.; Reszka, E. (2015): Matrix metalloproteinases and genetic mouse models in cancer research: a mini-review. In: *Tumour biology : the journal of the International Society for Oncodevelopmental Biology and Medicine* 36 (1), S. 163–175.

Woodbury, D.; Schwarz, E. J.; Prockop, D. J.; Black, I. B. (2000): Adult rat and human bone marrow stromal cells differentiate into neurons. In: *Journal of neuroscience research* 61 (4), S. 364–370.

Xiao, H.; Li, H.; Yu, G.; Xiao, W.; Hu, J.; Tang, K.; Zeng, J.; He, W.; Zeng, G.; Ye, Z.; Xu, H. (2014): MicroRNA-10b promotes migration and invasion through KLF4 and HOXD10 in human bladder cancer. In: *Oncology reports* 31 (4), S. 1832–1838.

Xu, B.; Geerts, D.; Bu, Z.; Ai, J.; Jin, L.; Li, Y.; Zhang, H.; Zhu, G. (2014): Regulation of endometrial receptivity by the highly expressed HOXA9, HOXA11 and HOXD10 HOX-class homeobox genes. In: *Human reproduction (Oxford, England)* 29 (4), S. 781–790.

Yamamoto-Shiraishi, Y.-i.; Kuroiwa, A. (2013): Wnt and BMP signaling cooperate with Hox in the control of Six2 expression in limb tendon precursor. In: *Developmental biology* 377 (2), S. 363–374.

Yang, H.; Zhou, J.; Mi, J.; Ma, K.; Fan, Y.; Ning, J.; Wang, C.; Wei, X.; Zhao, H.; Li, E. (2015): HOXD10 acts as a tumor-suppressive factor via inhibition of the RHOC/AKT/MAPK pathway in human cholangiocellular carcinoma. In: *Oncology reports* 34 (4), S. 1681–1691.

Yock, T. I.; Krailo, M.; Fryer, C. J.; Donaldson, S. S.; Miser, J. S.; Chen, Z.; Bernstein, M.; Laurie, F.; Gebhardt, M. C.; Grier, H. E.; Tarbell, N. J. (2006): Local control in pelvic Ewing sarcoma: analysis from INT-0091--a report from the Children's Oncology Group. In: *Journal of clinical oncology : official journal of the American Society of Clinical Oncology* 24 (24), S. 3838–3843.

Yu, H.; Ge, Y.; Guo, L.; Huang, L. (2017): Potential approaches to the treatment of Ewing's sarcoma. In: *Oncotarget* 8 (3), S. 5523–5539.

Zakany, J.; Duboule, D. (2007): The role of Hox genes during vertebrate limb development. In: *Current opinion in genetics & development* 17 (4), S. 359–366.

Zarzynska, J. M. (2014): Two faces of TGF-beta1 in breast cancer. In: *Mediators of inflammation* 2014, S. 141747.

Zha, Y.; Ding, E.; Yang, L.; Mao, L.; Wang, X.; McCarthy, B. A.; Huang, S.; Ding, H.-F. (2012): Functional dissection of HOXD cluster genes in regulation of neuroblastoma cell proliferation and differentiation. In: *PloS one* 7 (8), e40728.

Zhang, B.; Li, N.; Zhang, H. (2017): Knockdown of Homeobox B5 (HOXB5) Inhibits Cell Proliferation, Migration, and Invasion in Non-Small Cell Lung Cancer Cells Through Inactivation of the Wnt/β-Catenin Pathway. In: *Oncology research*.

Zhang, M.-l.; Nie, F.-q.; Sun, M.; Xia, R.; Xie, M.; Lu, K.-h.; Li, W. (2015): HOXA5 indicates poor prognosis and suppresses cell proliferation by regulating p21 expression in non small cell lung cancer. In: *Tumour biology : the journal of the International Society for Oncodevelopmental Biology and Medicine* 36 (5), S. 3521–3531.

Zhang, Q.; Jin, X. S.; Yang, Z. Y.; Wei, M.; Liu, B. Y.; Gu, Q. L. (2013): Upregulated Hoxc6 expression is associated with poor survival in gastric cancer patients. In: *Neoplasma* 60 (4), S. 439–445.

Zhang, X.; Zhu, T.; Chen, Y.; Mertani, H. C.; Lee, K.-O.; Lobie, P. E. (2003): Human growth hormone-regulated HOXA1 is a human mammary epithelial oncogene. In: *The Journal of biological chemistry* 278 (9), S. 7580–7590.

Zhang, Z.; Chen, J.; Jin, D. (1998): Platelet-derived growth factor (PDGF)-BB stimulates osteoclastic bone resorption directly: the role of receptor beta. In: *Biochemical and biophysical research communications* 251 (1), S. 190–194.

Zhao, J.-c.; Zhang, L.-x.; Zhang, Y.; Shen, Y.-f. (2012): The differential regulation of Gap43 gene in the neuronal differentiation of P19 cells. In: *Journal of cellular physiology* 227 (6), S. 2645–2653.

Zhao, X.; Sun, M.; Zhao, J.; Leyva, J. A.; Zhu, H.; Yang, W.; Zeng, X.; Ao, Y.; Liu, Q.; Liu, G.; Lo, Wilson H Y; Jabs, E. W.; Amzel, L. M.; Shan, X.; Zhang, X. (2007): Mutations in HOXD13 underlie syndactyly type V and a novel brachydactyly-syndactyly syndrome. In: *American journal of human genetics* 80 (2), S. 361–371.

Zheng, L.; Zhu, K.; Jiao, H.; Zhao, Z.; Zhang, L.; Liu, M.; Deng, W.; Di Chen; Yao, Z.; Xiao, G. (2013): PTHrP expression in human MDA-MB-231 breast cancer cells is critical for tumor growth and survival and osteoblast inhibition. In: *International journal of biological sciences* 9 (8), S. 830–841.

Zhong, H.; De Marzo, A M; Laughner, E.; Lim, M.; Hilton, D. A.; Zagzag, D.; Buechler, P.; Isaacs, W. B.; Semenza, G. L.; Simons, J. W. (1999): Overexpression of hypoxia-inducible factor 1alpha in common human cancers and their metastases. In: *Cancer research* 59 (22), S. 5830–5835.

Zhong, Z.-B.; Shan, M.; Qian, C.; Liu, T.; Shi, Q.-Y.; Wang, J.; Liu, Y.; Liu, Y.; Huang, Y.-X.; Pang, D. (2015): Prognostic significance of HOXD13 expression in human breast cancer. In: *International journal of clinical and experimental pathology* 8 (9), S. 11407–11413.

Zhou, Z.; Bolontrade, M. F.; Reddy, K.; Duan, X.; Guan, H.; Yu, L.; Hicklin, D. J.; Kleinerman, E. S. (2007): Suppression of Ewing's sarcoma tumor growth, tumor vessel formation, and vasculogenesis following anti vascular endothelial growth factor receptor-2 therapy. In: *Clinical cancer research : an official journal of the American Association for Cancer Research* 13 (16), S. 4867–4873.

Zorzi, A. P.; Bernstein, M.; Samson, Y.; Wall, D. A.; Desai, S.; Nicksy, D.; Wainman, N.; Eisenhauer, E.; Baruchel, S. (2013): A phase I study of histone deacetylase inhibitor, pracinostat (SB939), in pediatric patients with refractory solid tumors: IND203 a trial of the NCIC IND program/C17 pediatric phase I consortium. In: *Pediatric blood & cancer* 60 (11), S. 1868–1874.

Zoubek, A.; Dockhorn-Dworniczak, B.; Delattre, O.; Christiansen, H.; Niggli, F.; Gatterer-Menz, I.; Smith, T. L.; Jürgens, H.; Gadner, H.; Kovar, H. (1996): Does expression of different EWS chimeric transcripts define clinically distinct risk groups of Ewing tumor patients? In: *Journal of clinical oncology : official journal of the American Society of Clinical Oncology* 14 (4), S. 1245–1251.

9. Publication

Parts of this doctoral thesis have already been published:

Heyking, Kristina von; **Roth, Laura**; Ertl, Miriam; Schmidt, Oxana; Calzada-Wack, Julia; Neff, Frauke; Lawlor, Elizabeth R.; Burdach, Stefan; Richter, Guenther Hs (2016). The posterior HOXD locus: Its contribution to phenotype and malignancy of Ewing sarcoma. Oncotarget 7/2016: 41767–41780

10. Appendices

10.1 List of figures

10.2 List of tables

11. Acknowledgements

An dieser Stelle möchte ich mich bei allen bedanken, die zum Gelingen dieser Doktorarbeit beigetragen haben.

Mein besonderer Dank gilt:

Herrn Prof. Dr. Stefan Burdach und Herrn PD Dr. Günther Richter für die Möglichkeit, an diesem interessanten Thema am Forschungszentrum für krebskranke Kinder der TUM arbeiten zu dürfen, für die freundliche Aufnahme in die Arbeitsgruppe, für das mir entgegen gebrachte Vertrauen sowie für die Begleitung und die Korrektur meiner Arbeit, die hauptsächlich durch die Else-Kröner-Fresenius Stiftung und die Wilhelm-Sander Stiftung finanziert wurde.

Frau Dr. Kristina von Heyking, für die höchst kompetente, tolle Betreuung, für die Einarbeitung in die experimentelle Tätigkeit, für die Hilfe bei der Durchführung der Experimente, für die Durchsicht meiner Arbeit und für ihre fortwährende Unterstützung.

Frau Dr. Julia Calzada-Wack und Frau Dr. Frauke Neff vom Institut für Pathologie am Helmholtz Zentrum München für die sorgfältige und schnelle Durchführung der histologischen Untersuchungen.

Herrn Dr. Andreas Kirschner und Herrn Dr. David Schirmer für ihre tatkräftige Unterstützung bei der Durchführung der Mausexperimente.

Außerdem danke ich natürlich auch allen anderen Mitarbeitern des Forschungszentrums für krebskranke Kinder der TUM für die gute kollegiale Zusammenarbeit, die große Hilfsbereitschaft, die interessanten Gespräche und Anregungen und für die schöne Zeit im Labor.

Und zu guter Letzt bedanke ich mich bei Oma, Mama, Papa, Katharina, Anna, Roxi und Simon für ihre großartige Unterstützung, ihren emotionalen Rückhalt, ihr Vertrauen in das Gelingen dieser Arbeit und dafür, dass sie immer für mich da sind! Danke!